



**TECHNOLOGICAL INNOVATIONS  
IN ENDOBRONCHIAL LUNG CANCER  
DIAGNOSTICS**

Roel L. J. Verhoeven

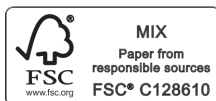


# **Technological innovations in endobronchial lung cancer diagnostics**

**Roel Lambertus Johannes Verhoeven**

The research described in this thesis was carried out within the Radboud Institute for Health Sciences at the Department of Pulmonary diseases and Medical Ultrasound Imaging Center (Radboud University Medical Center, Nijmegen, the Netherlands). This work was funded by research grants from the Radboudumc Medical Innovation and Technology expert Center (MITeC), the Ankie Hak fund, Pentax Medical Europe, AstraZeneca and Philips Medical.

Financial support for publication of this thesis was kindly provided by Pentax Medical Europe, Philips Medical and the Radboudumc.



Copyright © 2020 by R.L.J. Verhoeven. All rights reserved. No part of this publication may be reproduced or transmitted in any form or by any means, electronic or mechanical, including photocopy, recording, or any information storage and retrieval system, without permission in writing from the author.

**ISBN:** 978-94-6421-332-4

**Design by** Bregje Jaspers | ProefschriftOntwerp.nl

**Print by** Ipskamp Printing, Enschede

# **Technological innovations in endobronchial lung cancer diagnostics**

## **Proefschrift**

ter verkrijging van de graad van doctor  
aan de Radboud Universiteit Nijmegen  
op gezag van de rector magnificus prof. dr. J.H.J.M van Krieken,  
volgens besluit van het college van decanen  
in het openbaar te verdedigen op maandag 7 juni 2021  
om 16.30 uur precies

door

**Roel Lambertus Johannes Verhoeven**

geboren op 20 mei 1992  
te 's-Hertogenbosch

**Promotor**

Prof. dr. ir. C.L. de Korte

**Copromotor**

Dr. E.H.F.M. van der Heijden

**Manuscriptcommissie**

Prof. dr. A.F.T.M. Verhagen

Prof. dr. M.M. Rovers

Prof. dr. D.J. Slebos (Rijksuniversiteit Groningen)







## Table of contents

<b>Chapter 1</b>	General introduction and thesis outline	9
<b>Endobronchial techniques in advanced stage lung cancer</b>		
<b>Chapter 2</b>	Optimal endobronchial ultrasound strain elastography assessment strategy: an explorative study <i>Respiration, 2018; 97(4):337-347.</i>	23
<b>Chapter 3</b>	Predictive value of endobronchial ultrasound strain elastography in mediastinal lymph node staging: the E-predict multicenter study results <i>Respiration, 2020;99(6):484-492.</i>	49
<b>Chapter 4</b>	Accuracy and reproducibility of endoscopic ultrasound B-mode features for observer based lymph nodal malignancy prediction <i>Respiration, Accepted for publication, 2021.</i>	65
<b>Endobronchial techniques in early stage lung cancer</b>		
<b>Chapter 5</b>	Cone-beam CT image guidance with and without electromagnetic navigation bronchoscopy for biopsy of peripheral pulmonary lesions <i>Journal of Bronchology &amp; Interventional Pulmonology, 2021;28(1):60-69.</i>	81
<b>Chapter 6</b>	Multi-modal tissue sampling in cone beam CT guided navigation bronchoscopy; the accuracy of different sampling tools and rapid on-site evaluation of cytopathology <i>Submitted, 2020.</i>	97
<b>Chapter 7</b>	Cone-beam CT and augmented fluoroscopy guided navigation bronchoscopy; radiation exposure and learning curve <i>Submitted, 2020.</i>	111
<b>Chapter 8</b>	Summary	127
<b>Chapter 9</b>	General discussion and future perspectives	137
<b>Chapter 10</b>	Nederlandse samenvatting	149
<b>Appendices</b>	Bibliography	163
	Research data management	175
	PhD portfolio	176
	List of publications & presentations	178
	Dankwoord	182
	Curriculum Vitae	189





# CHAPTER 1

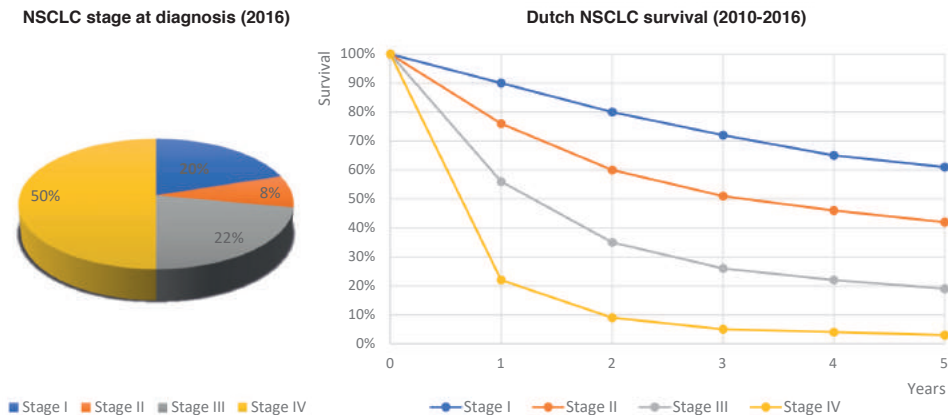
General introduction and thesis outline



## 1.1 Lung cancer

Lung cancer is the most prevalent form of cancer worldwide, exceeding 2.2 million new cases every year. The incidence will continue to rise in the upcoming years, with the expectation that numbers will increase to as much as 3.2 million cases in 2035 [2]. Every year since 2015 has seen more than 13.000 patients in the Netherlands receive the diagnosis lung cancer [1]. When considering national disease burden based on all pathology, lung cancer takes 6<sup>th</sup> place in the Netherlands [3].

Lung cancer can be divided into different subtypes, with the vast majority of histology findings classified as non-small-cell lung cancer (NSCLC, totalling approximately 85%). Non-small-cell lung cancer predominantly consists of subtypes adenocarcinoma, squamous-cell carcinoma, and large-cell carcinoma [4,5]. Unfortunately, this disease often only presents itself with symptoms at a late stage, leading to approximately 50% of diagnoses being end-stage disease (stage IV, Figure 1.1). Once other organs are involved – as indicated by disease stage IV – 5 year overall survival drops to approximately 5% (Figure 1.1). Comparing this to the 61% 5 year overall survival in patients with stage I disease, a stage where there's no disease presence other than a primary tumor, demonstrates that early diagnosis brings an improved outcome. Combining late diagnosis and poor prognosis shows approximately 80% of patients die within 5 years after having received their diagnosis [1]. Yet as even the earliest stage of disease remains to have very high mortality, all possibilities of improving outcome remain of high interest. One important aspect is to more timely and accurately diagnose and stage patients with a suspected or proven lung cancer. By accurate and timely diagnosis, unneeded disease progression and under- and overtreatment can be prevented. In this thesis, it is investigated how innovative technology in flexible endoscopy might help improve the diagnostic and staging trajectory of lung cancer.



**Figure 1.1** – Non-small-cell lung cancer (NSCLC) statistics. Left: The distribution of disease stage at moment of diagnosis of patients in the Netherlands (2016). Right: Overall 5-year survival of the different stages of NSCLC in the Netherlands, once a diagnosis has been obtained. Source: IKNL [1].

## 1.2 Lung cancer diagnosis

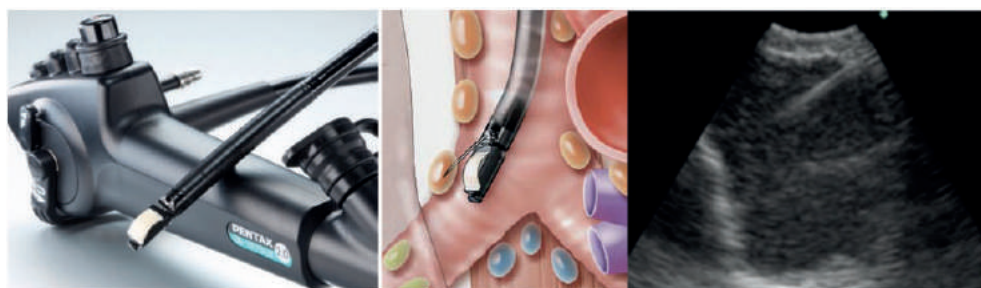
In the current situation, the patient most often finds its way to the department of pulmonology by first-line healthcare referral after having already developed advanced stage disease symptoms. At patient presentation, an initial suspicion of lung cancer is then further proofed by performing imaging such as X-ray or CT imaging. If these imaging modalities show a likely disease presence, it is recommended and routine clinical practice to perform a FluoroDeoxyGlucose – Positron Emission Tomography (FDG-PET) scan that is simultaneously combined with CT imaging (PET-CT scan) [6]. The FDG-PET scan allows for evaluation of the metabolic activity, while the CT scan gives spatial information. Together, they enable an assessment of both the metabolic activity of the primary tumor as well as possible lymph node and distant metastatic disease presence. PET-CT imaging thus allows for a first imaging-based disease diagnosis and staging. With this information, the further needed work-up of (endoscopic) diagnostic modalities can be determined.

## 1.3 Lung cancer staging

In staging NSCLC disease extent, the tumor (T), node (N) and metastatic spread outside the original organ (M) are assessed. By this so-called TNM classification, disease staging and concurrent treatment options can be determined [7]. The T descriptor mainly involves tumor size, generally ranging from T1 ( $\leq 3$  cm) to T4 ( $> 7$  cm). The N descriptor describes regional lymph node metastasis. In lung cancer, lymph nodal disease spread often follows specific predictable drainage patterns. The extent of nodal spread has shown prognostic of disease outcome, and ranges from N0-N3. N0 herein indicates absence of lymph nodal involvement. An N1 describes a nodal involvement maximally delimited by ipsilateral hilar or lymph nodes situated more peripheral in the lung. An N2 involvement indicates subcarinal and ipsilateral mediastinal involvement. An N3 involvement implies contralateral mediastinal or hilar nodes, or, involvement of any scalene or supraclavicular lymph nodes. The M descriptor implies distant metastasis into different organs, including the contralateral lung lobe and pleural or pericardial involvement. Combining the T, N and M descriptors results in the lung cancer stage (range I-IV). Patients with stage I-II disease, having N1 involvement at most, will generally receive treatment with curative intent (surgery, radiotherapy). Stage III disease most often includes N2/N3 involvement and will generally imply concurrent or sequential chemo-radiotherapy followed by immunotherapy or surgery. Stage IV – end-stage disease – involves distant metastasis. As there is systemic involvement, treatment of stage IV disease includes systemic treatment options like chemotherapy, immunotherapy or other targeted agents. From this staging algorithm it can be determined that disease staging and subsequent treatment and survival of NSCLC is mostly determined by metastatic (lymph nodal) involvement.

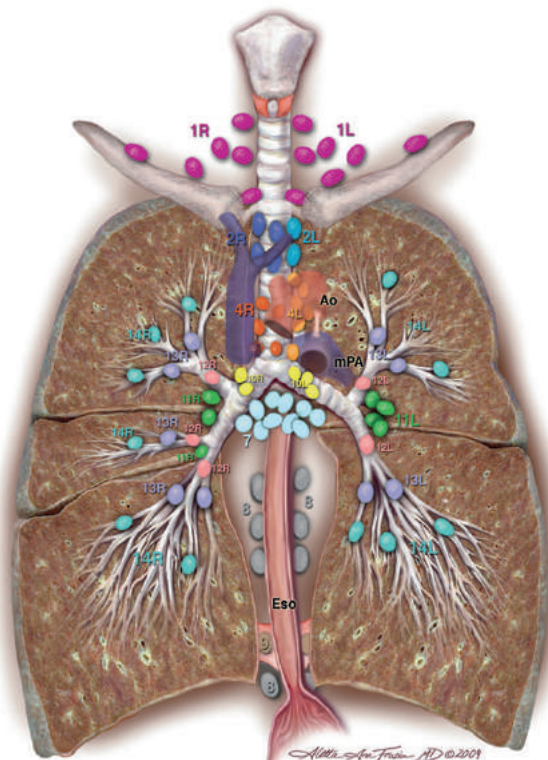
## 1.4 Advanced stage disease (Part I)

While PET-CT imaging can enable an initial imaging based diagnosis and staging, its combined 62% sensitivity and 90% specificity reveals the technique is not always accurate in diagnosis and staging [9]. Consequently, especially the lymph nodal involvement of the disease should be confirmed by tissue sampling if any imaging based suspicion of metastasis has been raised [6]. In staging and therewith lymph node sampling of a suspected (advanced) disease, the three routinely utilized modalities are endobronchial ultrasound – transbronchial needle aspiration (EBUS-TBNA), endosophageal ultrasound – fine needle aspiration (EUS-FNA) and mediastinoscopy. Of these modalities, the EBUS-TBNA and EUS-FNA procedures are least invasive, have lowest complication rates, are best tolerated, and most cost-effective [10]. By navigating through the natural orifice of the bronchial tree or oesophagus with these modalities, the lymph nodes can be assessed. These procedures use a video camera and ultrasound transducer positioned at the distal tip of a flexible endoscope to assess the differently defined anatomical lymph node regions (Figure 1.2). Routine clinical work-up of a suspected advanced stage disease involves combining an EBUS-TBNA and EUS-FNA procedure for systematically assessing all mediastinal and hilar lymph nodes under ultrasound guidance. Preferably, lymph node sampling is performed in at least zones 4L, 4R, 7, and any other lymph nodes showing increased metabolic activity or CT-scan based enlarged size [6,10] (Figure 1.3). Alongside PET and CT imaging, intra-procedural ultrasound imaging findings are often used to decide on aspiration of (additional) nodes (e.g. [12,13]). To prevent cross-contamination of tissue samples between nodes, the physician should start with the lymph node most distal from the suspected tumor and from there work back to nodes more proximal to the tumor. If needed and possible, the tumor itself should also be assessed [6]. Performing a single needle aspiration of a lymph node herein takes at least 3 minutes [14]. A combined EBUS-EUS approach has a sensitivity of 86% and



**Figure 1.2** – Left: Image of an ultrasound video-endoscope for performing EBUS-TBNA procedures. Middle: Illustration of EBUS-TBNA based lymph node aspiration using a hollow needle as advanced through the working channel of the endoscope. Right: Clinical ultrasound image of an enlarged lymph node being sampled with a hollow aspiration needle. Left and middle images by Pentax [8].

negative predictive value of 92% [15]. Thus, approximately one in seven malignant nodes will not be accurately identified as such by endosonographic staging. If EBUS-TBNA and/or EUS-FNA sampling results are negative or deemed unrepresentative and suspicion of nodal involvement remains, performing a mediastinoscopy is therefore indicated [6,10]



**Figure 1.3** – Illustration depicting the lymph node regions as routinely used for TNM staging in NSCLC. Every number herein defines a lymph node region. Depending on the primary tumor location, these lymph node regions can be used for determining disease involvement and therewith staging. Image by Rusch *et al.* and the IASLC [11], re-used with permission.

In mediastinoscopy, a surgical incision and dissection of the pretracheal space is required for gaining access to the lymph nodes, being more invasive and having higher complication rates [12]. Using a rigid endoscope and rigid tools, the lymph nodes can then be sampled for tissue collection, allowing for an evaluation of tissue histology. As a randomized controlled trial showed, this sequential staging approach has highest accuracy. Where mediastinoscopy and endosonographic staging had only 79% and 85% sensitivity, the combined approach had 94% sensitivity [12].



### 1.4.1 Endosonography for stratifying risk of malignancy

To increase the diagnostic yield and efficiency of endosonographically guided needle aspiration in EBUS-TBNA and EUS-FNA procedure, and therewith possibly avoid the necessity of additional staging procedures such as mediastinoscopy, it has been suggested to further utilize available ultrasonographical information for better differentiation of likely malignant lymph nodes. The first studies suggesting that endosonographic features of lymph nodes could help predict the chance of lymph node malignancy came after the initial introduction of EUS-FNA in the 1990's [16]. However, as an expert panel report also concludes, individual study findings of greyscale ultrasound imaging have shown heterogeneous in accuracy thus far and are therefore limited in widespread use [17].

### 1.4.2 Ultrasound and strain elastography

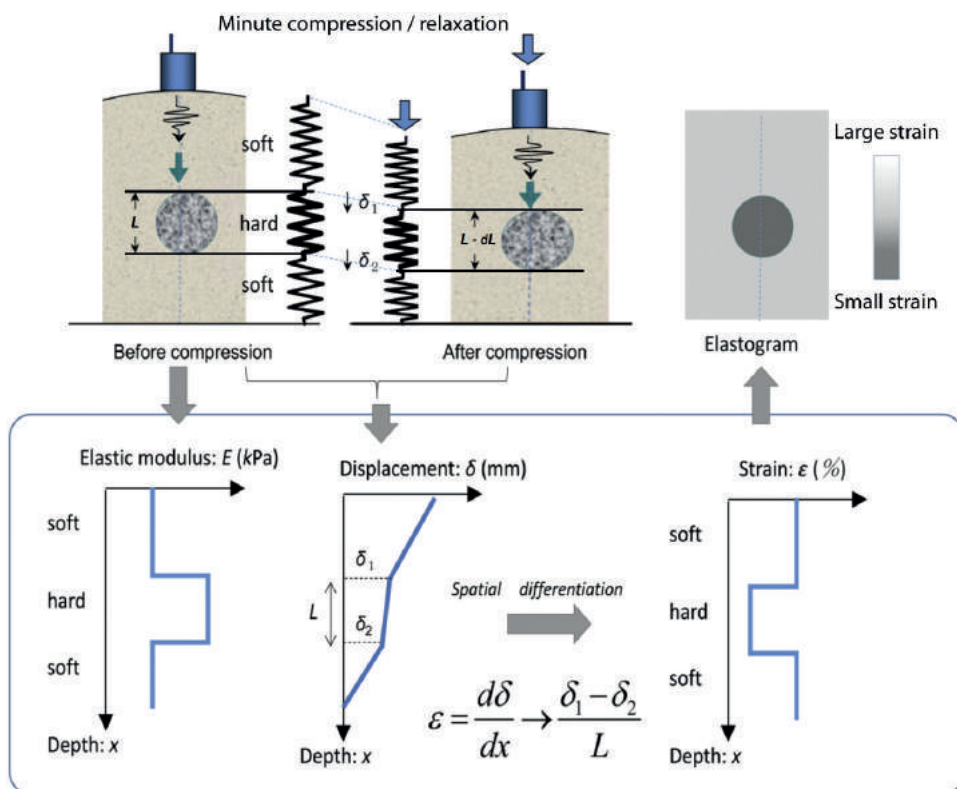
Ultrasound strain elastography is a relatively new endosonographic technique, giving information on soft tissue by deriving tissue elasticity in real time. It provides additional information to conventionally used endosonographic B-mode imaging, which is based on imaging acoustical properties of tissues. As multiple studies in other medical specialties have found, a lower strain in lymph nodes or tumors was found to be correlated with higher chance of malignancy and could be measured by means of ultrasound strain elastography [18,19].

Ultrasound strain elastography can be performed in multiple ways. For example, pre- and post-strain radio-frequency (RF) signals can be used for determining elastic properties of soft tissue [20,21]. To be able to reconstruct the strain, backscattered signals of the tissue at a first acquisition (pre-compression) are compared to a second acquisition (post-compression, Figure 1.4). The time shift between the tissue reflections at the different time points can then be quantified by for example a cross-correlation method. Since the speed of sound is considered to be constant, a time delay estimate can be transformed into a tissue displacement. After determining the displacement at every depth, its derivative can be computed for finding the relative strain [22]. The received RF signal contains not only the envelope but also the phase information, allowing a much more accurate quantification of strain than if only the envelop (echogram) were used. Since the phase information is available only in the axial direction and lacking in the lateral direction, strain is hard to determine accurately in the lateral direction [23]. Geometrically seen, the local axial strain can be estimated by formula 1 below [20]:

$$S_n = \frac{t_{n+1} - t_n}{2dz/c} \quad \begin{array}{l} S_n = \text{Local axial strain} \\ t_n = \text{time shift for segment } n \\ dz = \text{difference in axial length} \\ c = \text{speed of sound} \end{array} \quad (1)$$

The derived axial strain measurements are not a generalized strain as used to describe the Young's modulus (see Formula 2 below). To calculate the Young's modulus, one needs to know both (applied) stress and (obtained) strain. As the stress cannot be accurately derived for the whole 2D image in ultrasound strain elastography, the strain is only indirectly related to the Young's modulus (and thus an artefactual representation of it).

$$\text{Young's modulus: } E = \frac{\text{tensile stress}}{\text{extensional strain}} \quad (2)$$



**Figure 1.4** – Schematic illustration of how axial strain is derived from pre- to post-compression ultrasound imaging. On the top left, the tissue is in its initial state. A first RF signal is acquired. Top middle image: after introducing an axial force, a second RF signal is acquired. The displacement is calculated by using a cross correlation algorithm that correlates the RF signals before and after compression. The relative strain can be computed by taking the finite difference of tissue displacement at every depth in these two measurements. In endosonography, minute compression is hypothesized to be introduced by pulsation of the cardiovascular system. Image adapted from Shiina *et al.* (2015) [24].

The stress that is applied to create a deformation in endosonographic strain elastography is a result of the patient's own pulsating heart and vasculature. The force of these deformation sources is unknown, as it is both patient and location dependent. However, knowing the lymph nodal map [11] it can be derived that lymph nodes are found in between the EBUS transducer and the pulsating vasculature that is causing strain. As opposed to the operator being the source of the palpation in the axial direction from a proximal point of view, axial imaging is thus theorized to be possible by using the pulsating vasculature from a distal point of view with reference to the EBUS endoscope, with the lymph node in between source and transducer. As it is a relative measure, not knowing what force is applied to obtain such strain, the visualized strain is normalized over every image. Although semi-quantitative, it can potentially provide valuable information on relative lymph node elasticity and therewith the chance of lymph node malignancy.

## 1.5 Early stage disease (Part II)

As stated before, lung cancer is one of most lethal malignancies in the Netherlands, most importantly because of the advanced stage disease at diagnosis. To improve survival, current guidelines advocate low-dose CT-based screening in a population high at risk of developing lung cancer. An increasing number of countries have started or are preparing to start a national lung screening program [25–30]. These preparations are based in part on the findings of lung cancer screening studies. An example of these are the American National Lung Screening Trial (NLST) and the recently concluded Dutch-Belgian NELSON screening trial. Both trials showed that a CT screening of a high risk population could reduce lung cancer mortality by more than 20% as compared with the radiography control group [26,31]. This decreased mortality could mainly be attributed to a shift towards early stage lung cancer findings. However, these screenings also find numerous non-malignant lesions situated in the peripherals of the lung. An example is the NLST, which found that 39.1% of the participants developed at least one lesion of more than 4 mm in diameter. Of those patients with lesions, 72.1% needed additional diagnostics procedures for further nodule evaluation [26]. The NELSON study, having different inclusion criteria and study specifications, found that 9.2% of the participants needed at least one additional CT scan during the 10-year trial [31]. Eventually however, in both NLST and the NELSON trial more than 96% of the suspected peripheral pulmonary lesions were found to be benign [25,26].

Yet even without the implementation of a CT screening for a population at risk for developing lung cancer, we are seeing small peripheral lesions in the lung being diagnosed increasingly often. With the widespread availability of CT in more recent times, scanning is more easily performed. A CT scan not purposefully requested for lung disease will not rarely reveal one or more pulmonary lesions. A pooled analysis of 11 studies showed that in 13% (range 2-24%) of CT scans that were not purposefully requested for lung disease, one or more pulmonary

lesions suspected of malignancy were found. In these CT scans, 1.5% (range 0-4.0%) of patients were eventually diagnosed with lung cancer [32]. At current, the early stage disease patients in the Netherlands are exclusively identified through these incidental findings.

### **1.5.2 Diagnostic algorithms**

As opposed to staging advanced stage disease where lymph nodes can be reached and sampled under real-time guidance for confirming lung cancer, early stage disease requires a different approach. Early stage disease involves only the suspicion of a primary lesion, which is often small in size and located in the peripherals of the lung. Because of their small size and peripheral location, reaching them for obtaining a diagnosis and concurrently providing a treatment is complex. This can also partially be reflected by the fact that multiple different guidelines and calculators for determining on how to cope with peripheral pulmonary lesions exist [32–37].

Generally, three strategies for a suspected early stage lung cancer can be described: observational CT follow-up / watchful waiting, minimally invasive diagnostic techniques, or, (limited) surgical excision for further diagnosis and patient management. Based on the probability of malignancy, patient preferences and feasibility of the approach, one of strategies will be preferred above the other. The risk of malignancy is herein determined by multiple factors and can be influenced by the use of different algorithms [32–37]. Based on these algorithms, the British Thoracic Society (BTS) guidelines for example dictate a <10% risk of malignancy warrants watchful waiting, 10-70% should indicate non-surgical biopsy and a >70% risk of malignancy could allow for immediate surgical diagnosis. If chance of malignancy is deemed sufficiently high and surgical resection is considered infeasible, immediate radiotherapy might also be considered. The cut-offs herein are determined by weighing the risk of malignancy and need of tissue diagnosis against procedure effectiveness and invasiveness.

### **1.5.3 Non-surgical biopsy**

Peripheral lesions that ought to be diagnosed by minimal invasive means can be subjected to a multitude of clinical work-up diagnostics. Differences in modality costs (and country variation), heterogeneous study results of the different modalities, manufacture differences, needed expertise, and availability of modalities all hamper a straightforward guideline in reaching for the peripheral pulmonary nodules. However, a clear preference for first utilizing an endobronchial approach exists, as it is least invasive [32–34,37].

### **1.5.4 Endobronchial approaches**

The fluoroscopy (C-arm) guided transbronchial biopsy procedure using the conventional bronchoscope has been a widely used means for the endobronchial diagnosis of peripheral lesions in previous decades (pooled yield 34%, [34]). As the originally available bronchoscopes had diameters too big to pass beyond the segmental bifurcations, this method relied on

advancing biopsy tools through the working channel and into the hypothesized bronchi that would lead to the suspected lesion. Fluoroscopy was used as a coarse guidance method for tissue sampling and often no direct endobronchial visualization of accurate lesion sampling was possible.

In more recent years, several more promising new modalities have become available that are able to provide additional guidance for endobronchial diagnosis of peripheral pulmonary lesions. For an overview and more thorough explanation on these modalities, see i.e. [38–42]. A meta-analysis by Wang *et al.* (2012) showed that the individual diagnostic yield of most readily available modalities such as virtual endoscopy navigation guidance, electromagnetic navigation guidance, radial endobronchial ultrasound imaging guidance, ultrathin bronchoscopes and a guide-sheath based approach had diagnostic yields ranging from 67%-73.2% and an overall pooled diagnostic yield of approximately 70% [39]. These modalities are already a big improvement when compared to the conventional fluoroscopy guided trans-bronchial biopsy. But, a diagnostic yield of approximately 70% shows that room for improvement remains.

### **1.5.5 Transthoracic techniques**

If the endobronchial approach fails to provide an outcome or is deemed infeasible, additional more invasive staging is often indicated [32,34,43]. TTNA, or trans thoracic needle aspiration, is a more invasive technique than the earlier introduced endobronchial techniques. Instead of an endobronchial approach, this technique encompasses a percutaneous biopsy performed under CT guidance. TTNA has been reported and widely accepted as the golden standard for diagnosis of peripheral pulmonary lesions, with a diagnostic yield of approximately 90%. However, by traversing the thoracic wall it is also known to have high pneumothorax rate. The pooled pneumothorax complication rate is found to be 18.8-25.3%, of which 6-7% requires a chest tube placement [32,44]. In contrast, the different endobronchial approaches have 1.5% pooled chance of pneumothorax, requiring chest tube placement in only 0.6% [39].

### **1.5.6 Suboptimal diagnostics**

When both endobronchial techniques as well as TTNA did not provide outcome or are deemed infeasible and risk of malignancy is significant, more invasive techniques and follow up are indicated. These techniques are not necessarily diagnostic only, as they also involve a therapeutic nature. The follow-up is herein based on patient characteristics as well as patient preferences. A suspected peripheral lesion which was not or could not be diagnosed by minimally invasive diagnostics is likely to be referred for surgery or radiotherapy. In the surgical approach, a wedge resection will generally be performed. This involves removal of the suspected lesion with a minority of normal lung tissue and can be deemed a diagnostic but also immediate therapeutic option. If this wedge shows the lesion to be malignant by intra-procedural frozen section analysis, a continuation of the procedure into a lobectomy for curative surgical treatment is likely considered. Radiotherapy is a strictly therapeutic

technique, irradiating the suspected lesion to kill any tumor cells without pursuing any further sure diagnosis of the lesion.

As the British Thoracic Society guidelines (2015) and van IJsseldijk *et al.* (2019) conclude, the lack of confirmative tissue diagnostics preceding to surgery and radiotherapy leads to a significant amount of patients with benign disease receiving unnecessary treatment [32,45]. This unnecessary treatment poses the patient with risks and reduced lung function whilst adding significant costs to healthcare.

All considered, the demand for safe, fast and accurate diagnostic tools is high and is anticipated to increase rapidly as screening programs are being initiated. Ideally, an endobronchial approach easily accessible and having high diagnostic accuracy would overcome the need of the currently used sequential increasingly invasive diagnostic and consecutive treatment approach. The currently available techniques herein do not seem to fulfil this emerging demand.

## 1.6 Thesis outline

**Part I** - Part I of this thesis is focused on the clinical use of endobronchial ultrasound and ultrasound strain elastography for predicting lymph node malignancy in an advanced stage lung cancer (suspicion). Chapter 2 details a first clinical study exploring the value of ultrasound strain elastography for predicting lymph node malignancy when a standardized measurement protocol is used in a single center. Chapter 3 describes the predictive value of strain elastography for lymph node malignancy in an international multi-center trial. Aside assessment of the predictive value of strain elastography alone, it further describes if strain elastography information can be added to clinical information such as FDG-PET and lymph node size to further increase the clinical value. In chapter 4, the predictive value of ultrasound B-mode features for lymph node malignancy is described. By collecting observer scorings on ultrasound features in multiple centers, the predictive value of reported ultrasound B-mode features are derived. The reproducibility of ultrasound B-mode feature scoring is furthermore given.

**Part II** - The second part of this thesis (chapters 5-7) elaborates on endobronchial diagnostics for early lung cancer staging, also termed navigation bronchoscopy. Chapter 5 describes the ability of a combination of navigation bronchoscopy technologies and imaging to accurately reach and diagnose peripheral lesions. Imaging is herein provided by cone beam CT systems, as often available in the interventional radiology suite and the hybrid operating theatre. Chapter 6 specifically describes the accuracy of the differently available navigation bronchoscopy tissue acquisition methodologies. The accuracy of individual cytology and histology sampling tools along with the value of rapid on-site evaluation of cytopathology in a cone beam CT guided navigation bronchoscopy setting is described. Chapter 7 describes the cone beam CT mediated navigation bronchoscopy in an extended series of consecutive patients and the forthcoming availability of a specific tailoring of imaging protocols to the navigation bronchoscopy procedure. By having monitored diagnostic accuracy and radiation exposure over time, from initialization of the procedure until having performed more than 200 procedures, the learning curve of different facets of the procedure are described.

In chapters 8 and 9, the work as described in chapters 2-7 of this thesis are summated and discussed. A future perspective with regards to the described research is given.







# CHAPTER 2

**Optimal endobronchial ultrasound strain  
elastography assessment strategy:  
an explorative study**

**Authors**

R.L.J. Verhoeven, C.L. de Korte, E.H.F.M. van der Heijden.

**Published in**

Respiration. 2018; 97(4): 337–347

## 2.1 Abstract

### Background

In lung cancer staging, mediastinal lymph nodes are currently aspirated using endobronchial ultrasound transbronchial needle aspiration (EBUS-TBNA) based on size and FDG-PET avidity. EBUS strain elastography (SE) is a new technique that may help predict the presence of malignancy. However, a standardized assessment strategy for EBUS-SE measurement is lacking.

### Objectives

The aim of this study was to determine the optimal assessment strategy for investigating the predictive value of EBUS-SE in mediastinal lymph nodes.

### Methods

Two qualitative visual analogue scale strain scores and two semiquantitative strain elastography measurements (a strain histogram and strain ratio) were acquired in 120 lymph nodes of 63 patients with (suspected) lung cancer. The dataset was randomized into an 80% training dataset to determine cut-off values. Performance was consecutively tested on the remaining 20%, and, the overall dataset.

### Results

The semiquantitative mean histogram scoring strategy with a cut-off value of 78 (range 0–255) showed the best and most reproducible performance in prediction of malignancy with 93% overall sensitivity, 75% specificity, 69% positive predictive value, 95% negative predictive value, and 82% accuracy. Combining the EBUS-SE mean histogram scoring outcome with PET-CT information increased the post-test probability of disease in relevant clinical scenarios, having a positive test likelihood ratio of 4.16 (95% CI 2.98–8.13) and a negative test likelihood ratio of 0.14 (95% CI 0.04–2.81) in suspicious lymph nodes based on FDG-PET or CT imaging.

### Conclusions

EBUS-SE can potentially help predict lymph node malignancy in patients with lung cancer. The best semiquantitative assessment method is the mean of the strain elastography histogram.

## 2.2 Introduction

Endobronchial ultrasound transbronchial needle aspiration (EBUS-TBNA) has evolved from a diagnostic procedure to a staging procedure, and is now recommended as the first line staging procedure in lung cancer [9,10]. For accurate and complete staging, it is imperative that the endoscopist performs a full and systematic evaluation of the entire mediastinum. The evaluation should start in the contralateral hilum and proceed to the ipsilateral hilum, and preferably combine endobronchial ultrasound (EBUS) evaluation with esophageal ultrasound evaluation using the EBUS scope (EUSb) [10]. The goal of EBUS has herein shifted from the confirmation of metastatic disease to proving the absence of metastatic disease. Besides the available CT and FDG-PET information, ultrasound characteristics are often used for selecting nodes to aspirate in daily clinical practice. A study by Fujiwara *et al.* (2010) introduced B-mode ultrasound characteristics round shape, distinct lymph node margins, heterogeneous echogenicity and presence of a central necrosis sign as independent predictive markers for malignancy [46]. Later however, Evison *et al.* (2015) showed that heterogeneous echogenicity was the only significant predictor of malignancy [47]. Several other studies also found discording results in using these ultrasound features [48–50], resulting in limited widespread diagnostic application of these echo characteristics [17].

Additional tools like ultrasound strain elastography have become available that may help predict the probability of malignancy in mediastinal lymph nodes. Ultrasound strain elastography visualizes relative tissue stiffness by measuring axial tissue deformation. In EBUS-TBNA specifically, the periodical motion of the heart and greater vessels cause tissue deformation. Monitoring this tissue deformation by means of ultrasound over time enables a derivation of relative tissue strain which is a marker of tissue stiffness. A region of tissue that is heavily deformed over time when compared to another region in the same image is derived to be relatively soft (and thus high in strain). A region that is barely deformed by this same deformation force is derived to be relatively stiff (and thus low in strain). In ultrasound strain elastography, the received signal intensities over time are correlated to one another for quantifying these deformations. As current ultrasound technology only allows accurate cross-correlation of signal intensity along the propagation direction of ultrasound itself, it should however be acknowledged that it is primarily an axial measurement of strain (for more information, also see supplemental material). Ultrasound strain elastography has already shown valuable in differentiating benign from malignant lesions in thyroid and breast, where an external force can be used and standardized [19,51–53]. Several pilot studies now report that endoscopic ultrasound strain elastography can also be used for differentiating malignant and benign lymph nodes in the mediastinum with high accuracy, with lesions low in strain being more likely malignant [54–61]. However, the optimal method for scoring the presentation of the strain elastography values in EBUS applications remains unclear [62]. Several qualitative and semi-quantitative techniques have been reported so far. For qualitative presentation of strain, visual analogue scale (VAS-) scoring techniques

can be used. This is done by converting calculated relative strain into a color gradient and superimposing it on the B-mode image. This strain color image is then used for scoring the lymph node region of interest upon its major color component [55,58,59,63] or pattern-color combination [19]. Another frequently reported method is the semi-quantitative strain ratio measurement [58,60,64]. This technique requires that the operator manually selects the lymph node region and a secondary surrounding tissue region. By doing so, a ratio of strain can be calculated [58,60,64,65]. A third less frequently used method is the semi-quantitative strain histogram scoring method. This method quantifies the relative strain found in a manually selected lymph node area, and presents this as a histogram of strain counts [66].

Ideally, every assessment is operator independent, swift and safe. Yet in EBUS several factors will influence measurement results as a consequence of the technological principles used in strain elastography (also see supplemental material). For example, the position of the target node in relation to the source of compression and the tip of the EBUS scope affects the measured axial strain in EBUS strain elastography (EBUS-SE).

In this explorative study, we aim to determine the optimal EBUS-SE scoring and assessment strategy in patients with suspected or proven lung cancer. This is done by comparing the performance of predicting mediastinal lymph node malignancy among different scoring methods. We hypothesize that the strain histogram method will give the best overall predictive accuracy for diagnosing the lymph node malignancy since this will be the most operator independent and thus objective technique. We furthermore hypothesize that EBUS-SE will increase predictive value of mediastinal lymph node ultrasound imaging. To do so, we aim to explore what the clinical effect of adding EBUS-SE is on the probability of malignancy in combination with FDG-PET and CT imaging.

## **2.3 Materials and methods**

### **2.3.1 Study subjects**

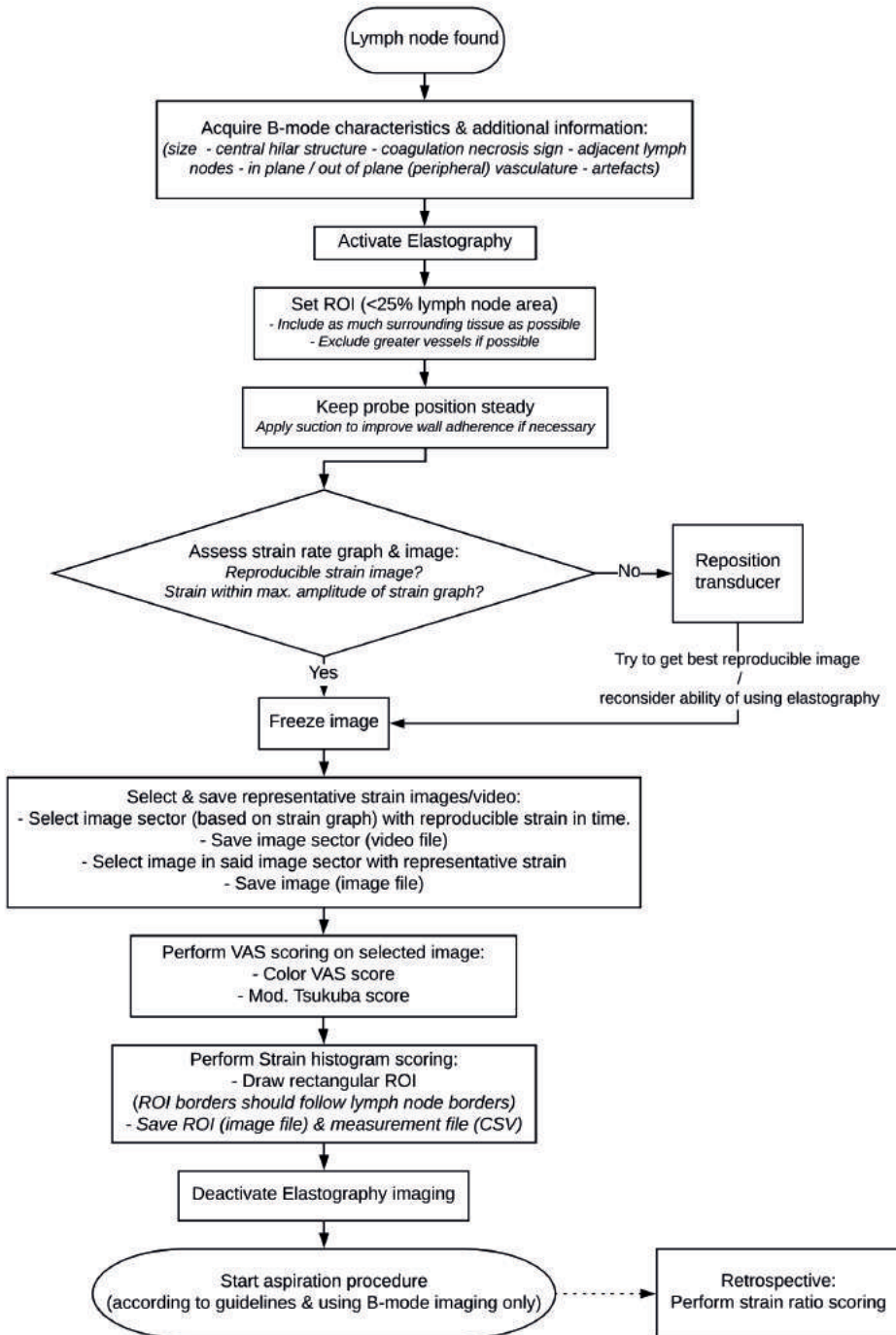
All patients in the Radboud University Medical Center (Nijmegen, The Netherlands) who had an indication for a diagnostic or staging EBUS-TBNA procedure for suspicion of lung cancer were eligible and included. This study was conducted with approval of independent ethics committee as part of the E-predict multi-center study (NCT02488928) and all included patients gave informed consent. The inclusion period ranged from July 2015 to April 2016. All subjects had no history of prior radio- or chemotherapy and no general EBUS-TBNA contra-indications.

### 2.3.2 Study design

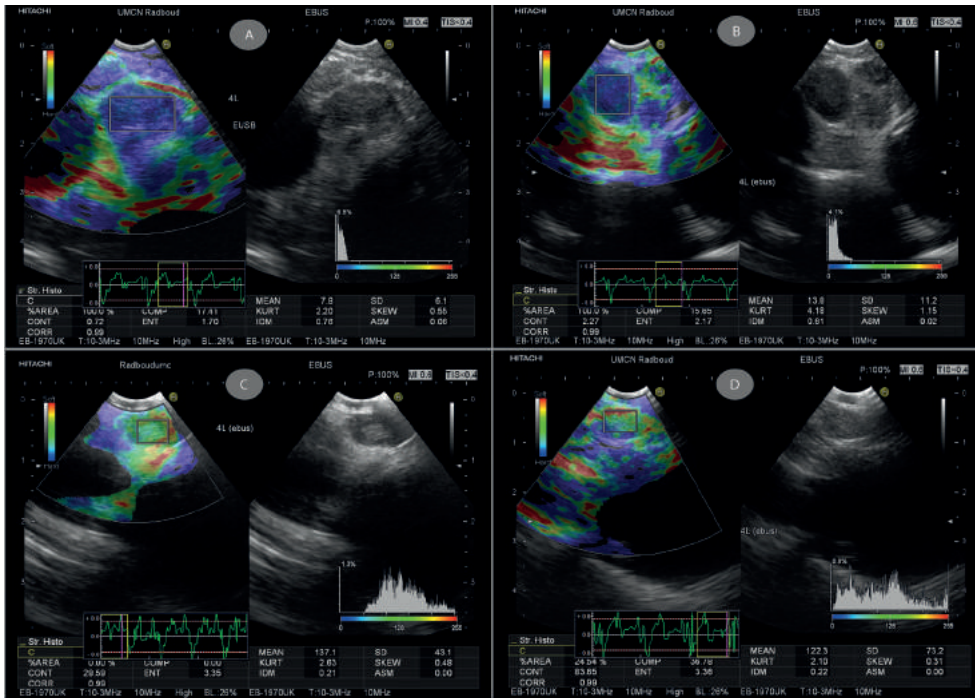
The EBUS-TBNA procedures were performed according to local and international guidelines [6,10]. Measurements were acquired using the Hitachi Preirus Hi Vision processor (Hitachi corporation, Tokyo, Japan) with Hitachi Real Time Elastography software in combination with Pentax EB-1970UK echo-endoscopes (Pentax Medical, Tokyo, Japan). The recommended diagnostic work-up of our hospital was used; all nodes with short-axis size >10 mm on CT, ultrasound based short axis size >5 mm or FDG-PET avid nodes in at least regions 4L, 4R and 7 were routinely aspirated. FDG-PET scans were obtained and evaluated by the radiologist following the European Association of Nuclear Medicine guidelines [67]. While Standard Uptake Values of individual lymph nodes were not routinely reported, a cut-off of 2.5 was typically used. EBUS strain elastography measurement collection and assessment was performed using a standardized operating protocol (see supplemental data & Figure 2.1.). In brief, real-time dual ultrasound B-mode and elastography imaging were used for data collection of both B-mode lymph node ultrasound characteristics (size, shape, margin, echogenicity, central hilar structure presence and coagulation necrosis sign [46]) and quantitative and qualitative EBUS-SE measurements. After these measurements, routine EBUS-TBNA sampling was performed under guidance of B-mode ultrasound alone. Cytology and consecutive histology (if available) of the EBUS-TBNA specimen combined with clinical follow-up were used as the gold standard for determining individual lymph node diagnosis.

### 2.3.3 EBUS Strain Elastography evaluation techniques

**Qualitative evaluation** - For visual scoring of strain, two visual analog scale scoring methods based upon earlier reports were used [55,58,63]. The first VAS system requires the operator to classify the image into one of five groups based upon the major color component. From low to high strain respectively, these scores correspond to; 1: predominantly blue, 2: blue and green, 3: predominantly green, 4: green and red, 5: predominantly red (see Figure 2.2). The second qualitative VAS scoring method used a modified version of the Tsukuba score, a scoring system based on a combination of the visualized color and the pattern of the strain image. This scoring method has shown to be promising in classification of breast lesions [19]. Scoring was however slightly altered by the authors to accommodate for the differences in breast US and EBUS imaging. The operator grades the lymph node EBUS-SE image following a six-category classification system (Figure 2.3).


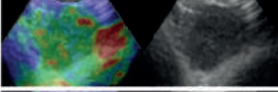

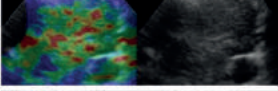

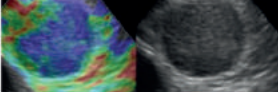

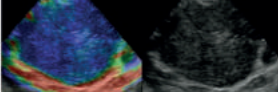

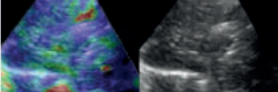

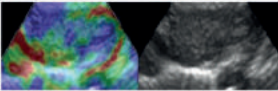


**Figure 2.1** – Summarized measurement acquisition protocol for obtaining reproducible strain elastography measurements. Abbreviations: Image sector – a set of subsequent imaging frames as automatically selected by the Hitachi Strain Elastography software upon freezing the ultrasound image; ROI – Region of Interest; VAS – Visual Analogue Scale.



**Figure 2.2** – Typical examples of EBUS strain elastography imaging of 4L lymph nodes as captured by Hitachi – Real Time Strain Elastography software on the Preirus Hi Vision processor (Hitachi Corporation, Tokyo, Japan) in combination with Pentax EB-1970UK endoscope (Pentax medical, Tokyo, Japan). In each panel on the left, conventional B-mode image with strain map overlay in color; the yellow box is the manually set region of interest (ROI) selection for calculation of the strain histogram mean. The different colors correspond to measured relative strain. Red corresponds to high deformation, green to intermediate measured deformation and blue to relatively low deformation. On the right side of each panel, the B-mode image can be seen and used as reference. On the bottom left of each panel a strain rate graph is shown, to be used for quality control and frame selection of elastography measurements. On the bottom right of each panel the strain histogram as calculated based on the selected ROI is shown. Finally, the strain histogram parameters are presented in the table on the bottom of each panel. Panel A – D: all depict 4L lymph nodes, Panel A: EUSb approach, Panels B-D: EBUS approach. Panels A and B: malignant nodes. Panel C and D: benign nodes.

**Semi-Quantitative EBUS-SE evaluation** - For semi-quantitative scoring of EBUS-SE, two measurement methods are evaluated (see data supplement). The first measurement method is the mean strain elastography histogram. This requires a (rectangular) hand-selection of a lymph node region of interest. After selection, strain values are computed from the selected area and relayed back to the operator through a histogram of strain counts (see Figure 2.2). The second semi-quantitative scoring method is the strain ratio. Herein, the lymph node region of interest as selected during the strain histogram method are compared against a hand-selected surrounding reference tissue area using the Matlab Image Processing Toolbox (version 9.1.0, MathWorks, Inc., Natick, MA, USA, see Figure 2.4). As opposed to the other methods, the strain ratio was measured after completion of the EBUS-procedure by one operator (RLJV) blinded for patient details and pathology outcome.

Schematic illustration	Typical image	Classification standard	Score
		Strain is seen in the entire hypoechoic area (the entire lesion is shown in green similar to the surrounding tissue).	1
		Strain is seen within most of the hypoechoic area but some areas show no strain (the lesion is a mixture of red, green and blue).	2
		Strain appears only in the periphery, no strain in the center of the lesion (center of the lesion is blue, the periphery is green).	3
		No strain is measured within the lesion (the entire lesion is shown in blue).	4
		No strain is measured within the lesion nor in the surrounding tissues (the lesion and the surrounding tissues are blue).	5
		Typical artefact seen when blood vessels invade the lymph node. Red in the center of the vessel surrounding, green in the vicinity.	X

**Figure 2.3** – Modified Tsukuba score classification system used for visual analog scale scoring of lymph node EBUS SE, adapted from Itoh *et al.* (2006). The depicted typical images are all EBUS-SE lymph nodes images. The original Tsukuba score system as introduced for breast imaging was adjusted to accommodate for differences in endobronchial and breast imaging, where the scoring system was originally designed for [19].

### 2.3.4 Statistics

The performance of the different EBUS strain elastography scoring techniques was evaluated by a-priori randomizing the final dataset into an 80% training dataset for determining scoring method cut-off values and using the remaining 20% of data to test the scoring method performance on unseen data. To evaluate the performance of the models, sensitivity, specificity, negative predictive value (NPV), positive predictive value (PPV), accuracy, negative and positive likelihood ratios and post-test probability of malignancies (using the likelihood ratios) with their respective 95% confidence intervals (CI) are calculated among the separate and combined datasets. Area under the curve (AUC) is calculated for continuous variables.

To exploratively correlate strain elastography imaging to outcome, pathology results were classified as malignant or benign. Patients diagnosed with granulomatous disease or patients of which measurement data was incomplete were excluded from the final dataset before randomization and analysis (Figure 2.5). The statistical computing language R and interface R-studio (version 1.1.414) were used for statistical analysis [68].

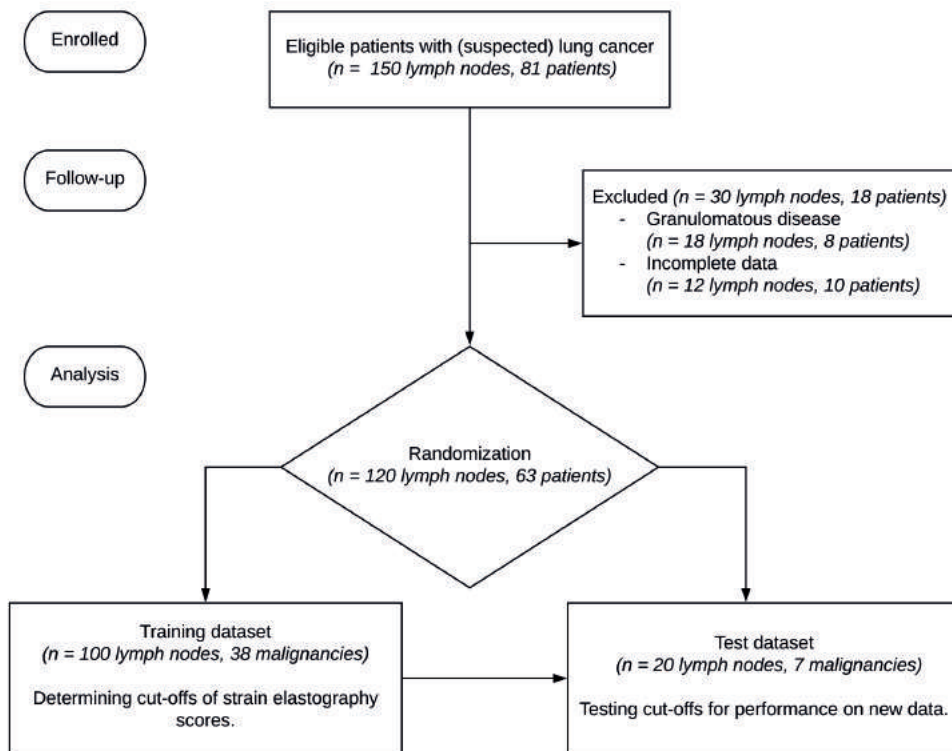




**Figure 2.4** – Visualization of user interface as programmed with Matlab for post procedure strain ratio extraction (version 9.1.0., Mathworks, Inc., Natick, MA, USA). The original prospectively selected rectangular region of interest for calculating the strain histogram was automatically segmented and used to compare a retrospectively selected ellipsoid reference tissue region of interest. An input dialogue was additionally used for qualitative rating of the ability to select an adequate ellipsoid reference tissue region of interest.

## 2.4 Results

In total, 150 lymph node strain elastography measurements were obtained in 81 patients. After exclusion of other pathologies and incomplete measurements, 120 lymph nodes in 63 unique patients remained (Figure 2.5). A total of 45 lymph nodes herein proved to be malignant based on EBUS-TBNA alone (43 lymph nodes, 28 patients) or by surgical follow-up of false negative benign EBUS-TBNA cytology findings (2 lymph nodes, 2 patients). For the N=75 lymph nodes (42 unique patients) eventually classified as benign, follow-up data was available in 61 nodes (81%). Surgical proof of benign EBUS-TBNA findings was available in 41 lymph nodes (55%) by either resection (15 nodes, 9 patients) or mediastinoscopy (26 nodes, 13 patients). Long-term clinical follow-up was available in 20 lymph nodes (27%, 12 patients) with a median follow up time of 23 months (min. 3 – max. 34). No follow-up of benign EBUS-TBNA findings was available in 14 lymph nodes (19%, 9 patients) due to rapid disease progression (6 nodes, 5 patients) and loss to follow-up (8 nodes, 4 patients).



**Figure 2.5** – CONSORT flow diagram of the study design.

The general patient demographics and lymph node details are summarized in Table 2.1. The lymph nodes were randomized into the training and test dataset (Figure 2.5). The a-priori defined training dataset included 100 randomly selected lymph nodes. The remaining testing dataset consisted of 20 lymph nodes. Prevalence of malignancy or pre-test probability of malignant disease in both datasets was approximately equal at 0.38 and 0.35, respectively. The results of general B-mode ultrasound feature classification are presented in the data supplement (Table 2E.1). In the final dataset, 79 of 120 lymph nodes (66%) were classified as FDG-PET positive. No PET-scan was available in 3 patients (3 lymph nodes), and no contrast-CT was available in 1 patient (1 lymph node).

**Table 2.1** – On the left, overall patient demographics and lymph node characterization. Lymph node size is given as mean (min – max) in mm. On the right, measured lymph nodes per region as counts (N) and as distribution of counts of malignant (mal) to benign (ben) findings. Abbreviations used: SA: short axis, NA: not available, NSCLC: non small cell lung cancer, SqCC: squamous cell carcinoma, NOS: not otherwise specified, LCNEC: large cell neuroendocrine carcinoma, EB: endobronchial, EUSb: Esophageal using EBUS scope, LMB: Left Main Bronchus, RMB: Right Main Bronchus, mal: malignant, ben: benign

Patient Demographics		Measured Lymph nodes		
Study subjects	63	<i>Region</i>	<i>N (mal/ben)</i>	<i>% total</i>
Mean age	64.3 yr (range 41-83 yr)	2L	1 (1/0)	0.8%
Sex	39 Male (61%) / 24 Female (39%)	2R	2 (2/0)	1.6%
<b>Aspirated lymph node characteristics</b>		4L (EB)	23 (11/12)	19.2%
CT size (SA)	11.95 mm (2-41 mm)	4L (EUSb)	7 (4/3)	5.8%
FDG-PET avidity	79 FDG+ / 38 FDG- / 3 NA	4R	25 (7/18)	20.8%
US size (SA)	9.95 mm (4-26 mm)	7 (LMB)	3 (0/3)	2.5%
<b>Lymph node pathology outcome</b>		7 (RMB)	23 (4/19)	19.2%
Normal	75 (62.5%)	7 (EUSb)	10 (5/5)	8.3%
Malignant	45 (37.5%)	10L	0 (0/0)	0%
NSCLC Adenocarcinoma	19 (15.8%)	10R	2 (1/1)	1.6%
NSCLC SqCC	15 (12.5%)	11L	10 (3/7)	8.3%
NSCLC NOS	1 (0.8%)	11R	14 (7/7)	11.7%
Small Cell Lung Carcinoma	5 (4.2%)			
LCNEC	3 (2.5%)			
Invasive ductal carcinoma	2 (1.6%)			

### 2.4.1 EBUS-SE scoring method assessment cut-off values

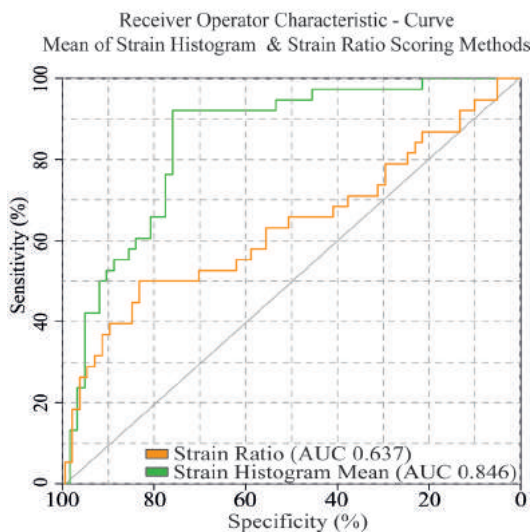
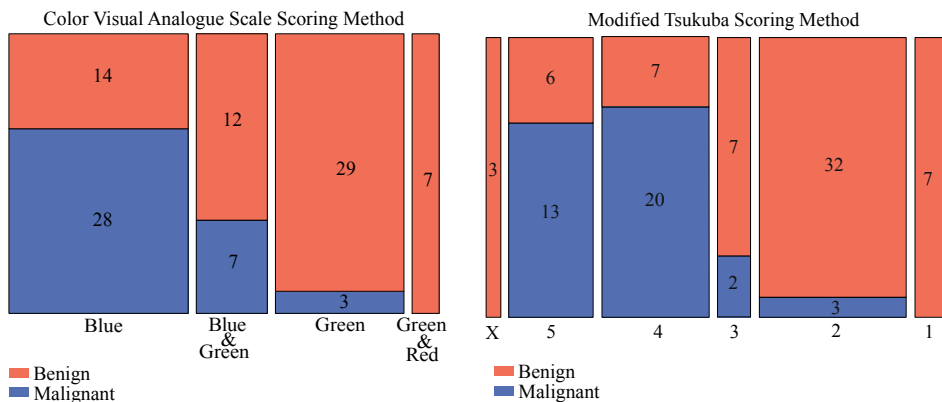
Cut-off values of all four strain elastography scoring methods were first optimized by analyzing performance on the training dataset using accuracy, AUC (in the cases of strain histogram and strain ratio scoring) and individual predictive values sensitivity, specificity, NPV and PPV. For the color VAS scoring system, optimal predictive performance was found if lymph nodes categorized as ‘predominantly blue’ or ‘blue and green’ were grouped together (predicting malignancy) versus all other categories grouped (predicting benign outcome, Figure 2.6). The modified Tsukuba scoring method performed best when placing the cut-off at the two lowest of five scores (Figure 2.6), grouping score 4-5 as malignant and score 1-3 as benign. For the semi-quantitative measurements, the ROC curve analysis of the strain histogram method (AUC 0.846, Figure 2.6) showed a relative mean strain value of <78 (range 0-255, with a lower value representing less strain) to be most predictive of malignancy. The strain ratio was most predictive of malignancy when the mean of the lymph node strain divided by the reference tissue strain was more than 1.67 (AUC 0.637, Figure 2.6). During retrospective strain scoring (also see Figure 2.4), R.L.J.V. furthermore scored the selection of reference tissue upon adequacy when taking into account technical and clinical boundary conditions. Selecting adequate reference tissue was reported qualitatively as being difficult

in 50% of cases. Reported causes were diverse, such as a lack of homogeneous reference tissue, depth dependency artefacts, or, too small regions of interest for obtaining a single adequate secondary measurement.

### **2.4.2 EBUS-SE predictive value**

With above described cut-off values, the different predictive values as introduced in the Methods section were calculated on both datasets. The results are summarized in Table 2.2, calculation of likelihood ratios are furthermore presented in Supplemental Table 2E.2. The prospectively collected Color VAS scoring, Modified Tsukuba scoring and Strain histogram scoring had similar accuracies in the training dataset of 76%, 82% and 82%, respectively. The most notable difference in individual performance factors among these methods were found in sensitivity and NPV. Sensitivity and NPV are upwards of 76% in all three methods. Less false negatives were however found in the strain histogram method, having a sensitivity of 92% and NPV of 94% (being 3-16% higher than the other two methods). Consequently, it also had the lowest negative post-test probability of malignancy (0.06). Following the specificity and PPV, positive post-test probability of malignancy seems to be similar in the three methods at around 0.70. While performance among the three prospective methods seems comparable, the strain ratio most markedly has lower sensitivity (50%) and NPV (73%) in the training dataset, which is further reflected by the lower accuracy (71%).

When the cut-offs of the four scoring methods are consecutively used to analyze performance on the testing dataset, the accuracies remain within the earlier determined 95% CI of the training dataset (Table 2.2). However, the positive and negative post-test probability of malignancy as based on the likelihood ratios (Table 2E.2) do show differences. All collected methods except strain ratio showed no false-negatives in the test dataset. Consequently, both the Color VAS score and Modified Tsukuba score performed better than the 95% CI as deterred from the training dataset. Furthermore, we would expect a higher than 0.58 positive post-test probability of malignancy of the Modified Tsukuba scoring method based on training dataset results (0.61-0.82 95% CI).



**Figure 2.6** – Results of EBUS Strain elastography scoring through multiple methods.

Top: Distribution of malignancies and normal lymph nodes along the qualitative Color VAS scoring method (top left) and the modified Tsukuba scoring method (top right) in the training dataset. The width of column corresponds to amount of measurements as proportion of total (training dataset, n = 100). The count of measurements are superimposed on the columns of every score. Both VAS scores show a sharp decline in malignancy prevalence if the scoring does not involve a majority of lymph node tissue being blue (Color VAS score Blue & Blue and green, mod. Tsukuba score 4 & 5). It furthermore stands out that the score X in the modified Tsukuba method was used in five artefactual cases of measurements, whereas this was not possible in the color VAS score nor semi-quantitative strain ratio and histogram scoring, and lymph nodes as such will have been rated otherwise.

Bottom: Receiver Operator Characteristic curve of strain ratio and mean of strain histogram, based on the training dataset. Area under the curve of the strain histogram mean is 0.846. Area under the curve of the strain ratio is 0.637. The top most left of both ROC's correspond to cut-off values of <78 and >1.67 for the strain histogram mean and strain ratio to predict malignancy, respectively. In these cases, the strain histogram mean has 92% sensitivity and 76% specificity while the strain ratio has 84% specificity and 50% sensitivity.

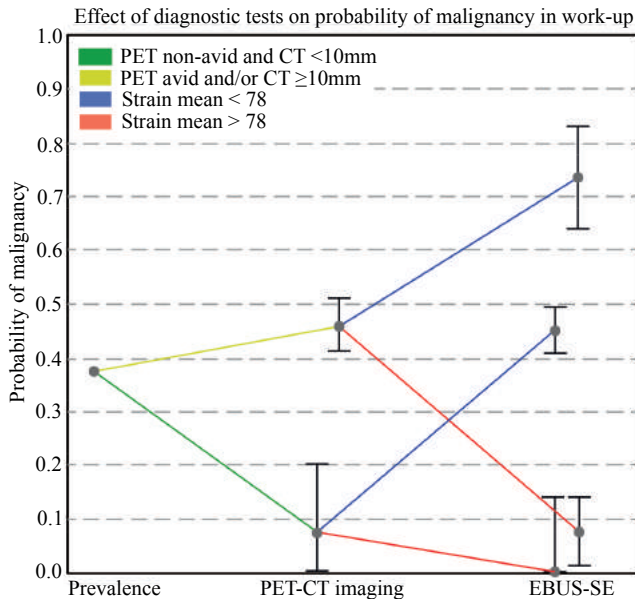
**Table 2.2** – Summary of main EBUS Strain Elastography scoring method performance results. Scoring method performance was obtained by randomly partitioning the total dataset into a training (80%) and test dataset (20%). The cut-off scores of the scoring methods are first determined by optimization of performance on the training dataset. Transferability of performance using these scores is subsequently assessed in the test dataset. The post-test probabilities of malignancy are determined by the pre-test probability of malignancy and the likelihood ratios as defined in Supplemental Table 2E.2. \* Denotes significant differences between training and test dataset, being outside the 95% CI as determined in the training dataset. Abbreviations used: Sens: sensitivity, Spec: specificity, PPV: positive predictive value, NPV: negative predictive value, VAS: visual analog scale.

<b>EBUS Strain Elastography scoring method</b>	<b>Sens</b>	<b>Spec</b>	<b>PPV</b>	<b>NPV</b>	<b>Accuracy (95% CI)</b>	<b>Positive post-test probability of malignancy (95% CI)</b>	<b>Negative post-test probability of malignancy (95% CI)</b>
<b>Training dataset (100 lymph nodes, 38 malignancies – pre-test probability of malignancy 0.38)</b>							
Color VAS score	76%	77%	67%	84%	77% (68-85%)	0.67 (0.56 – 0.78)	0.16 (0.08 – 0.23)
Modified Tsukuba score	87%	79%	72%	91%	82% (73-89%)	0.72 (0.61 – 0.82)	0.09 (0.03 – 0.16)
Strain histogram mean	92%	76%	70%	94%	82% (73-89%)	0.70 (0.61 – 0.80)	0.06 (0.00 – 0.13)
Strain ratio	50%	84%	65%	73%	71% (61-80%)	0.66 (0.50 – 0.80)	0.27 (0.20 – 0.33)
<b>Test dataset (20 lymph nodes, 7 malignancies – pre-test probability of malignancy 0.35)</b>							
Color VAS score	100%	69%	64%	100%	80%	0.64	0.00*
Modified Tsukuba score	100%	62%	58%	100%	75%	0.58*	0.00*
Strain histogram mean	100%	69%	64%	100%	80%	0.64	0.00
Strain ratio	29%	85%	50%	69%	65%	0.5	0.31
<b>Overall dataset (120 lymph nodes, 45 malignancies – pre-test probability of malignancy 0.375)</b>							
Color VAS score	80%	76%	67%	86%	78%	0.67	0.14
Modified Tsukuba score	89%	76%	69%	92%	81%	0.69	0.08
Strain histogram mean	93%	75%	69%	95%	82%	0.69	0.05
Strain ratio	47%	84%	64%	72%	70%	0.64	0.28

When combining performances of both the training and test dataset, the mean of the strain histogram shows to best predict lymph node malignancy. It has lowest negative post-test probability of malignancy while accuracy is similar to the best of methods. The mean of the strain histogram furthermore shows similar performance when testing on new and unseen data.

### **2.4.3 Effect of EBUS-SE on probability of malignancy assessment**

Based on the analysis of the different EBUS-SE scoring methods, the strain elastography histogram mean scoring method is used to further investigate if EBUS-SE could be of potential added value in clinical workup. This is investigated by calculating the effect on the probability of malignancy when combined with PET-CT imaging information of both the abnormal and normal mediastinal lymph nodes in the overall dataset (see Figure 2.7 & Supplemental Tables 2E.2-3). Based on available combined PET avidity and/or CT size  $\geq 10$  mm, a group of normal (N=26) and suspicious (N=90) mediastinal lymph nodes were identified in our complete dataset. In these groups, probability of malignancy was 8% and 46%, respectively. Explorative analyses shows addition of EBUS-SE histogram scoring in the subgroup of suspicious lymph nodes increases post-test probability of malignancy from 46% to 73% (positive likelihood ratio 4.61, 95% CI 2.98-8.13). Oppositely, a negative EBUS-SE histogram analysis in this group of suspicious nodes reduces the post-test probability of malignancy from 46% to 8% (negative likelihood ratio 0.143, 95% CI 0.04-2.81, Figure 2.7 & Supplemental Table 2E.3). In the subgroup of imaging normal lymph nodes, a mean EBUS SE histogram  $<78$  increased the probability of malignancy from 8% to 45%. And if EBUS-SE outcome indicated non-malignancy in the PET/CT negative lymph nodes, probability of malignancy dropped from 8% to 0%, negating two cases where PET-CT imaging was found false negative (Figure 2.7, Supplemental Table 2E.3).



**Figure 2.7** – Graphical representation of added value of performing cumulative diagnostic tests in our complete dataset. The first point on the left at 0.375 corresponds to prevalence of malignancy in our complete dataset (116 lymph nodes). PET and/or CT imaging is able to increase probability of malignancy to 46% if found positive. Negative PET and CT imaging is able to decrease probability of malignancy from 37.5% to 7.8%. After having performed PET-CT imaging, EBUS-SE imaging is performed. In PET-CT suspected nodes (N=90), probability of malignancy increases from 46% to 73% if EBUS-SE imaging is positive. If EBUS-SE imaging is negative in these suspected nodes, the probability of malignancy decreases to 7.9%. In normal lymph node findings based on PET-CT imaging (N=26), probability of malignancy decreases from 7.8% to 0% if negative on EBUS-SE imaging (>78 strain histogram mean). If these lymph nodes are however EBUS-SE imaging positive (<78 strain histogram mean), probability of malignancy increases from 7.9% to 45%.

## 2.5 Discussion

EBUS-SE could potentially be a sensitive technique to help predict lymph node malignancy in patients with lung cancer. We found that the semi-quantitative mean histogram scoring method with a cut-off value of 78 (range 0-255) showed the best, most objective and most reproducible performance in prediction of malignancy with 93% overall sensitivity, 75% specificity, 69% positive predictive value, 95% negative predictive value, and 82% accuracy. Exploratively combining lymph node relative stiffness by using the EBUS-SE histogram mean scoring outcome with CT and / or PET-CT information further increased confidence in post-test probability of disease, having a positive test likelihood ratio of 4.16 (2.98-8.13 95% CI) and a negative test likelihood ratio of 0.14 (0.04-2.81 95% CI) in imaging suspicious lymph nodes. EBUS-SE scoring may thus enable a better prediction and separation of lymph nodes with high and low probability of disease but will not replace a tissue diagnosis. It can however be a helpful tool for guiding which node to aspirate in a distinct region, or ultimately, deciding



whether to proceed with, or omit, additional diagnostic procedures if ROSE or conclusive cytology results are unavailable (especially when FDG-PET information is lacking). Yet, care needs to be taken in interpreting these results. This explorative study is of limited size and further research to corroborate our findings using a standardized assessment procedure based on clinical findings and technological considerations is recommended.

### **2.5.1 Differences in EBUS-SE Scoring methods**

In the qualitative scoring, both the scoring of a major color component (Color VAS method) and a combined scoring of pattern and color (modified Tsukuba score) perform similar in terms of overall accuracy. Our proposed use of the modified Tsukuba scoring system has not previously been introduced in EBUS applications. Even though we expected that taking into account both pattern and color above color alone would provide more information, it does not seem to be of clear additional value over the color VAS system in this dataset.

Three studies used a scoring system like the color VAS scoring system, with comparable results [55,59,63]. He *et al.* reported best accuracy if the visualized color was over 50% blue, then indicative of malignancy with an accuracy of 73.7%. Huang *et al.* (2017) and Izumo *et al.* (2014) introduced an additional cut-off; only predominantly blue lesions were indicative of malignancy, while predominantly non-blue lesions were indicative of benign lymph nodes. By leaving out an intermediary group (part-blue, part non-blue) they were able to report an overall accuracy in these categories of 91.4% and 96.7%, respectively. Leaving out uncertain cases (part blue, part non-blue) was not done in our study for accurate comparison of scoring methods (but see Figure 2.6). Possibly, such a method could increase diagnostic success.

In semi-quantitative scoring, the majority of previous pilot studies report using the strain ratio for scoring [58,60,64]. Our study however clearly shows that the mean value of the strain as obtained from the histogram has best performance. As reflected by the comparatively low performance of the strain ratio scoring method, we found that the strain ratio outcome relied heavily on the selected secondary reference tissue region in EBUS. Adequate selection of a uniform secondary reference tissue while taking into account the technical and clinical boundary conditions is difficult not only because of limited tissue uniformity but also heterogeneous sources of strain. Likely, this is one of the reasons why other pilot studies investigating EBUS-SE with strain ratios reported different cut-off values [69] and collected multiple measurements for combining them into one average reference value [58,60,64]. A potential limitation of our study is that we collected strain ratio measurements retrospectively rather than prospectively, which could have affected the strain ratio scoring outcome.

### **2.5.2 Combining EBUS-SE with other predictive variables**

FDG-PET and/or CT imaging of lymph nodes in this study had sensitivities comparable to the reported literature [9], but a lower combined specificity of 33% (Table E2.3). This could in

part be explained by the systematic staging of all lymph nodes by EBUS-TBNA as applied in our clinical practice. Combining EBUS-SE with pre-test contrast CT and FDG-PET avidity however was able to improve the predictive accuracy of lymph node pathology in both PET-CT negative and positive imaging cases. The relative stiffness as measured by EBUS-SE thus seems to show additional value to the metabolic and size information as given by FDG-PET and CT. Yet again, care needs to be taken in interpreting the results of adding EBUS-SE information to PET and CT negative nodes, as only 26 lymph nodes of which 2 false negative lymph nodes were available for an exploratory analysis. While adding EBUS-SE correctly changed diagnosis to malignant in both cases and could be promising, additional studies are warranted.

Besides PET-CT information, ultrasound B-mode characteristics as described by Fujiwara *et al.* (2010) [46] were also collected in this explorative study (Supplemental Table 2E.1). Since different studies have shown conflicting results in the value of these features, we did not integrate these into a combined predictive value nor integrate them with EBUS-SE findings [46–50]. Analysis of these features in our dataset showed presence of heterogeneous echogenicity and a central necrosis sign to be most predictive of malignancy, with positive likelihood ratios of 5.83 and 3.65. An AUC of 0.73 of the B-mode based size of lymph nodes revealed a correlation between size and malignancy.

### **2.5.3 General remarks**

The mean lymph node short axis diameter in this study was 9.9 mm (range 4-26 mm). This indicates it was not a population with bulky mediastinal disease but rather a group with low disease burden. Malignant lymph node involvement can be heterogeneous and microscopic. This is cause for concern in both TBNA and strain elastography of individual lymph nodes. TBNA provides only limited information about the complete node, as it samples limited amounts of tissue within the node. Strain elastography can provide information about the entire node, but is based only on the strain of tissue upon deformation. Whether elastography is able to differentiate between micro-metastatic disease accurately and if it may guide the site of aspiration within a lymph node to detect intranodal fields at risk of micro-metastatic disease is unclear. The current dataset does not allow this level of analysis.

### **2.5.4 Observer scoring variability**

A general point of concern for all EBUS-SE measurement methods is the inter- and intra-observer variability in lymph node scoring and frame selection through different platforms. System settings and operator protocol can affect EBUS-SE measurement outcome (also Supplemental data). A standardized operating procedure is essential. In this current study, the prospective elastography measurements and scoring were done by one pulmonologist using a standardized operating protocol (EvdH). Inter-observer variability was thus minimal in order to adequately study differences in scoring method performance. Reproducibility of this technique based upon operator expertise, operator color acuity, anatomical site and

region needs to be further investigated. Widespread implementation of this technique can only be realized when system settings and operator methods are unified. Transferability of these findings to other diseases like for example sarcoidosis are unknown and also need to be studied. In doing so, we recommend to use the mean of the strain histogram for scoring as it showed to have best performance in this study, requires the least operator input and will have highest inter-observer agreement based upon technique background.

## 2.6 Conclusion

EBUS-SE is a sensitive technique which may help predict lymph node malignancy in patients with lung cancer. In this study we found that the semi-quantitative mean histogram scoring method with a cut-off value of 78 (range 0-255) showed the best and most reproducible performance in prediction of malignancy with 93% overall sensitivity, 75% specificity, 69% positive predictive value, 95% negative predictive value, and 82% accuracy. Combining EBUS-SE mean histogram scoring outcome with CT and/or PET-CT information increased confidence on post-test probability of disease, having a positive test likelihood ratio of 4.16 (2.98-8.13 95% CI) and a negative test likelihood ratio of 0.14 (0.04-2.81 95% CI) in suspicious lymph nodes based on PET or CT imaging. We further present a standard operating procedure for EBUS-SE assessment and future research.

## 2.7 Statement of ethics

The research was conducted ethically in accordance with the latest World Medical Association Declaration of Helsinki. The study protocol was approved by the independent local medical ethical committee and institutional review body before start of subject inclusion. Informed consent was obtained. The study is registered and can be found on ClinicalTrials.gov (identifier: NCT02488928).

## 2.8 Acknowledgements

We would like to thank Olga Schuurbijs M.D. PhD. and Wouter Hoefsloot M.D. PhD. for their contributions and comments. We would furthermore like to thank Priya Vart, PhD, assistant professor biostatistics, for his advice on statistical analysis.

## 2.9 Supplemental data

### 2.9.1 Technical introduction

Endobronchial ultrasound strain elastography is an ultrasound technique giving information on soft tissue by deriving elastic properties in real time. As Ying *et al.* and others state in their studies, the elastic modulus of lymph nodules were found to be correlating with tumour malignancy and could be measured by means of strain elastography [18,70,71]. Several pilot reports on use of these commercial techniques in EBUS have shown promising results [55,58–61,72–74]. To be able to reconstruct a strain image, backscattered signals of the tissue at a first acquisition (pre-compression) are compared to a second acquisition (post-compression). The time shift between the tissue reflections is then found by a cross-correlation method. Since the speed of sound is considered to be constant, this time delay estimate can be transformed into a tissue displacement. When the displacement at every depth is known, a finite difference of these displacement estimates can be used to determine the relative deformation along the imaging line, also known as axial strain [22]. Due to technical limitations of ultrasound systems, real-time strain is hard to determine in the lateral scanning direction [23]. Strain elastography is thus described as being an axial deformation and strain measurement only, different in origin than that of other reported B-mode US features [46]. All major ultrasound manufacturers such as Hitachi, Philips, Siemens Toshiba and General Electric have now commercialized strain elastography [75–77]. Although these manufacturers differ in detailed approach, the basics are similar. In this supplement, additional considerations for using ultrasound elastography as clinical diagnostic tool in EBUS are given together with complementary (clinical) information to the article.

### 2.9.2 Materials and methods

For acquisition of images and performing measurements in this explorative study (Figure 2.1, the Hitachi Preirus Hi Vision processor (Hitachi Corporation, Tokyo, Japan) with Hitachi Real Time Elastography (version EZU-TE5) and strain histogram software (version EZU-TESH1) installed were used in combination with Pentax medical - Ultrasound Video Bronchoscopes EB-1970UK (Pentax Medical, Tokyo, Japan).

#### **Technical limitations in EBUS-SE & potential sources of artefacts**

The stress that is applied to create a deformation in EBUS strain elastography was derived to be originating from the patient's own pulsating heart and vasculature, as manual palpation by means of the EBUS endoscope is impossible. The amount and direction of force of these deformation sources are unknown, as they are both patient and location dependent. Given the lymph nodal map [11], it is however derived that axial strain imaging is possible by using the pulsating vasculature found distal to the EBUS transducer, with the lymph node in between source and transducer. The scoring of strain elastography is stated to be relative, since the force applied to obtain strain is unknown. The software of the different commercial systems therefore normalize the strain in every image for both visualization and calculation.

This means the axial strain is semi-quantitative and will cover the entire visualized/calculated elasticity spectrum. By doing so, it relays how much strain is measured inside the region of interest when compared to surrounding tissue. When performing in-vivo imaging of mediastinal lymph nodes, several potential pitfalls and artefacts that are a consequence of the technical background of strain elastography imaging were found and are summarized below (also see [22,24,78,79]).

**Anatomical structures** - In EBUS strain elastography we ought to use the distal pulsating vasculature as source of stress only. One should assess if the lymph node itself is also invaded by vasculature, cysts, lymphatic structures or necrosis by using B-mode and Doppler. These structures add additional sources of strain or alternatively, are easily deformed and affect axial strain imaging accuracy [80]. If several structures in or out of plane are found, the possibility of using strain elastography should be reconsidered.

**Amount of (axial) deformation** - The amount of tissue deformation and movement influences the quality of the strain measurement. Some cases of highly enlarged pathological lymph nodes act as additional spring load and prevent sufficient deformation for quantification by the ultrasound system. This is recognizable by a generalized lack of strain rate graph amplitude (low strain). Alternatively, too much tissue displacement (>5%) [81,82] or non-axial displacement disables the underlying algorithm to correlate deformation in subsequent images. Inaccurate findings can be recognized by a non-periodical and chaotic strain image and strain rate graph with high amplitude and/or a temporally incoherent visualized strain (for a strain rate graph example, also see the lower left of each panel in Figure 2.2). In this explorative study a variety of cases where pulsatile forces caused overall tissue movement were found. Patient or transducer movement also caused measurements to be aborted in several cases if applying suction or relocating the transducer did not improve imaging.

**Energy absorption** - As a resultant of energy absorption and spherical dissipation, the deformation obtained through applied stress decreases further away from the deformation source. The majority of (non-linear) deformation is absorbed relatively near to the stress source. For measurement reproducibility, a ROI should therefore include mediastinal tissue together with the mediastinal lymph node, but exclude the direct vicinity of the strain source (i.e. pulsating vasculature). This holds for both visualizing strain as for scoring strain, as non-linearity of scoring is potentially introduced otherwise. Last but not least, one should consider that the signal to noise ratio of the system becomes lower at increasing depth, giving rise to less accurate derivations [23,79,81].

**Region of interest size** - As stated earlier, measured strain values are normalized over the chosen visualized region of interest. Sufficient reference tissue should be included in visualization to give an accurate representation of relative strain. As Ciurea *et al.* and Havre *et al.* state, lesions were rated softer if the ROI for calculating strain was chosen too

small relative to the lesion [78,83]. To have an adequate sized reference region, Havre *et al.* suggests to make the ROI size such that the lesion will be 25-50% of total ROI size [78]. Based upon our experience, we suggest to use this rule of thumb conservatively, with 25% or less being a better estimate than 50%.

**Software presets** - Initial software set-up of the ultrasound processing system and variation in measurement technique determine reproducibility and accuracy of lesion scoring [78]. The visualized strain is a relative measure. In relaying the relative strain information back to the user, visualization can be arbitrary. However, by changing software settings and thus visualization, efforts to quantify strain are also affected. In using strain elastography in clinical practice, both the imaging protocol for performing EBUS strain elastography as the software settings should be standardized. This is applicable both in strain visualization as in performing measurements through all scoring methods.

### 2.9.3 Supplementary Figures and Tables

**Table 2E.1** – Performance of US B-mode features [46] to predict the presence of lymph node malignancy. B-mode ultrasound features were prospectively scored on all lymph nodes (n=120). Receiver Operator Characteristic – Area under the curve of ultrasound based short axis size was 0.73. The 95% CI of the accuracy and LR+ and LR- are placed between brackets. These results are partially in conflict with other reported findings (i.e. [47–50]) and were therefore not used in subsequent (multi-feature) analysis. Abbreviations: SA - Short Axis, CHS – Central Hilar Structure, CNS – Central Necrosis sign, LR+ - Positive Likelihood Ratio, LR- - Negative Likelihood Ratio, Inf - Infinity.

US features	Sens.	Spec.	PPV	NPV	Acc. (95% CI)	LR+ (95% CI)	LR- (95% CI)
<b>SA Size <math>\geq 10</math> mm</b>	60%	68%	53%	74%	65% (56%-73%)	1.88 (1.25-2.90)	0.59 (0.37-0.84)
<b>Shape</b>	93%	51%	53%	93%	67% (57%-75%)	1.89 (1.50-2.46)	0.13 (0.00–0.32)
<b>Margin</b>	13%	79%	27%	60%	54% (45%-63%)	0.63 (0.20–1.41)	1.10 (0.92-1.29)
<b>Echogenicity</b>	64%	75%	60%	78%	71% (62%-79%)	3.65 (2.19-7.14)	0.43 (0.26-0.62)
<b>CHS</b>	98%	13%	41%	100%	46% (37%-55%)	1.15 (1.03-1.25)	0.03 (0.00–0.46)
<b>CNS</b>	16%	97%	78%	66%	67% (57%-75%)	5.83 (1.56-Inf)	0.87 (0.73-0.96)

**Table 2E.2** – PET, CT and EBUS-SE likelihood ratios and their 95% confidence intervals between brackets. Calculated with given predictive values sensitivity, specificity, NPV and PPV and Bayesian statistics. \*Outside 95% CI as derived in training dataset. VAS – Visual Analogue Scale

	Positive Likelihood Ratio (95% CI)		Negative Likelihood Ratio (95% CI)	
	Training dataset	Validation dataset	Training dataset	Validation dataset
<b>Color VAS-score</b>	3.26 (2.02 – 5.66)	3.25	0.34 (0.17 – 0.54)	0.00*
<b>Mod. Tsukuba score</b>	4.14 (2.63 – 7.44)	2.60*	0.167 (0.05 – 0.33)	0.00*
<b>Strain histogram mean</b>	3.81 (2.52 – 6.40)	3.25	0.10 (0.00 – 0.24)	0.00
<b>Strain ratio</b>	3.10 (1.66 – 6.71)	1.86	0.60 (0.40 – 0.80)	0.84*
<b>Overall dataset</b>				
<b>Color VAS-score</b>	3.24 (2.17 – 5.31)		0.29 (0.14 – 0.47)	
<b>Mod. Tsukuba score</b>	3.70 (2.52 – 5.99)		0.15 (0.04 – 0.29)	
<b>Strain histogram mean</b>	3.68 (2.55 – 5.74)		0.09 (0.00 – 0.21)	
<b>Strain ratio</b>	2.92 (1.60 – 5.82)		0.64 (0.45 – 0.82)	
<b>PET avid</b>	1.79 (1.43 – 2.31)		0.142 (0.00 – 0.34)	
<b>CT-scan <math>\geq 10</math> mm</b>	2.13 (1.63 – 2.88)		0.158 (0.04 – 0.34)	
<b>PET avid and/or CT-scan <math>\geq 10</math> mm</b>	1.42 (1.20 – 1.70)		0.141 (0.00 – 0.42)	
<b>PET avid and/or CT-scan <math>\geq 10</math> mm, then elastography</b>	4.61 (2.98 – 8.13)		0.143 (0.04 – 2.81)	
<b>PET non-avid and CT-scan <math>\leq 10</math> mm, then elastography</b>	1.35 (1.18-1.57)		0 (0.00-0.27)	

**Table 2E.3** – Performance of PET, CT and EBUS strain elastography for predicting lymph nodal malignancy alone or when used in combination (overall dataset, N = 120 lymph nodes, prevalence of malignancy = 0.375). PET avidity was scored by the radiologists and evaluated following the European Association of Nuclear Medicine guidelines [67]. For assessing the added value of strain elastography to PET and CT, the strain histogram mean scoring method was used. Interpretation of combined results is as follows: if PET- and/or CT-scan shows suspicious, being bigger than 10 mm or FDG-PET avid, it is considered a positive test\*. If none of both applies (<10 mm and FDG-PET negative), it is considered a negative test†. By adding strain histogram mean scoring to either a positive test (N = 90) or negative test (N=26), the added value of strain elastography in clinical work-up was exploratively assessed (see Figure 2.7).

Known predictors of malignancy	N	Sens.	Spec.	PPV	NPV	Accuracy (95% CI)	Negative post-test probability of malignancy (95% CI)	Positive post-test probability of malignancy (95% CI)
PET (positive/negative)	117	93%	48%	52%	92%	65% (56-74%)	0.079 (0.00 – 0.17)	0.52 (0.46 – 0.58)
CT-scan ( $\geq 10$ / < 10 mm)	119	91%	57%	56%	91%	70% (60- 78%)	0.087 (0.02 – 0.17)	0.56 (0.49-0.63)
PET avid AND/OR CT $\geq 10$ mm	116	95%	33%	46%	92%	56% (46-65%)	0.078 (0.00 – 0.20)	0.46 (0.42 – 0.51)
PET avid AND/OR CT $\geq 10$ mm & mean strain*	90	88%	81%	73%	92%	63% (76-90%)	0.079 (0.02 – 0.14)	0.73 (0.64 – 0.83)
PET non-avid AND CT <10 mm & mean strain†	26	100%	26%	44%	100%	53% (44- 63%)	0 (0.00 – 0.14)	0.45 (0.41 – 0.49)









# CHAPTER 3

**Predictive value of endobronchial ultrasound strain elastography in mediastinal lymph node staging: the E-predict multicenter study results**

## **Authors**

R.L.J. Verhoeven, R. Trisolini, F. Leoncini, P. Candoli, M. Bezzi, A. Messi, M. Krasnik, C.L. de Korte, J.T. Annema, E.H.F.M. van der Heijden

## **Published in**

Respiration 2020;99(6):484-492.

## 3.1 Abstract

### Background

Systematic assessment of lymph node status by endobronchial ultrasound-guided transbronchial needle aspiration (EBUS-TBNA) is indicated in (suspected) lung cancer. Sampling is herein guided by nodal size and FDG-PET characteristics. Ultrasound strain elastography (SE) might further improve risk stratification. By imaging tissue deformation over time, SE computes relative tissue strain. In several tissues, a lower strain (deformation) has been associated with a higher likelihood of malignancy.

### Objectives

To assess if EBUS-SE can independently help predict malignancy, and when combined with size and FDG uptake information.

### Methods

This multicenter ( $n = 5$  centers) prospective trial included patients with suspected or proven lung cancer using a standardized measurement protocol. Cytopathology combined with surgery or follow-up imaging (>6 months) were used as reference standard.

### Results

Between June 2016 and July 2018, 327 patients and 525 lymph nodes were included (mean size 12.3 mm, malignancy prevalence 0.48). EBUS-SE had an overall AUC of 0.77. A mean strain <115 (range 0–255) showed 90% sensitivity, 43% specificity, 60% positive predictive value, and 82% negative predictive value. Combining EBUS-SE (<115) with size (<8 mm) and FDG-PET information into a risk stratification algorithm increased the accuracy. Combining size and SE showed that the 48% a priori chance of malignancy changed to 11 and 70% in double negative or positive nodes, respectively. In the subset where FDG-PET was available ( $n = 370$ ), triple negative and positive nodes went from a 42% a priori chance of malignancy to 9 and 73%, respectively.

### Conclusions

EBUS-SE can help predict lymph node malignancy and may be useful for risk stratification when combined with size and PET information.

## 3.2 Introduction

Systematic endobronchial ultrasound (EBUS) combined with esophageal endosonographic evaluation (EUS/EUSb) is currently the recommended first line staging procedure in lung cancer [9]. During a systematic evaluation of the entire mediastinum - going from the contralateral hilum to the ipsilateral hilum - all lymph nodes should be carefully assessed [10]. Information from both CT and FDG-PET are generally used to define risk of malignancy in lymph nodes, subsequently guiding the sampling strategy. In routine clinical practice, every node which is FDG-PET avid or has a CT based short axis size  $\geq 10$  mm should be aspirated. And, if CT or PET-CT has shown abnormal mediastinal findings, at least three different mediastinal lymph node stations (4R, 4L, 7) should for example be sampled [10]. When no PET scan information is available or the lymph node shows low uptake, B-mode ultrasound characteristics and the short axis diameter as measured during EBUS/EUSb are often used to determine when to aspirate. However, there is no consensus on the lower limit in ultrasound size for aspiration. While the 10 mm short axis size as equal to CT is often used, cut-offs ranging from 5 to 10 mm are found across studies [13,47,84–87]. Studies assessing B-mode criteria such as node heterogeneity, shape and a central hilar structure have also been found to be contradictory in their results [17]. A recent meta-analysis found that ultrasound features might indeed correlate with malignancy, but should be further studied to determine their true predictive capability [88].

Endobronchial Ultrasound strain elastography (EBUS-SE) is one of relatively new ultrasound features. It has proven promising in risk stratification of likely malignant lymph nodes among different studies [89]. EBUS-SE derives tissue strain by monitoring how tissue deforms over time as a force is being applied. Its working principle can be best compared to classical palpation. In short, a region of tissue that is heavily deformed when compared to another region in the same image is derived to be high in strain (easily deformed). A region that is barely deformed when compared to another region by this same force is derived to be low in strain (low deformation). In EBUS-SE, this tissue deformation is measured primarily in the axial direction (depth direction). The periodical motion of the heart and greater vessels are hypothesized to exert the needed force on surrounding tissue. For calculating the relative strain, the received ultrasound signal needs to be monitored over time. By mapping how the signal varies over time (while a force is being exerted), one can compute the deformation. A relative strain can be derived from this deformation and is generally relayed to the user through a colour-coded overlay projected over the B-mode image. Several qualitative and semi-quantitative techniques to assess the calculated relative strain have been reported. We recently showed that the strain histogram method will give the best overall accuracy for predicting lymph node malignancy, as it is the most operator independent and thus objective technique [90]. More detailed information on EBUS-SE assessment technique and SE-technology can also be found in Chapter 2 [90,91].

In this international, prospective multicenter study, we investigated the predictive value of EBUS-SE in patients with suspected or proven lung cancer in daily clinical care. Using a standardized measurement strategy, we assess if EBUS-SE can help predict malignancy in lymph nodes as an individual predictive value, and, if it can help enhance prediction by combining EBUS-SE information with FDG-PET information and EBUS lymph node short axis size. The interobserver variability is furthermore determined.

### **3.3 Materials and methods**

#### **3.3.1 Study subjects**

This prospective international multicenter study (n=5) was registered under Clinicaltrials.gov number NCT02488928. The study was conducted in accordance with the declaration of Helsinki, and, ethics committee approval was obtained for each center. Patients of 18 years and older with an EBUS indication for a suspected or proven lung cancer were eligible. Prior chemo- or radiotherapy were exclusion criteria due to hypothesized tissue altering effects. All measurements were obtained using Pentax EB1970UK and EB19-J10U ultrasound bronchoscopes (Pentax Medical, Japan), and Hitachi Preirus Hi Vision US processors (Hitachi Corp, Japan) with unified software settings in each center.

#### **3.3.2 Study design**

To assess if EBUS-SE can help predict lymph node malignancy, two main research questions were formulated. (1) Can EBUS strain elastography by itself help predict malignancy of mediastinal lymph nodes in a multicenter setting? Divided into two sub-questions: (a) is strain a predictive parameter, and (b) can it be used as a reproducible measurement technique in daily clinical care? And research question (2): can we improve the current risk stratification by further incorporating EBUS-SE information with lymph node size and FDG-PET avidity information?

#### **3.3.3 Materials and methods**

All participating centers received similar training on EBUS-SE technique and pitfalls preceding to study participation. Systematic EBUS-TBNA staging was performed following international and local guidelines [6, 10, 11]. EBUS-SE measurements of to-be-aspirated lymph nodes were acquired at the discretion of the endoscopist. A standardized measurement protocol using the strain histogram scoring technique was used to quantify measured lymph node strain as previously reported in more detail (see [90,91]). Compared to previously published data [90], the EBUS-SE software settings were updated. As such, the EBUS-SE mean strain cut-off was re-analyzed for optimal performance in the present study. Known prognostic variables such as FDG-PET avidity, CT size and ultrasound B-mode characteristics were collected by the endoscopist [46]. The local FDG-PET reports as available for the endoscopist were used for further analysis. No central reading on FDG-PET was performed. Strain measurement

reproducibility was furthermore scored subjectively by the operator as 'heavily changing', 'slightly changing', or 'reproducible' based on the strain rate graph and corresponding colour-overlays [90].

### 3.3.4 Analysis

Strain elastography measurements and corresponding case report forms were coded, digitalized and completed by the site investigator. The case report forms were correlated with strain measurements by author RV (blinded). Individual lymph node cytopathology and subsequent surgical results were used for correlation to EBUS-SE measurements. When no follow-up tissue sample was available, an imaging based clinical follow-up of at least 6 months was used. Statistical analysis was performed using R-studio [68]. The performance of predictors was assessed using contingency tables and predictors derived from these, accompanied by their 95% confidence intervals (CI). Predictors include sensitivity, specificity, negative predictive value (NPV), positive predictive value (PPV), accuracy, receiver operator characteristic (ROC) curves, negative likelihood ratios (LR-), positive likelihood ratios (LR+) and pre- to post-test probabilities of malignancies calculated from these. The predictive value of continuous variables was assessed through the area under the curve (AUC) of the ROC. To analyse the added value of predictive variables to one another (chronologically), an ANOVA of different predictive models was made using a chi-squared test (PET alone, PET and EBUS short axis size combined, PET and EBUS short axis size further combined with EBUS-SE). Inter-observer variability of strain was assessed by comparing ROCs among different hospitals, adjusted for non-paired data [92]. During analysis, a relatively low false negative rate of imaging results was prioritized above overall accuracy for obtaining highest staging accuracy.

## 3.4 Results

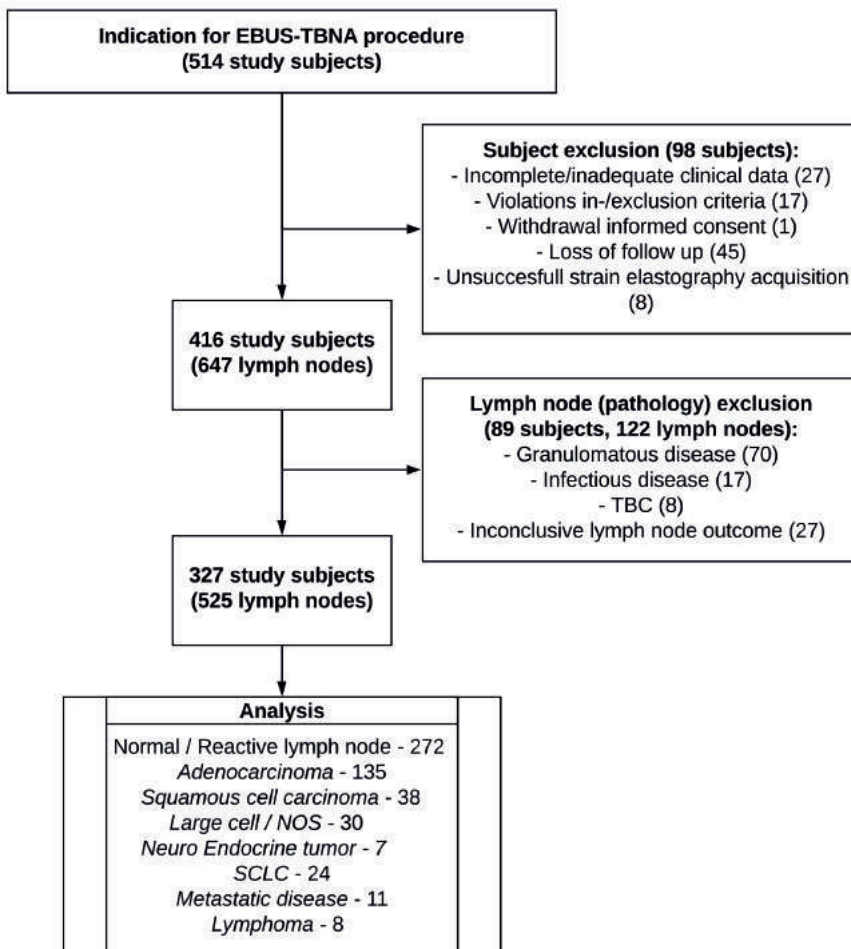
Between May 2016 – July 2018, measurements of 525 lymph nodes from 327 unique patients were included for study analysis (CONSORT diagram, Figure 3.1). Of the included 525 lymph nodes on which EBUS-TBNA and elastography measurements were performed, 228 were found malignant through initial cytopathology findings, 170 received further surgical verification and 127 underwent additional clinical and imaging follow-up to confirm benign disease. Overall prevalence of malignancy was 48%. Study demographics and lymph node information are shown in Tables 3.1 and 3.2, respectively.

### 3.4.1 EBUS strain elastography performance

ROC analysis was performed to assess EBUS strain elastography predictive value. In Table 3.1, ROC analysis of the mean strain as obtained from all five centers showed an AUC of 0.77 (95% CI 0.73-0.81). The AUC of individual hospitals ranged between 0.67-0.85. Pairwise ROC comparison of individual hospitals showed that EBUS-SE performance did not vary

significantly across centers. Comparing the highest to lowest AUC and largest volume to smallest volume performances gave P-values of 0.072 and 0.41, respectively (Table 3.3).

In 456 out of 525 lymph nodes in this multicenter study an adequate track record on temporal reproducibility of EBUS-SE measurements was available. The endoscopists subjectively rated EBUS-SE lymph node measurements as 'heavily changing' in 41 measurements (8.9%); 'slightly changing' in 135 measurements (29.6%); and 'reproducible' in 280 (53.3%) measurements. To assess if strain elastography performance varied with reproducibility scoring, ROC comparison of the differently scored subsets was performed. No significant differences were found ( $p>0.4$ ). To obtain a representative dataset, all measurements were included for analysis.



**Figure 3.1** – CONSORT diagram of study inclusion.



Distinctive cut-off values of the strain histogram mean were studied to identify clinically relevant scenarios. As a stand-alone predictive parameter of malignancy, a strain mean cut-off value of <115 (range 0-255) was found most suitable, having high sensitivity (90%) and NPV (82%) with moderate specificity (43%) and PPV (60%, Table 3.4). Using this cut-off as the only criterium for predicting malignancy, the positive likelihood ratio (LR+) of 1.58 would change the 0.48 pre-test probability of malignancy (being equal to prevalence of disease) to a 0.60 post-test probability of malignancy. The found negative likelihood ratio (LR-) of 0.23 would imply that the 0.48 pre-test probability of disease decreases to 0.18 if mean strain was measured to be more than 115 (Table 3.4).

### 3.4.2 Size and FDG-PET performance

The variables size and FDG-PET avidity have long shown their value for lymph node malignancy prediction in routine clinical practice. The predictive value of these variables along with EBUS-SE as found in this study are summarized in Table 3.1 and Table 3.4. In the data subset where FDG-PET information was available (370 lymph nodes), PET avidity showed high sensitivity (88%) and NPV (83%) at moderate specificity (42%). Overall FDG-PET accuracy was 61%, and, FDG-PET performance did not significantly differ across centers ( $p>0.05$ , Table 3.1). ROC Analysis of EBUS based lymph node short axis size showed an overall AUC of 0.78 (95% CI 0.74-0.82) and non-significant ( $p>0.05$ ) performance differences across centers in pairwise ROC comparison (Table 3.1). Further analysis of different size-based cut-offs showed how the diagnostic utility of EBUS based lymph node size varied with the chosen cut-off (Table 3.4). Using  $\geq 10$  mm short axis size as predictor for malignancy resulted in a LR- of 0.39. Sixty-five out of all 253 malignancies in this dataset would then be falsely classified as benign (25.7%). A size minimum of  $\geq 8$  mm as cut-off value would reduce false negatives to 31 in this dataset, being 12.3% of the total amount of malignancies (LR- 0.26). The increase in sensitivity (74 to 88%) gained by preferring the  $\geq 8$  mm criterium however comes at a cost of more false positives. Whereas a  $\geq 10$  mm cut-off had a LR+ of 2.2, an  $\geq 8$  mm cut-off had a LR+ of only 1.66 (Table 3.3).

**Table 3.1** – Demographical data and overall overview on predictive variables as studied in the E-predict multi-center trial.

Abbreviations: NM – Non Malignant, M – Malignant, US – Ultrasound short axis size (in millimeter), AUC – Area Under the Curve, PET acc. – PET scan overall accuracy as calculated per center, Strain AUC – AUC of EBUS-SE per center as found by ROC analysis, 95% CI – 95% Confidence Interval.

Center	Patients / Lymph nodes	Sex (F/M)	Age (min-max)	Disease Prevalence (N/MM)	US Short axis Size (min-max)	US Size AUC (95% CI)	Strain AUC (95% CI)	PET Acc. (# avail.)
Nijmegen	143 / 256	54 / 89	64 (26-90)	0.42 (149/107)	10.9 (3-50)	0.76 (0.69-0.82)	0.75 (0.68-0.81)	0.58 (232)
Amsterdam	28 / 41	14 / 14	65 (48-78)	0.37 (26/15)	11.1 (3-13)	0.68 (0.49-0.86)	0.67 (0.49-0.84)	0.58 (26)
Bologna	72 / 102	32 / 40	67 (42-83)	0.61 (40/62)	13.3 (4-41)	0.81 (0.72-0.90)	0.82 (0.74-0.90)	0.73 (52)
Firenze	42 / 80	14 / 28	68 (52-85)	0.34 (53/27)	12.0 (5-30)	0.70 (0.58-0.82)	0.85 (0.76-0.95)	0.65 (52)
Fano	42 / 46	13 / 29	68 (35-90)	0.91 (4/42)	19.1 (9-48)	0.74 (0.51-0.97)	0.82 (0.64-0.99)	0.75 (8)
<b>Total</b>	<b>327 / 525</b>	<b>127 / 200</b>	<b>66 (26-90)</b>	<b>0.48 (272/253)</b>	<b>12.3 (3-50)</b>	<b>0.78 (0.74-0.82)</b>	<b>0.77 (0.73-0.81)</b>	<b>0.61 (370)</b>

**Table 3.2** – Lymph node characteristics. Lymph node regions according to the IASLC nodal definition from the 8th TNM classification as included in this multi-center trial, followed by counts and percentages [11]. Two counts of mediastinal pulmonary masses can furthermore be found, interpreted as continuous with a previous lymph node margin, but now indistinguishable. Abbreviations: L – Left, R – Right, Leb – Left endobronchial, Eso – esophageal, LMB – Left main bronchus, RMB – Right main bronchus, P – Posterior.

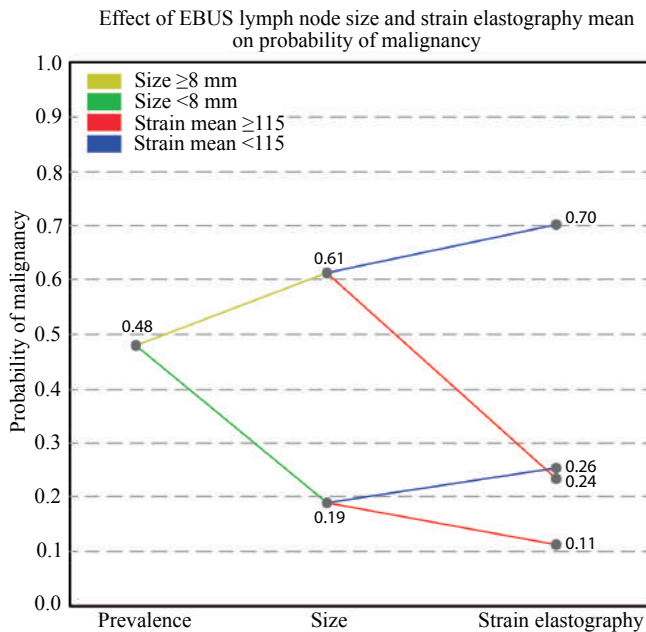
Mediastinal lymph node region: Number of measurements / Percentage	
<b>2 L:</b>	4 / 0.8%
<b>4 L</b>	65 / 12.4%
<b>7 LMB:</b>	17 / 3.2%
<b>10 L:</b>	5 / 1%
<b>11 L:</b>	57 / 10.9%
<b>12 L:</b>	3 / 0.6%
<b>Mediastinal lymph node region: Number of measurements / Percentage</b>	
<b>2 R:</b>	13 / 2.5%
<b>4 R:</b>	125 / 23.8%
<b>7 RMB:</b>	126 / 24%
<b>10 R:</b>	7 / 1.3%
<b>11 R:</b>	59 / 11.2%
<b>12 R:</b>	7 / 1.3%
<b>Mediastinal pulmonary mass: 2 / 0.4%   3 P: 2 / 0.4%   8 R: 2 / 0.4%</b>	

**Table 3.3** – Pair-wise AUC comparison of ROC curves computed from strain elastography measurements in individual centers. P-value as found by two-sided testing (unpaired).

	Nijmegen	Amsterdam	Bologna	Firenze	Fano
<b>Nijmegen</b>	-	0.41	0.17	0.06	0.47
<b>Amsterdam</b>	-	-	0.13	0.07	0.25
<b>Bologna</b>	-	-	-	0.59	0.97
<b>Firenze</b>	-	-	-	-	0.71
<b>Fano</b>	-	-	-	-	-

### 3.4.3 Clinical scenarios

**Combining strain elastography with size** - After assessing the different scenarios in which size and strain imaging could be combined in clinical practise, it was found that a lymph node size  $\geq 8$  mm in combination with a strain cut-off of  $< 115$  would best stratify risk of malignancy in this dataset. Analysis of this stratification showed that adding strain to EBUS-measured lymph node short axis size could significantly help stratify risk of malignancy as compared to stratification based upon EBUS-measured short axis size alone ( $P < 0.001$ ). If using these cut-offs to assume that all lymph nodes of  $\geq 8$  mm and the subset of lymph nodes  $< 8$  mm that had strain  $< 115$  were considered malignant, an overall sensitivity of 95%, NPV 86%, specificity 30% and PPV 56% was found (Table 3.4). The risk stratification methodology can however better be interpreted by a decision tree diagram. A more detailed visualization of how risk of malignancy changes with found variable outcome is shown in Figure 3.2. By this stratification methodology, double imaging positive lymph nodes (being  $\geq 8$  mm and low in strain) would have a 70% chance of being malignant in this dataset. Oppositely, double imaging negative lymph nodes ( $< 8$  mm and high in strain) would have an 11% chance of being malignant and thus false negative.



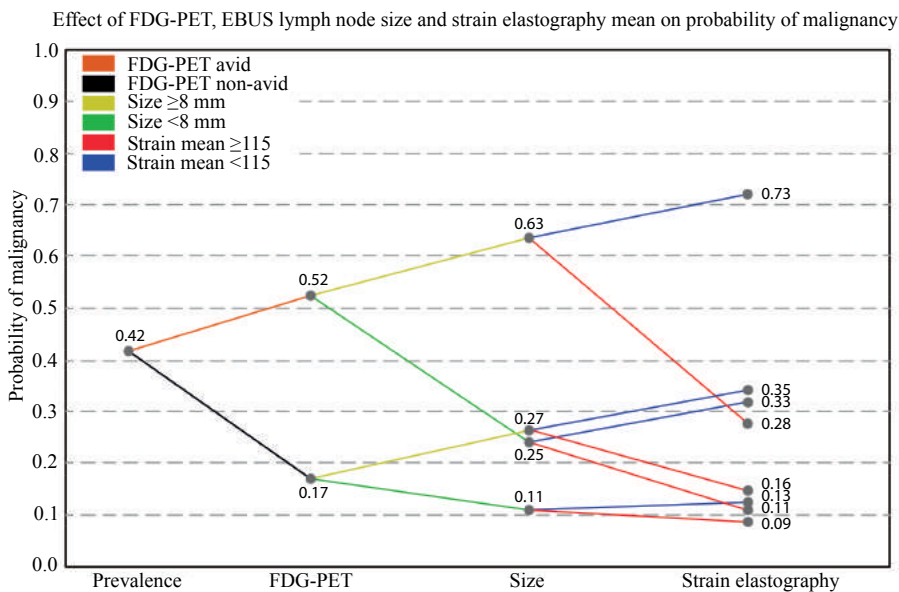
**Figure 3.2** – Clinical scenario combining EBUS size and EBUS-SE for predicting probability of mediastinal lymph node malignancy. This analysis was performed on all lymph nodes where both data was available ( $n=525$  lymph nodes). The initial prevalence of disease is used as starting point (pre-test probability of malignancy). From there, the post-test probability of malignancy is updated based upon the EBUS short axis size information. If EBUS size is  $\geq 8$  mm, probability of malignancy increases. If EBUS size is  $< 8$  mm, probability of malignancy decreases. After having obtained the intermediate EBUS size-based probability of malignancy, the EBUS-SE measurement outcome is further included to assess the contribution of EBUS-SE to the probability of malignancy. A strain  $< 115$  is associated with an increase in probability of malignancy. A strain  $\geq 115$  is associated with a decrease in probability of malignancy.

**Table 3.4** – Overall predictive performance of study variables. The EBUS-SE mean strain as found by the strain histogram technique and EBUS short axis size are first summarized with different cut-offs. Secondly, the combined size and strain are introduced. The theoretical workflow herein is as follows; all lymph nodes above the size cut-off are grouped as suspicious of malignancy. Lymph nodes whom have shown smaller than this size are secondly assessed by strain elastography. Only if the mean strain has shown higher than the strain cut-off will these lymph nodes be grouped as non-malignant. If the strain shows lower than the cut-off (lower strain/less deformation), lymph nodes will be grouped as suspected of malignancy (also see Figure 3.2). Lastly, the dataset for which FDG-PET, US size and US strain were available (N=370 out of the original 525 lymph nodes) is described. This dataset was used to provide a multi-modal work-up of malignancy risk estimation as has been depicted in Figure 3.3. Prevalence of malignancy in this subset was 0.42. Prevalence in the overall dataset was 0.48.

Abbreviations: N – number of measurements available, Prev. – Prevalence of disease, Sens – Sensitivity, Spec – Specificity, PPV – Positive Predictive value, NPV – Negative Predictive value, Acc. – Accuracy, CI – Confidence Interval, TP – True Positive, FN – False Negative, TN – True Negative, FP – False Positive, LR+ - Positive Likelihood ratio, LR- - Negative Likelihood ratio, | (symbol) - or.

Variable	N	Prev.	Sens.	Spec.	PPV	NPV	Acc. (95% CI)	TP	FP	TN	FN	LR-	LR+
<b>Strain [0-255]</b>													
<78	525	0.48	0.64	0.76	0.71	0.7	0.70 (0.66-0.74)	163	66	206	90	0.47	2.67
<115	525	0.48	0.90	0.43	0.60	0.82	0.66 (0.61-0.70)	227	154	118	26	0.23	1.58
<b>Size</b>													
≥8 mm	525	0.48	0.88	0.47	0.61	0.81	0.67 (0.62-0.71)	222	144	128	31	0.26	1.66
≥10 mm	525	0.48	0.74	0.66	0.67	0.73	0.70 (0.66-0.74)	188	92	180	65	0.39	2.2
<b>Size &amp; Strain</b>													
≥8 mm   <78	525	0.48	0.94	0.33	0.57	0.86	0.63 (0.58-0.67)	238	181	91	15	0.18	1.4
≥8 mm   <115	525	0.48	0.98	0.22	0.54	0.91	0.58 (0.54-0.63)	247	213	59	6	0.09	1.26
≥10 mm   <78	525	0.48	0.88	0.49	0.61	0.81	0.68 (0.63-0.72)	223	140	132	30	0.24	1.73
≥10 mm   <115	525	0.48	0.95	0.30	0.56	0.86	0.61 (0.57-0.66)	240	190	82	13	0.17	1.36
<b>PET-information (subset)</b>													
FDG-PET	370	0.42	0.88	0.42	0.52	0.83	0.61 (0.56-0.66)	137	124	90	19	0.29	1.52
Size ≥8 mm	370	0.42	0.84	0.52	0.56	0.82	0.66 (0.61-0.71)	131	102	112	25	0.31	1.75
Size ≥10 mm	370	0.42	0.69	0.71	0.63	0.76	0.70 (0.65-0.75)	108	63	151	48	0.44	2.38
Strain <115	370	0.42	0.87	0.46	0.54	0.83	0.64 (0.58-0.68)	136	115	99	20	0.28	1.61

**Combining strain elastography with size and FDG-PET** - To enable a risk stratification analysis using FDG-PET avidity, EBUS short axis size and EBUS-SE information, the subset of data where FDG-PET was available was analysed (n=370). While prevalence of lymph node metastases in this subset of data was slightly lower (0.42), the accuracies of the predictive values EBUS size and EBUS-SE did not significantly differ from that of the overall dataset (Table 3.4). Assessing several scenarios in this subset showed that both an EBUS size and EBUS-SE cut-off similar to the previous model could be used, being a size of 8 mm and a strain cut-off of 115. Combining FDG-PET avidity and EBUS size with EBUS-SE significantly enhanced lymph node malignancy prediction when compared to a risk stratification based upon FDG-PET and EBUS based short axis size alone ( $P < 0.001$ ). The resulting risk stratification model is shown in Figure 3.3. In all sub-scenarios where FDG-PET and size information have been combined, EBUS-SE increases or decreases likelihood of malignancy in cases of low and high strain respectively. If all three predictors were negative, a 9% chance of malignancy remained. If all three predictors were positive, lymph nodes had a 73% chance of malignancy.



**Figure 3.3** – Clinical scenario combining PET, EBUS size and EBUS-SE for predicting probability of mediastinal lymph node malignancy. This analysis was performed on all lymph nodes where all three data were available (n=370 lymph nodes). The initial prevalence of disease is used as starting point (pre-test probability of malignancy). From there, the post-test probability of malignancy is updated based upon FDG-PET avidity information. FDG-avid lymph nodes had an increased probability of malignancy, whereas non-avid lymph nodes decreased the probability of lymph nodes being malignant. From there, the post-test probability of malignancy is updated based on the EBUS-measured lymph node short axis size information. If size is  $\geq 8$  mm, probability of malignancy increases. If EBUS size is  $< 8$  mm, probability of malignancy decreases. Following the obtained intermediate PET and EBUS size based probability of malignancy, the EBUS-SE measurement is included to assess its contribution on the probability of malignancy. A strain  $< 115$  is associated with an increase in chance of malignancy. A strain  $\geq 115$  is associated with a decrease in chance of malignancy.

### 3.5 Discussion

To our knowledge, this is the first study utilizing a standardized assessment protocol to show the added predictive value of EBUS-SE in relevant daily clinical scenarios in multiple centers. We confirm earlier single center studies that showed an association between relative strain and presence of lymph node malignancy [88,89]. In this study, we show that strain elastography is an independent predictive variable. Furthermore, we show that EBUS-SE can be used in conjunction with EBUS lymph node short axis size and FDG-PET information to help better select which nodes must be further evaluated. Using two clinical scenarios, we show how EBUS-SE can help further risk stratify chance of malignancy. The addition of EBUS-SE in clinical practice could increase EBUS-TBNA staging accuracy. It might help intra-procedural decision making in case of multiple nodes within a region or unrepresentative ROSE (i.e. insufficient percentage of lymphoid cells to confirm lymph node aspirate), and, it might help decision making on further work-up after EBUS-TBNA in case of unrepresentative cytology findings.

Strain elastography is a relative measure and can therefore vary with measurement technique and time. Standardization and training are important for EBUS-SE implementation [90]. In this study, the performance variability of EBUS-SE was found insignificant between centers and operators. Yet, we signify the need of additional technical research to further improve reproducibility and standardization across systems and manufacturers. Moreover, when one starts using EBUS-SE, efforts should be made to assess how well EBUS-SE risk stratification performs by their hands. It is unknown beyond the here studied population and observers how performance might be influenced by differences in patient cohorts and measurement technique settings.

Strain is a continuous variable with range 0-255, similar to EBUS size. We present scenarios using a distinct cut-off. Continuous variables have gradual onset rather than distinctive values and risk of malignancy is thus not fully reflected by one value. Again, the discussed scenarios were chosen because a low false negative rate was prioritized above overall accuracy for obtaining highest staging accuracy.

The differences in EBUS-SE performance of Nijmegen in this study and previously published results are not fully understood (AUC 0.75 vs. 0.846) [90]. Possibly, a more rigorous selection for measurement inclusion was previously applied since the protocol was kept similar. Although unlikely, the updated software setting could also have had a small effect. With the updated software settings and low false negative prioritization, we now find an optimal cut-off value of 115 (previously; 78).

The present guidelines do not specifically state distinct cut-off values for aspiration of lymph nodes during an EBUS-staging procedure. In general, as used per CT imaging,  $\geq 10$  mm is

often chosen as cut-off value for increased chance of malignancy. We confirm that this size cut-off indeed showed good overall accuracy (70%) in predicting lymph node malignancy in our dataset. However, it should be considered that good overall accuracy does not necessarily correlate to high sensitivity. Earlier studies have used cut-off values varying from 5 to 10 mm with success [13,47,84–87]. Based on our results we propose to at least routinely include nodes of  $\geq 8$  mm for aspiration when no additional predictive variables are used. Using this criterium in our dataset would however still result in 12.3% of malignant lymph nodes being missed. This is already a major step forward when compared to a 10 mm cut-off, which would equal to as much as 25.6% of malignant lymph nodes being missed. Ideally, lymph nodes smaller than 8 mm should also be considered for aspiration, but the more recent large multicenter trials have used this 8 mm cut-off value successfully [13,93]. We would recommend further research on this subject to enable adjustment of the guidelines accordingly.

For assessing mediastinal lymph node involvement, FDG-PET imaging is recommended [6,9]. Its results cannot be omitted once available. The endoscopist is likely to aspirate avid nodes regardless of size or EBUS-SE. In this study, PET-imaging was available across centers as per their routine clinical practice. No central reading was performed, possibly affecting FDG-PET accuracy variability. Binomial proportion testing however showed insignificant FDG-PET accuracy differences across centers.

Lymph nodes were included for aspiration based on criteria other than strain elastography. In that respect, none of the included lymph node aspirations were carried out without an inclusion bias. Future work should assess SE using systematic inclusion rather than based to the operator's own insights. Furthermore, additional studies should assess if a multi-frame strain analysis that is cross-compatible across systems and manufacturers can be introduced to further increase temporal reproducibility, widespread availability, and, diagnostic performance.

### **3.6 Conclusion**

EBUS strain elastography helps predict malignant lymph node involvement in patients with lung cancer. The addition of ultrasound strain elastography to EBUS short axis size and FDG-PET avidity further improves risk stratification for malignancy.

### **3.7. Statement of Ethics**

The research was conducted ethically in accordance with the latest World Medical Association Declaration of Helsinki. The study is registered and can be found on ClinicalTrials.

gov (identifier: NCT02488928). The study protocol was approved by the medical ethical committees in both the Netherlands and Italy, where subject inclusion took place after having obtained informed consent.









# CHAPTER 4

**Accuracy and reproducibility of endoscopic  
ultrasound B-mode features for observer-based  
lymph nodal malignancy prediction**

## **Authors**

R.L.J. Verhoeven, F. Leoncini, J. Slotman, C.L. de Korte, R. Trisolini, E.H.F.M. van der Heijden, on behalf of the E-predict study group

**Accepted for publication in**

Respiration, 2021.

## 4.1 Abstract

### Background

Endoscopic ultrasound routinely guides lymph node evaluation for the staging of a known or suspected lung cancer. Characteristics seen on B-mode imaging might help the observer decide on the lymph nodes of risk. The influence of nodal size on the predictivity of these characteristics and the agreement with which operators can combine these for malignancy risk prediction is to be determined.

### Objectives

We evaluated (1) if prospectively scored individual B-mode ultrasound features predict malignancy when further divided by size and (2) assess if observers were able to reproducibly agree on still lymph node image malignancy risk.

### Methods

Lymph nodes as visualized by EBUS were prospectively scored for B-mode characteristics. Still B-mode images were furthermore collected. After collection, a repeated scoring of a subset of lymph nodes was retrospectively performed (n=11 observers).

### Results

Analysis of 490 lymph nodes revealed the short axis size is an objective measure for stratifying risk of malignancy (ROC Area Under Curve 0.78). With  $\geq 8$  mm size, 210/237 malignant lymph nodes were correctly identified (89% sensitivity, 46% specificity, 61% positive predictive value, 81% negative predictive value). Secondary addition of B-mode features in  $< 8$  mm nodes had limited value. Retrospective analysis of intra- and inter-observer scoring furthermore revealed significant disagreement.

### Conclusions

Lymph nodes of  $\geq 8$  mm size and preferably even smaller should be aspirated regardless of other B-mode features. Observer disagreement in scoring both small and large lymph nodes suggests it is infeasible to include subjective features for stratification. Future research should focus on (integrating) other (semi-) quantitative values for improving prediction.

## 4.2 Introduction

Once a suspected or proven lung cancer with abnormal mediastinal findings has been found through CT- and/or PET-CT imaging, guidelines recommend systematic lymph nodal assessment and aspiration through EBUS-TBNA (Endobronchial Ultrasound - Transbronchial Needle Aspiration) and preferably combined with EUS-FNA (Esophageal Ultrasound - Fine Needle Aspiration) [10]. Whilst a minimum of 3-4 lymph node aspirations is required by endoscopic examination if CT and/or PET-CT has shown abnormal findings (>10 mm short axis size on CT and/or FDG-PET avidity), also less suspected findings on endoscopic imaging (>5 mm short axis findings on ultrasound) might subsequently incur ultrasound guided aspiration [6,10,86,94]. In cases where the decision making is not clear-cut, ultrasound imaging is often used to help decide on which lymph nodes to aspirate. Several studies have assessed which routinely available endoscopic ultrasound B-mode features help differentiate malignant and benign lymph nodes. The five identified and studied B-mode features include size, nodal heterogeneity, margin distinctiveness, presence of a central necrosis sign and a central hilar structure [46]. As multiple studies have found, individual features or a combination thereof might have predictive value [46–49,88,95–98]. However, the results in these predominantly single center studies differ. Consequently, no formal recommendation on the widespread use of these features has been given [17].

Possible reasons for the found differences in prospective value of B-mode features might be differences in lymph node disease burden under study and/or a lack of consistent information in the features for enabling accurate prediction of malignancy. In clinical practice, one of first determinants on the need of sampling therefore might remain to be the CT and US based lymph node short axis size. The influence of the lymph node size on scoring performance of the other identified B-mode features is however not well established. Some single center studies report aspirating all lymph nodes of >5 mm short axis size (i.e. [46,86]) whereas several multi-centric studies report a  $\geq 8$  mm node as a lower margin for enabling aspiration regardless of the presence of any other features (i.e. [13,93]). It is however especially sub-centimeter lymph nodes which are subjected to B-mode feature evaluation, with the endoscopist deciding intra-procedurally to proceed with sampling or not. The predictive value in doing so is however complicated not only by differences in reported performance across studies, a disagreement in interpretation of B-mode imaging and features could also be a potential pitfall [95,98]. As we have moved towards systematic sampling in endoscopic staging in order to prevent the need of more invasive cervical mediastinoscopy staging, one can question if subjective scoring of  $\leq 8$  mm lymph nodes remains desirable, or, if all lymph node regions should be aspirated regardless.

The aim of the present study is to assess the performance characteristics of the reported ultrasound features evaluated during endosonography in a multi-center international study when further specified by lymph node size. In this study, we therein specifically assess if

the often used and clinically feasible 8 mm size cut-off could be further helped by B-mode features in deciding upon aspiration. To assess the reproducibility (inter- and intra-observer variability) of compounded endoscopic B-mode feature scoring for predicting lymph nodal malignancy, we furthermore perform a multi-observer retrospective scoring of a subset of lymph node images.

## 4.3 Materials and Methods

### 4.3.1 Study subjects

This study was performed using prospectively collected and scored ultrasound B-mode images as gathered during the E-predict multi-center international trial, a study as described in Chapter 3 evaluating the value of ultrasound strain elastography for endosonographic prediction of lymph node malignancy (clinicaltrials.gov identifier: NCT02488928) [99]. All images were acquired and prospectively scored during endoscopic ultrasound guided fine needle aspiration procedures (EBUS/EUS) for a known or suspected lung cancer. For retrospective assessment of the reproducibility (inter- and intra-observer variability) of compounded endoscopic B-mode feature scoring in a subset of these prospectively collected images, several observers from different centers with varying experience were recruited on a voluntary basis.

### 4.3.2 Study design

This study is two-fold: (1) We prospectively evaluate performance characteristics of the endoscopist-reported ultrasound B-mode features in a multi-center multi-observer fashion. The performance characteristics are evaluated on all lymph nodes, and, in the subsets of <8 mm and  $\geq 8$  mm lymph nodes. (2) We investigate the observer variability in scoring the combination of B-mode features for predicting lymph node malignancy. By retrospective scoring of a subset of still lymph node images through multiple observers, intra- and inter-observer variability is assessed. Knowing pathology outcome, accuracy of endoscopist malignancy scoring (as based on compounded B-mode features) is exploratively assessed.

### 4.3.3 Materials and methods

(1) Prospective collection of B-mode feature scoring was performed as part of the E-predict study protocol, which included 525 lymph nodes (see Chapter 3 [99]). The investigators of the five recruiting centers prospectively scored features after careful examination on dynamic imaging: echogenicity (heterogeneous versus homogeneous), shape (round versus oval), margins (distinct versus indistinct), coagulation necrosis sign (present versus absent), central hilar structure (present versus absent) [46,99]. Lymph node short axis size was determined by intra-procedural caliper measurements. During analysis, combined feature scores as described by Hylton *et al.* were furthermore retrospectively computed for obtaining the recently introduced Canada Lymph Node Score [95]. Individual lymph node

cytopathology, subsequent surgical results and/or 6-month clinical follow-up were used as reference standard.

(2) For the retrospective assessment of variability in compounded endoscopic B-mode feature scoring for predicting lymph nodal malignancy, repeated scoring of a subset of the prospectively collected lymph nodes was performed. The subset included 200 lymph node images randomly selected from all prospectively included lymph nodes. The prevalence of disease was unknown to the observers. Only one single B-mode still image was presented and participants were asked to classify it into 'malignant' or 'benign'. Scoring was performed with in-house developed Mevislab software (MeVis Medical Solutions AG version 2.8.2, Bremen, Germany). A size measurement tool was available. Metadata (i.e. node location, patient and image characteristics) were removed. The observers did not receive any feedback on their lymph node rating. Intra-observer scorings were performed with at least one day in between scorings and a new random image order.

#### **4.3.4 Analysis**

Analysis was performed with R and Rstudio [68]. To assess the influence of size on B-mode feature scoring, analysis was performed on the overall dataset and the subsets in which lymph node sizes were  $<8$  mm and  $\geq 8$  mm. To assess the performance of B-mode features descriptive characteristics sensitivity, specificity, positive predictive value (PPV), negative predictive value (NPV) and accuracy along with counts are reported. For the continuous variable short axis size, the Receiver Operator Characteristic - Area Under the Curve (ROC-AUC) is furthermore presented.

For retrospective analysis on observer variability, a division into differently sized lymph nodes was also made (8 mm cut-off). Knowing there's considerable variation in individual observer learning curves in endobronchial ultrasound [100–102], we chose to further classify observer expertise into novice [ $<50$  endoscopic US staging procedures], intermediate [50–400 procedures] and expert [ $>400$  procedures]. Raw agreement [%] and Gwet's Agreement Coefficient (AC1) – correcting for by chance agreement - were calculated to assess the agreement of measurements [103,104]. An AC1 value of 1 would indicate perfect agreement, 0 would indicate at chance agreement,  $<0$  would indicate an agreement worse than as expected by chance. With no universal cut-off for determining good agreement but knowing its potential high impact, an AC1 minimum of 0.70 was considered desirable for inter-observer research and an AC1 minimum of 0.85 for intra-observer agreement.

## 4.4 Results

The E-predict multi center trial enrolled 525 lymph nodes from 327 study subjects between May 2016 and July 2018. For patient and lymph node characteristics, see [99]. For 490 lymph nodes (with 347 and 143 lymph nodes  $\geq 8$  mm and  $< 8$  mm, respectively) a full B-mode feature measurement was available for analysis. Overall prevalence of malignancy was 48%. Prevalence of malignancy in the  $\geq 8$  mm and  $< 8$  mm subsets were 61% and 19%, respectively. See Tables 4.1 and 4.2 for a summary on multi-center B-mode feature scoring performance.

**Table 4.1** – Performance of prospectively scored ultrasound features for predicting lymph node malignancy on the overall dataset of 490 lymph nodes ( $n = 490$ , disease prevalence 0.48). Sens. – Sensitivity, Spec.- Specificity, PPV – positive predictive value, NPV – negative predictive value, Acc. – accuracy, CI – confidence interval, TN – True Negative, TP – True positive, FN – False negative, FP – False positive. CHS – Central Hilar Structure, CNS – Central Necrosis sign.

	Sens.	Spec.	PPV	NPV	Acc. (95% CI)	TN	TP	FN	FP
<b>Size <math>\geq 10</math> mm</b>	0.75	0.64	0.66	0.73	0.70 (0.65-0.74)	163	178	59	90
<b>Size <math>\geq 8</math> mm</b>	0.89	0.46	0.61	0.81	0.67 (0.62-0.71)	116	210	27	137
<b>Echogenicity</b>	0.62	0.81	0.75	0.69	0.72 (0.67-0.76)	204	147	90	49
<b>Shape</b>	0.68	0.60	0.61	0.67	0.64 (0.59-0.68)	151	162	75	102
<b>Margin</b>	0.83	0.35	0.54	0.69	0.58 (0.54-0.63)	88	197	40	165
<b>CHS</b>	0.91	0.29	0.54	0.77	0.59 (0.54-0.63)	73	215	22	180
<b>CNS</b>	0.15	0.98	0.85	0.55	0.58 (0.53-0.62)	247	35	202	6
<b>US Canada score <math>&gt;3</math></b>	0.64	0.82	0.77	0.71	0.73 (0.69-0.77)	208	152	85	45
<b>US Canada score <math>&gt;4</math></b>	0.12	0.99	0.94	0.55	0.57 (0.62-0.52)	251	29	208	2
<b>Mean strain <math>&lt;115</math></b>	0.90	0.44	0.60	0.82	0.66 (0.62-0.70)	111	213	24	142

### 4.4.1 B-mode size

Currently, the best made objective traditional B-mode feature is short axis size. In line with routine clinical use, it shows of value in a first identification and estimation of lymph nodes at risk of malignancy. As depicted in Figure 4.1, ROC-AUC of short axis size was 0.778 (95% confidence interval 0.737-0.819). The clinically often used 8 mm cut-off identified 210 out of 237 malignant lymph nodes and had 137 false positives (sensitivity 89%, specificity 46%, PPV 61%, NPV 81%). A slightly larger 10 mm cut-off had higher overall accuracy but also identified only 178 out of 237 malignant lymph nodes. As a first measure for identification and subsequent deciding on aspiration, an 8 mm criterion is an objective feature with relatively high sensitivity and NPV (Tables 4.1-4.2, Figure 4.1). A smaller than 8 mm size cut-off for including every identified lymph node would increase the sensitivity even further, although at the cost of specificity (Figure 4.1).



**Table 4.2** – Performance of prospectively scored ultrasound features for predicting lymph node malignancy in the subsets of data with lymph node short axis size <8 and ≥8 mm. PPV – positive predictive value, NPV – negative predictive value, Acc. – accuracy, CI – confidence interval, TN – True Negative, TP – True positive, FN – False negative, FP – False positive. CHS – Central Hilar Structure, CNS – Central Necrosis sign.

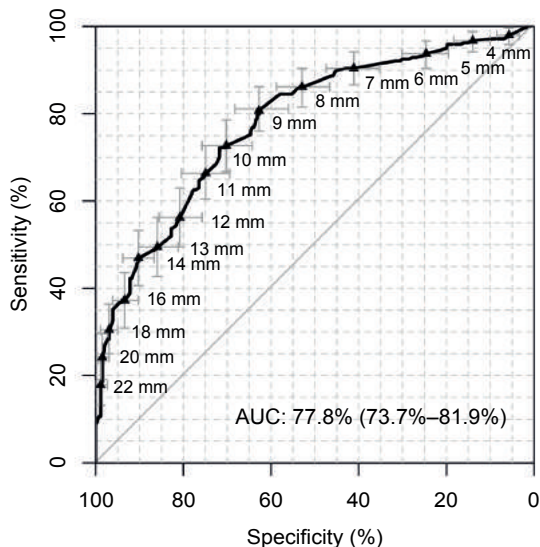
	Sens.	Spec.	PPV	NPV	Acc. (95% CI)	TN	TP	FN	FP
<b>Subset &lt;8 mm (n=143, disease prevalence 0.19)</b>									
<b>Echogenicity</b>	0.37	0.84	0.34	0.85	0.75 (0.67-0.82)	97	10	17	19
<b>Shape</b>	0.44	0.78	0.32	0.86	0.71 (0.63-0.79)	90	12	15	26
<b>Margin</b>	0.67	0.34	0.19	0.82	0.41 (0.32-0.49)	40	18	9	76
<b>CHS</b>	0.81	0.28	0.21	0.86	0.38 (0.30-0.46)	32	22	5	84
<b>CNS</b>	0.07	1.00	1.00	0.82	0.83 (0.75-0.88)	116	2	25	0
<b>US Canada score &gt;3</b>	0.07	1.00	1.00	0.82	0.83 (0.75-0.88)	116	2	25	0
<b>Mean strain &lt;115</b>	0.78	0.47	0.26	0.90	0.53 (0.45-0.62)	55	21	6	61
<b>Subset ≥8 mm (n=347, disease prevalence 0.61)</b>									
<b>Echogenicity</b>	0.65	0.78	0.82	0.59	0.70 (0.65-0.75)	107	137	73	30
<b>Shape</b>	0.71	0.45	0.66	0.50	0.61 (0.55-0.66)	61	150	60	76
<b>Margin</b>	0.85	0.35	0.67	0.61	0.65 (0.60-0.70)	48	179	31	89
<b>CHS</b>	0.92	0.30	0.67	0.71	0.67 (0.62-0.72)	41	193	17	96
<b>CNS</b>	0.16	0.96	0.85	0.43	0.47 (0.42-0.53)	131	33	177	6
<b>US Canada score &gt;3</b>	0.71	0.67	0.77	0.61	0.70 (0.65-0.75)	92	150	60	45
<b>US Canada score &gt;4</b>	0.14	0.99	0.94	0.43	0.47 (0.53-0.61)	135	29	181	2
<b>Mean strain &lt;115</b>	0.91	0.41	0.70	0.76	0.71 (0.66-0.76)	56	192	18	81

#### 4.4.2 Descriptive B-mode features

In our multicenter scoring, several B-mode features initially show of predictive value in the overall dataset (Table 4.1). When however looking into individual center outcomes, large differences in predictive value of several B-mode features were seen between centers (*Table to be published in the online supplement of the accepted manuscript due to size limitations*). Maximal sensitivity differences between centers were >20% for features echogenicity, shape and margin (overall sensitivity being 62%, 68% and 83%, respectively). A maximal specificity difference of 24.7% and 66.2% was furthermore seen in the features shape and margin, respectively (overall specificities 60% and 35%, *Table to be published in the online supplement of the accepted manuscript*). The features central hilar structure and a central necrosis sign had more similarity in outcome across centers. The central necrosis sign feature is not often found present in the different centers, but if so, a high risk of malignancy is warranted (specificities in all but one center: 91.7-100%, overall: 98%). The central hilar structure showed most conformity over all centers of classically used B-mode features other than size. With overall sensitivity 91%, specificity 29%, PPV 54% and NPV 77%, only 22 out of 237 malignant lymph nodes would have gone unnoticed in this dataset. Oppositely, with specificity 29% and PPV 54%, it has a high number of false positives (180/253). The

retrospectively calculated Canada lymph node score, recombining multiple B-mode features, showed relatively high accuracy (73%). It's clinical value in deciding on aspiration was however limited in our dataset, missing 85 out of 237 malignant nodes (sensitivity 64%).

Receiver Operator Characteristic - Ultrasound Short Axis Size



**Figure 4.1** – Receiver Operator Characteristic (ROC) of ultrasound measured lymph node short axis size. 95% confidence intervals of sensitivity and specificity at distinct short axis sizes in grey. AUC – Area Under the Curve (95% confidence interval between brackets).

#### 4.4.3 Clinical decision-making work-up

Considering the scenario where all lymph nodes  $\geq 8$  mm should be aspirated regardless of other imaging features - as it is the firstly available and most objective feature enabling a risk of prediction - further analysis of B-mode features for deciding on aspiration as specified by size was deemed necessary (Table 4.2).

In the subset of lymph nodes  $< 8$  mm, prevalence of malignancy was 19% ( $n=143$ ). With the exception of 'margin' and 'central hilar structure', all sensitivities are below 50%, indicating more than half of malignancies go unnoticed. The central hilar structure had most chance of identifying lymph node malignancy in  $< 8$  mm nodes with sensitivity 81% and NPV 86% (identifying 22 out of 27 lymph nodes). It however also resulted in a high number of false positives (84 out of 116 benign lymph nodes, Table 4.1). The ultrasound Canada score again had high overall accuracy, but considering disease prevalence did not show useful in further work-up on malignancy (sensitivity 7%).

In the subset of lymph nodes  $\geq 8$  mm the prevalence of malignancy was 61% (n=347). With this high overall risk of malignancy in this subset, the need of aspiration regardless of features seems warranted. Yet, if a further stratification need be made, the central hilar structure again showed most useful with high sensitivity (92%) and moderate NPV (72%). Overall accuracy of lymph nodal risk estimation was however highest by echogenicity (72%) and a Canada score  $>3$  (69%). Yet both echogenicity and the Canada score do not seem accurate enough for reliable clinical decision making, as they are neither sensitive nor specific enough in excluding or including malignant and benign findings with values  $<78\%$  (Table 4.2 & Table to be published in the online supplement of the accepted manuscript).

**Table 4.3** – Observer variability in retrospective scoring of a random subset of lymph nodes. Observer variability when only looking at malignant / benign lymph nodes and sizes  $<8$  and  $\geq 8$  mm are presented. The raw agreement is first presented (%), followed by the Gwet's AC1 coefficient.

	All lymph nodes			Malignant lymph nodes			Benign lymph nodes		
	All	$<8$ mm	$\geq 8$ mm	All	$<8$ mm	$\geq 8$ mm	All	$<8$ mm	$\geq 8$ mm
<b>Lymph nodes</b>	200	69	131	99	15	84	101	54	47
<b>Inter-observer variability</b>									
Expert (n=5)	74/0.48	71/0.54	76/0.59	79/0.66	77/0.59	80/0.70	69/0.40	69/0.53	68/0.39
Interm. (n=3)	71/0.42	73/0.57	69/0.47	76/0.58	78/0.57	75/0.61	66/0.35	72/0.58	59/0.21
Novice (n=3)	58/0.17	63/0.28	56/0.12	58/0.17	64/0.32	57/0.15	58/0.17	63/0.28	52/0.08
<b>Intra-observer variability</b>									
Expert 1	86/0.76	93/0.92	82/0.65	82/0.64	80/0.76	82/0.65	90/0.87	96/0.96	83/0.72
Expert 2	86/0.72	84/0.78	87/0.79	92/0.87	93/0.88	92/0.88	80/0.65	81/0.77	79/0.58
Interm. 1	80/0.60	78/0.69	80/0.69	84/0.72	87/0.76	83/0.74	75/0.52	76/0.68	74/0.57

#### 4.4.4 Compounded B-mode scoring - observer variability

For retrospective observer scoring, five experts, three intermediate observers and three novices were included. Two experts and one intermediate observer performed scoring twice to enable intra-observer variability assessment (Table 4.3). All observers scored the dataset of 200 lymph nodes within 20 minutes.

*Inter-observer variability* – In the overall dataset, the experts (n=5) had highest agreement, with Gwet's AC1 0.48 (raw agreement 74%, Table 4.3). Intermediate (n=3) AC1 was 0.42 (raw agreement 71%). The novices (n=3) showed an AC1 of only 0.17 (raw agreement 58%). Division of the overall dataset into subsets with  $<8$  and  $\geq 8$  mm size did not change raw agreement more than 5% as compared to the overall dataset. Analysis of observer variability against lymph node pathology shows experts and intermediates have more disagreement in scoring benign lymph nodes than malignant nodes (Table 4.3). Intermediate and expert observers had an AC1 0.58-0.66 (76-79% raw agreement) in malignant lymph nodes and an AC1 0.35-0.40 (66-69% raw agreement) in benign lymph nodes. These findings remained after differentiating by size.

*Intra-observer variability* – The experts showed moderate intra-observer agreement in the overall dataset, with an AC1 0.72-0.76 (raw agreements 86%) while the intermediate had an AC1 of 0.60 (raw agreement 80%). The Gwet's AC1 in intra-observer scoring of <8 mm lymph nodes varied from 0.69-0.92 (raw agreement 78-93%), whilst the >8 mm lymph nodes had AC1 0.65-0.79 (80-87% raw agreement).

*Observer accuracy* – The observer variability scoring on still images was used to explore B-mode compounding accuracy. Accuracy of predicting lymph node malignancy based on still B-mode images varied from 0.47-0.58 in novice to 0.60-0.72 and 0.63-0.71 in intermediate and expert, respectively. A division of the dataset by an 8 mm size cut-off did not show unequivocal changes in overall accuracy (Table 4.4). Further evaluation of compound scoring shows low overall sensitivity and PPV in <8 mm lymph nodes (both <0.42), indicating difficulty in identifying malignant nodes in this cohort. Oppositely, a low specificity and NPV in  $\geq 8$  mm lymph nodes in the majority of observers indicates that benign nodes are often not identified in the cohort of enlarged lymph nodes.

**Table 4.4** – Explorative observer prediction accuracy when asked to classify retrospective lymph node B-mode ultrasound images as either malignant or benign based on a compounding of visible B-mode features. PPV – positive predictive value, NPV – negative predictive value.

	Accuracy			Sensitivity			Specificity			PPV			NPV		
	All	<8 mm	≥8 mm	All	<8 mm	≥8 mm	All	<8 mm	≥8 mm	All	<8 mm	≥8 mm	All	<8 mm	≥8 mm
<b>Experts</b>	0.67	0.69	0.65	0.73	0.35	0.79	0.61	0.79	0.40	0.66	0.39	0.71	0.70	0.81	0.51
Expert 1	0.71	0.81	0.65	0.55	0.20	0.61	0.86	0.98	0.72	0.79	0.75	0.80	0.66	0.82	0.51
Expert 2	0.71	0.71	0.70	0.77	0.33	0.85	0.64	0.81	0.45	0.68	0.33	0.73	0.74	0.81	0.62
Expert 3	0.63	0.61	0.63	0.78	0.47	0.83	0.48	0.65	0.28	0.59	0.27	0.67	0.69	0.81	0.48
Expert 4	0.66	0.67	0.65	0.79	0.40	0.86	0.52	0.74	0.28	0.62	0.30	0.68	0.72	0.82	0.52
Expert 5	0.64	0.67	0.62	0.75	0.33	0.82	0.52	0.76	0.26	0.61	0.28	0.66	0.68	0.80	0.44
<b>Intermediates</b>	0.66	0.72	0.62	0.70	0.42	0.75	0.61	0.80	0.40	0.65	0.37	0.70	0.68	0.83	0.44
Intermediate 1	0.65	0.71	0.62	0.78	0.40	0.85	0.52	0.80	0.21	0.62	0.35	0.66	0.71	0.83	0.43
Intermediate 2	0.60	0.70	0.55	0.67	0.40	0.71	0.53	0.78	0.26	0.58	0.33	0.63	0.62	0.82	0.33
Intermediate 3	0.72	0.75	0.70	0.66	0.47	0.69	0.78	0.83	0.72	0.75	0.44	0.82	0.70	0.85	0.57
<b>Novices</b>	0.51	0.54	0.49	0.51	0.40	0.53	0.50	0.57	0.43	0.50	0.21	0.62	0.52	0.77	0.34
Novice 1	0.58	0.57	0.59	0.61	0.40	0.64	0.55	0.61	0.49	0.57	0.22	0.69	0.59	0.79	0.43
Novice 2	0.47	0.52	0.44	0.45	0.40	0.46	0.48	0.56	0.38	0.46	0.20	0.57	0.47	0.77	0.29
Novice 3	0.48	0.52	0.46	0.47	0.40	0.49	0.49	0.56	0.40	0.47	0.20	0.59	0.49	0.77	0.31

## 4.5 Discussion

This study evaluates whether individual B-mode features and a compounding thereof can be used to accurately and reproducibly predict lymph node malignancy in a dataset of 490 aspirated lymph nodes for which follow-up was available. While we find that the classically first available ultrasound short axis size is the most objective feature with reasonable predictive value (AUC-ROC 0.78), we also show that not one additional nor a combination of B-mode features is a do-it-all solution for predicting lymph node malignancy. Based on our findings and incorporating the purpose of endoscopic ultrasound guided needle aspiration as a systematic staging procedure in suspected lung cancer, we conclude that preferably all assessed lymph node regions should be aspirated regardless of size or features. At least all lymph nodes  $\geq 8$  mm should be subject to sampling regardless of other features due to a high prevalence of malignancy in this subgroup of nodes, but preferably smaller. In  $< 8$  mm lymph nodes, a central hilar structure (sensitivity 81%, NPV 86%) could also be used to stratify risk of malignancy, but the low specificity (28%) and considerable observer interpretation differences in feature scoring suggest it is of suboptimal outcome.

Our retrospective analysis of observer variability using still images as representation of compounded B-mode features shows that malignancy risk estimation cannot reliably be performed on still B-mode images. We find a relevant inter-and intra- observer agreement difference, and while exploratory, find compounded feature scoring had an accuracy of less than 72%. We therefore recommend not to decide on risk of malignancy or further work-up by compounding of only B-mode features.

Varying results have been reported on endoscopic B-mode lymph node imaging scoring agreement across different observers and within observers. Schmid-Bindert *et al.* retrospectively studied B-mode feature scoring through blinded procedural videos and reported inter-observer agreements of 88.6% and higher (n=2). Hylton *et al.* also had a database of videos, and in multiple observers (n=12) reports a raw agreement different for the individual features ranging from 62.6% for echogenicity to 81.7% for the central necrosis sign (Gwet's AC1 0.25-0.77) [95,98]. Our retrospective study determined the reproducibility of endoscopists B-mode feature compounding for predicting malignancy rather than individual B-mode feature scoring. In that regard, our study design was dissimilar to the aforementioned. In studying compounding, we find there is considerable inter-observer variability, leading to 20% and higher expert raw disagreement over all lymph node subsets. Intra-observer variability is a further concern. Intra-observer agreement of the experts and intermediate was  $\leq 86\%$  in the overall dataset when presented with the exact same image (AC1 0.72-0.76). Observer compounding of B-mode features is subject to significant variability. However, knowing assessment of stationary images is far from ideal and irrevocable, a 0.60-0.72 accuracy on predicting nodal malignancy by experts and intermediates also implicates prediction accuracy was better than at chance agreement. Analysis however shows a low

sensitivity and PPV for prediction in the subset of lymph nodes <8 mm size. Unfortunate, as this subset is most important for further work-up risk stratification and preventing understaging. The currently available B-mode features do not provide sufficient information for a highly accurate and reproducible prediction of lymph node malignancy. As we recently reported and show here, strain elastography may enable a semi-quantitative way of predicting malignancy, increasing sensitivity and NPV better than B-mode characteristics scoring [99]. Future research should be conducted and focus on implementation of computer aided diagnosis systems which could enable more consistent outcomes and possibly enable more accurate predictions. Integration of (other) (semi-)quantitative ultrasound features not easily objectified by the endoscopist should furthermore be investigated (i.e. [105]), along with the possibility of combining it with multiple modalities (such as strain elastography and/or PET-CT/CT findings [90,99]). Such systems may further allow tailoring to individual anatomical lymph node regions, i.e. weighing factors such as size or a presence of hilar structure differently.

#### **4.5.1 Study limitations**

The prospectively collected B-mode images and the scoring thereof by the observers were done in routine clinical practice during a multi-center trial on strain elastography. As systematic study inclusion and scoring of all assessed nodes was not mandatory, inclusion of lymph nodes could have been biased. A second limitation is the retrospective nature of our analysis on reproducibility, and, having only still B-mode ultrasound images available for scoring. Lastly, retrospective scoring was performed without taking notice of metadata (e.g. lymph node location, PET/CT information). This could have affected exploratively assessed scoring accuracy, but is not expected to negatively affect scoring variability.

#### **4.6 Conclusion**

Aside of the ultrasound B-mode short axis size, the currently used B-mode features do not provide sufficient information for good prediction of lymph nodal malignancy, and, reproducibility in their scoring shows to be an issue. In systematic staging, preferably all lymph nodes should be sampled. If any decision making on which nodes need to be aspirated is made aside of FDG-PET findings, the objective short axis size seems a relevant predictor. An  $\geq 8$  mm size has shown to be a clinically feasible cut-off, and could be used as a starting point. In systematic sampling, even smaller lymph node should however be considered. Future research should focus on implementation of computer aided diagnosis systems and further integration of multi-modality information for possibly improving nodal malignancy prediction.

## **4.7 Statement of Ethics**

The research was conducted ethically in accordance with the latest World Medical Association Declaration of Helsinki. The E-predict study from which the here presented data was obtained is registered and can be found on ClinicalTrials.gov (identifier: NCT02488928). This study is approved by the medical ethical committees in both the Netherlands and Italy, where subject inclusion took place after having obtained informed consent.

## **4.8 Acknowledgments**

We gratefully acknowledge our E-predict study team Piero Candoli, Michela Bezzi, Alessandro Messi, Mark Krasnik and Jouke Annema for contributing to the collection of the dataset used for this study.









# CHAPTER 5

**Cone beam CT image guidance with and without  
electromagnetic navigation bronchoscopy for  
biopsy of peripheral pulmonary lesions**

**Authors**

R.L.J. Verhoeven, J.J. Fütterer, W. Hoefsloot, E.H.F.M. van der Heijden

**Published in**

*Journal of Bronchology & Interventional Pulmonology*, 2021;28(1):60-69.

## 5.1 Abstract

### Background

Bronchoscopic diagnosis of small peripheral lung lesions suspected of lung cancer remains a challenge. A successful endobronchial diagnosis comprises navigation, confirmation and tissue acquisition. In all steps, 3D information is essential. Cone beam CT (CBCT) imaging can provide CT information and 3D augmented fluoroscopy imaging. We assess if CBCT imaging can improve navigation and diagnosis of peripheral lesions by two clinical workflows with a cross-over design: (1) a primary CBCT and rEBUS-based approach and (2) a primary electromagnetic navigation (EMN) and rEBUS-based approach.

### Methods

All patients with a peripheral lung lesion biopsy indication were eligible for study inclusion and randomly assigned to study arms. Commercially available equipment was used. The main study goals were to assess CBCT confirmed navigation success and diagnostic accuracy. Surgery or unambiguous clinical follow-up served as golden standard.

### Results

Eighty-seven patients with 107 lesions were included. Lesion mean longest axis size in the CBCT arm was 16.6 mm (n=47) and 14.2 mm in the EMN arm (n=40). The primary CBCT approach and primary EMN approach had 76.3% and 52.2% navigation success respectively. Addition of EMN to the CBCT approach increased navigation success to 89.9%. Addition of CBCT imaging to the EMN approach significantly increased navigation success to 87.5% per lesion. The overall diagnostic accuracy per patient was significantly lower than navigation success, being 72.4%.

### Conclusions

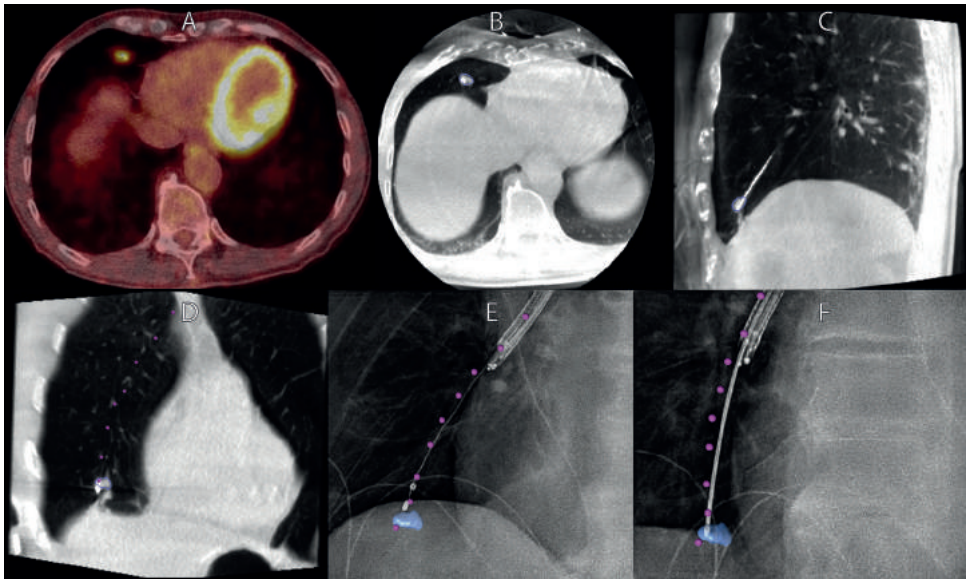
CBCT imaging is a valuable addition to navigation bronchoscopy. Although overall navigation success was high, the diagnostic accuracy remains to be improved. Future research should focus on improving the tissue acquisition methodology.

## 5.2 Introduction

Small peripheral pulmonary lesions suspected of lung cancer remain a diagnostic challenge. Despite computed tomography (CT) screening programs being implemented and a preference for minimally invasive diagnostics where possible [25–30], there are no unambiguous guidelines on the use of technology for an endobronchial approach. Over the last decade, several endobronchial techniques have become available that are able to increase the diagnostic yield of the conventional fluoroscopy guided transbronchial biopsy approach (pooled yield 31.3%) [37]. Techniques such as radial ultrasound mini-probe imaging (rEBUS), ultrathin bronchoscopy, virtual navigation bronchoscopy and electromagnetic navigation bronchoscopy (EMN) have been successfully implemented in clinical routine [34]. A meta-analysis by Wang-Memoli *et al.* showed that the diagnostic yield of these techniques ranged from 67% to 73%, and that their overall pooled diagnostic yield was approximately 70% [39]. The prospective multi-center NAVIGATE trial that evaluated EMN further substantiated this diagnostic yield in a total of 1105 patients. By EMN, in combination with fluoroscopy (91% of cases) and rEBUS imaging (57% of cases), they achieved a combined overall diagnostic yield of 73% and 67.3% in lesions smaller than 20 mm [106]. Although these are promising results when compared to the conventional transbronchial biopsy, a diagnostic yield of approximately 70% still demands further improvement.

Navigation bronchoscopy can technically be divided into three steps; navigation, confirmation and acquisition [107]. A successful diagnosis can only be obtained if all three steps are accurately performed. The integration of robotics in endoscopy is a new approach that could enhance accuracy in all three steps [108,109]. Yet, as lesions become smaller, have no bronchus sign, or are positioned at tight angulations relative to the airway, precise 3D imaging information likely becomes an essential need for accurate navigation and (transbronchial) biopsy. Furthermore, 3D information will also enable minimal invasive transbronchial treatment [107,110].

Cone beam CT (CBCT) imaging is a relatively new modality in interventional pulmonology, but, readily available as ceiling- or floor mounted C-arm system in the interventional radiology unit or hybrid operating room. CBCT Imaging allows for CT imaging as well as fluoroscopy. An initial CBCT scan does not only provide 3D information, it can be further used to delineate and overlay the lesion and pathway towards the lesion on regular fluoroscopy images (Figure 5.1 & 5.2). This overlay, also termed augmented fluoroscopy (AF), is accurately maintained in 3D during every movement of the C-arm. Repeated CBCT scans can provide exact 3D confirmation of lesion and biopsy-tool positioning. CBCT imaging can thus provide navigation guidance, confirmation of lesion access and biopsy guidance. Several recent studies investigated CBCT imaging, for its CT and fluoroscopic capabilities [111], in combination with ultrathin bronchoscopy and rEBUS [112], EMN [113,114], or transthoracic needle aspiration [115], reaching diagnostic yields of 70-84% [111–115]. However, to the best of

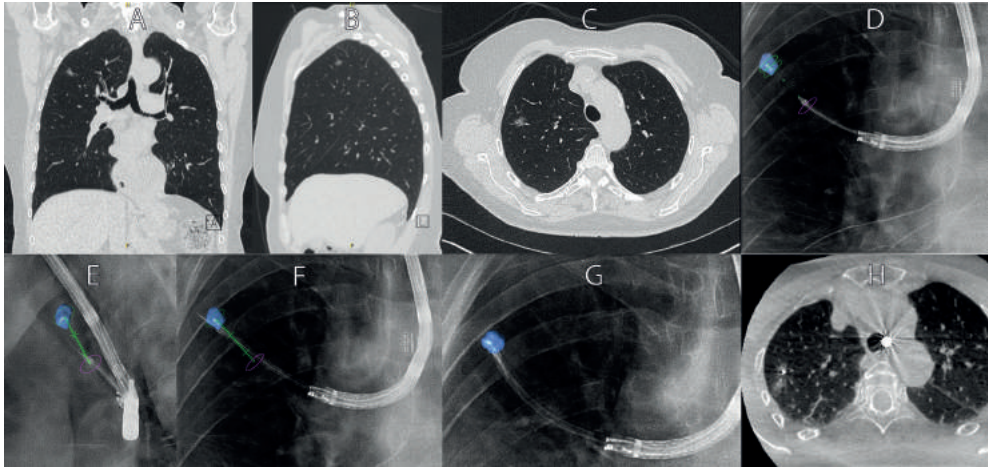


**Figure 5.1** – Case example of CBCT and augmented fluoroscopy based navigation.

Panel A: Pre-procedural PET-CT showing FDG uptake in 12x11x7 mm solid lesion in the lower right lobe, near the diaphragm. Panels B-D: Conformational CBCT after CBCT and AF based navigation. Panels E-F: Augmented fluoroscopy under two different angles for verification of biopsy positioning. Lesion delineated in blue. Envisioned endobronchial pathway as segmented on the workstation intra-procedurally augmented as purple dots. Histopathology analysis of biopsy specimens found granulomatous disease, further proven to be granulomatosis with polyangiitis through clinical follow-up.

our knowledge, no studies have systematically studied if CBCT and augmented fluoroscopy specifically improves navigation and diagnosis in an initial electromagnetic- and rEBUS-based navigation. Similarly, while multi-slice CT aided navigation bronchoscopy has been reported [111,116–120], no studies have reported how cone beam CT and an augmented fluoroscopy based navigation can provide for a do-it-all guidance modality.

In this study, we prospectively assess CBCT and AF image guidance for navigational bronchoscopy of peripheral pulmonary lesions. Using a combination of modalities in two separate workflows and utilizing a cross-over design, we investigate if: (1) CBCT with AF and rEBUS based navigation bronchoscopy can enable successful navigation and biopsy guidance, and (2) assess the added value of CBCT and AF imaging on a primary electromagnetic- and rEBUS-based navigation. In this study, navigation success is the primary outcome measure. If accessing the lesion by primary navigation methodology showed unsuccessful on CBCT imaging, a crossover between workflows was applied. The secondary outcome measure is diagnostic accuracy, relating true positives and true negatives to subjects included.



**Figure 5.2** – Case example of CBCT and augmented fluoroscopy based trans-parenchymal navigation. Panels A-C: Pre-procedural CT scan where a ground glass opacity of 10x9x6 mm in the right upper lobe is visible. Panels D-E: Multi-angle augmented fluoroscopy for verifying that the trans-parenchymal access tool is positioned correctly. Panel F: Utilizing the trans-parenchymal access tool for trans-parenchymal navigation towards the lesion. Panels G-H: After completing trans-parenchymal navigation the distal end of the catheter resides within the lesion. Histopathological analysis of biopsy specimens led to a diagnosis of adenocarcinoma in situ.

## 5.3 Materials and methods

### 5.3.1 Study subjects

This prospective single center study was approved by the local IRB. All patients with a peripheral pulmonary lesion suspected of lung cancer with an indication for minimally invasive biopsy were eligible for study inclusion. Clinical indication to perform a minimally invasive biopsy followed local clinical practice and was defined in our multidisciplinary tumor board in accordance to international guidelines [32]. Patients were eligible after informed consent was obtained and contra-indications for endobronchial procedures were absent. Patients with lesions that could be diagnosed without the need for any navigation guidance (i.e. <math><5^{\text{th}}</math> generation endobronchial lesions or mediastinal lymph node involvement on PET-CT) were excluded for this study. There was no further pre-selection for study inclusion based on patient or lesion characteristics. Randomization into one of both study arms was determined by CBCT scanner room availability, which alternated weekly. The primary CBCT-based workflow utilized a ceiling mounted Philips Allura Clarity FD20 scanner (Philips, Best, The Netherlands). The primary EMN-based workflow utilized Medtronic's SuperDimension EMN system (version 7.0, Medtronic, Minneapolis, USA) in combination with the floor mounted Siemens Artis Zeego CBCT system (Siemens Healthineers, Forchheim, Germany). See Figure 5.3 for a CONSORT flow diagram of subject inclusion.

### 5.3.2 Study design, materials and methods

Pre-procedural CT ( $\leq 1.0$  mm resolution) and/or PET-CT imaging was available in all patients. The pre-procedural CT was used to plan a navigation trajectory on the EMN planning platform irrespective of the primary study approach. Procedures were performed under general anesthesia, preferably via laryngeal mask (and if deemed impossible, by endotracheal tube). Standard flexible video bronchoscopes with 2.8 mm working channel were used for inspection bronchoscopy and consecutive catheter guidance (EB19-J10, Pentax Medical, Tokyo, Japan).

The primarily CBCT-based navigation started with an inspection bronchoscopy and a first CBCT scan (8s roll, Lungsuite, Philips) to identify and segment the lesion and pathway. The 3D segmentations were automatically overlaid during fluoroscopy at any given angle. This augmented fluoroscopy (AF) under multiple angles in combination with a rEBUS-based (UM-S20-17S Radial EBUS miniprobe, Olympus, Tokyo, Japan) confirmation was used for 3D guidance (Figures 5.1 & 5.2). Straight catheters with steerable curette (Guide sheath kit, Olympus, Tokyo, Japan) or catheters with pre-formed curvature (Medtronic Extended Working Channel, Minneapolis, USA) were used to navigate. Additional CBCT scans were made if AF confirmed positioning while rEBUS imaging remained uncertain, or vice versa. After confirming accurate positioning, tissue sampling was performed under AF-guidance. If the CBCT and AF-based approach remained unsuccessful, additional EMN guidance was added (cross-over).

The primary EMN workflow utilized the pre-procedurally segmented CT based pathway from the EMN planning platform for navigation guidance. After inspection bronchoscopy, the EMN system was calibrated. Navigation was consecutively performed per manufacturer's instruction using catheters with pre-formed curvature (Medtronic Extended Working Channel, Minneapolis, USA). If positioning was estimated to be accurate by the EMN system, the sensor was exchanged for the rEBUS probe. If rEBUS imaging confirmed lesion access, further confirmatory CBCT imaging was performed (6s roll, Syngo DynaCT, Siemens Healthineers). If no confirmation was obtained after repeated EMN and rEBUS-based attempts, CBCT scanning was performed to assess needed repositioning. Once a CBCT was performed, CBCT and AF imaging were used for subsequent biopsy guidance, and if necessary; navigation guidance (cross-over).

When endobronchial access showed difficult in either approach, trans-parenchymal access was pursued. In all cases, this was done with help of CBCT and AF. Tools to facilitate trans-parenchymal access varied, from TBNA needles and consecutive guide sheaths to using a dedicated device (Cross-Country needle, SuperDimension).

After successful navigation, tissue sampling was performed using commercially available tools in an identical order: brush when central in lesion, followed by needle and forceps

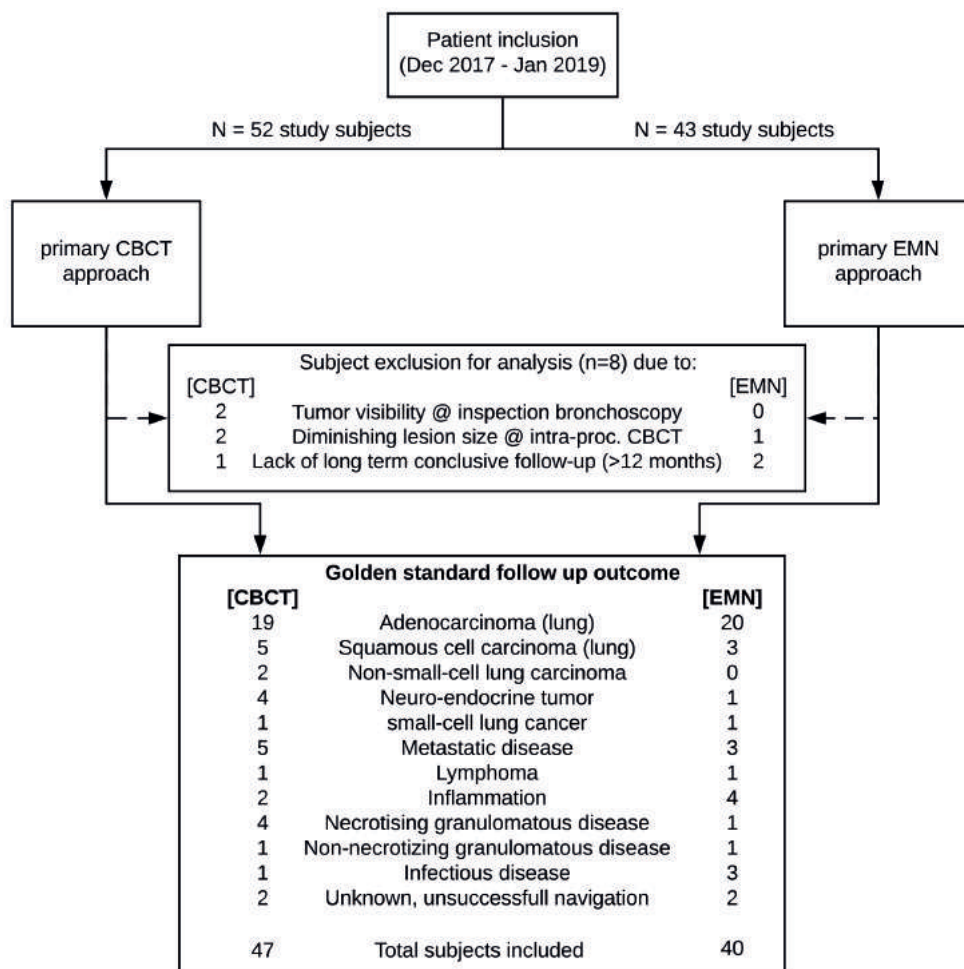


biopsy for all others, then if possible and deemed safe; cryobiopsy. Rapid on-site evaluation of cytopathology (ROSE) was always available for confirming lesion access. Histology samples were obtained regardless of ROSE outcome.

### 5.3.3 Analysis

All procedural actions, conclusions, considerations and their timing were noted. Procedural follow-up outcomes were found through electronic health records. Navigation outcome was termed 'centered' if CBCT imaging unambiguously showed center lesion access of tools. Navigations were termed 'in contact with' if CBCT imaging showed tool contact with the outer boundary of the lesion, but not a central access of the lesion. Navigations were termed unsuccessful if intra-procedural CBCT verification showed the lesion was not reached. Navigation success was thus defined as CBCT imaging confirmed tool positioning residing centrally within the lesion or in contact with the lesion (range: central – in contact with – unsuccessful). The diagnostic accuracy was defined on a patient level, where the count of true positive and true negative findings (i.e. analysis of at least one nodule corresponding to follow-up outcome) are related to the total amount of patients included. In case tissue biopsy showed malignancy, it was considered a true positive diagnosis. In case tissue biopsy was found to be benign or non-representative (e.g. blood, normal lung tissue), follow up with CT guided trans-thoracic needle aspiration, surgical biopsy or unambiguous long-term monitoring outcome (i.e.  $\geq 12$  months) served as gold standard to provide false- or true negative diagnostic procedural outcome.

Statistical programming language R and Rstudio were used for analysis [68]. Our sample size calculation showed that, to prove a 70% diagnostic accuracy with 15% margin of error and 95% confidence and be further able to directly compare approaches by cross-over design, a minimum sample size of 40 in every study arm was needed. A binomial proportions test using Pearson's chi squared test statistics was performed to assess if a study approach had significantly better chance of success ( $p < 0.05$ ). A student's t-test was used to compare means.



**Figure 5.3** – CONSORT FLOW diagram of study in- and exclusion.

## 5.4 Results

Between December 2017 and January 2019, 87 study subjects were included. Subject inclusion rate for both study arms unexpectedly varied due to altering room availability, resulting in a slightly higher inclusion in the CBCT arm (Table 5.1, Figure 5.3). A total of 8 study subjects were excluded from analysis due to the following reasons: visible tumor during inspection bronchoscopy (n=2); considerably altered lesion dimensions at procedural imaging (indicative of infectious disease rather than malignancy, n=3); and lack of sufficient follow-up (n=3). In the primary CBCT and AF based approach, 47 patients and 59 lesions were included. Combined, these lesions had a mean long axis diameter of 16.6 mm (1.12 cm<sup>3</sup> median volume). In the primary EMN approach, 40 patients and 48 lesions were included. Their mean lesion long axis diameter was 14.2 mm (0.80 cm<sup>3</sup> median volume). Detailed

patient and lesion characteristics are summarized in Table 5.1. A comparison of essential parameters showed that malignancy prevalence, lesion volume and bronchus sign presence did not significantly differ between study arms.

**Table 5.1** – Patient and nodule characteristics across both study arms. <sup>1</sup> not significantly different between study arms. <sup>2</sup> Bronchus sign as assessed on pre-procedural CT ( $\leq 1$  mm slice thickness) related to navigation outcome (range: within-edge-unsuccessful) as found by CBCT imaging. Abbreviations: LUL – Left Upper Lobe, RUL – Right Upper Lobe, RML – Right Middle Lobe, LLL – Left Lower Lobe, RLL – Right Lower Lobe.

Study characteristics	Primary CBCT and AF approach		Primary EMN approach	
Patients (male / female)	47 (16 / 31)		40 (20 / 20)	
Age (min – max)	65 years (41-85 years)		65 years (44-81 years)	
Lesions	59		48	
Malignancy prevalence <sup>1</sup> (lesions / study subjects)	83% / 83%		72.9% / 72.5%	
Median lesion volume <sup>1</sup>	1.12 cm <sup>3</sup> (0.05-19.90 cm <sup>3</sup> )		0.80 cm <sup>3</sup> (0.15-18.80 cm <sup>3</sup> )	
Mean long axis diameter <sup>1</sup>	16.6 mm (5–43 mm)		14.2 mm (7-48 mm)	
Bronchus sign <sup>1,2</sup> (@ $\leq 1$ mm CT)	62.7%		70.8%	
Within lesion navigations	71.1% (32/45)		77.8% (28/36)	
In contact with lesion	25% (2/8)		50% (3/6)	
Unsuccessful navigations	50% (3/6)		50% (3/6)	
Lesion locations	Overall	Malignant	Overall	Malignant
LUL / RUL	9 / 29	7 / 25	15 / 15	13 / 11
Lingula / RML	1 / 3	1 / 2	1 / 2	0 / 2
LLL / RLL	8 / 9	6 / 8	5 / 10	2 / 7

### 5.4.1 Navigation success

Navigation success rate using CBCT with AF and rEBUS as primary guidance modality was 76.3%, which is significantly better than that of the primary EMN- and rEBUS-based approach, being 52.2% ( $p=0.016$ , Table 5.2). The addition of EMN sensor guidance to the primary CBCT-approach improved navigation success from 76.3% to 89.9% per lesion (+13.6%,  $p=0.043$ ). Oppositely, addition of CBCT and AF guidance led to a 35.3% increase in navigation success in the primary EMN-approach, from 52.2% to 87.5% per lesion ( $p=0.0002$ , Table 5.2). Performing a primary CBCT and AF-based navigation resulted in a significantly higher fluoroscopy time and number of CBCTs when compared to a primary EMN approach (Table 5.3). A bronchus sign (based on  $\leq 1$  mm resolution CT) was found less often in unsuccessful navigations and navigations only in contact with the lesion (42% of cases vs 66.4% overall,  $p=0.006$ , Table 5.1).

### 5.4.2 Diagnostic accuracy

Whereas combining all navigation modalities (rEBUS, EMN, CBCT) resulted in an overall navigation success in 93% of patients, the overall diagnostic accuracy in the combination of both study arms was significantly lower (72.4%,  $p=0.0007$ ). The diagnostic accuracy with the combined use of technologies was 70.2% and 75% for the primary CBCT- and EMN-arm, respectively ( $p=0.797$ , nonsignificant difference). For this, a mean of approximately 10 biopsies were taken using 3.4 different biopsy tools across both study arms. Using this combination of biopsy tools with intermittent image verification took approximately 24 minutes in both study arms (Table 5.3).

### 5.4.3 Navigation time

Average navigation time across study arms was 27.4 minutes (Table 5.3). Navigation time in the EMN arm was considerably higher than in the CBCT arm, largely due to the calibration time of the EMN system (5.7 minutes). In both arms a CBCT was made for verification in all but three primary EMN cases, where rEBUS combined with fluoroscopy gave unambiguous confirmation and the operator decided to perform first sampling preceding to CBCT verification, which then showed malignancy in ROSE. The time to obtain a CBCT was different in both study arms, using the two different systems. It took an average of 7.9 minutes on the floor mounted system (EMN-arm) and 4.3 minutes for the ceiling mounted system ( $p<0.0001$ , CBCT-arm, Table 5.3). Segmenting the lesion and pathway for augmentation on the work station after having obtained a CBCT was often done in parallel with other procedural tasks. This took an average of 6.4 minutes on the floor mounted system and 5.3 minutes on the ceiling mounted system (time from having obtained CBCT to first use of AF by physician, non-significant differences).

### 5.4.4 Added navigation guidance

Reasons to add EMN-guidance in the CBCT-arm were a need for guidance combined with catheter steerability ( $n=7$  patients) and one case where the pathway on pre-procedural planning could not be found during intra-operative CBCT imaging. Causes for adding CBCT and AF-imaging to the EMN arm were cases where the planned pathway was shown incorrect intra-procedurally ( $n=2$ ), where EMN had difficulty distinguishing multiple parallel bronchi ( $n=1$ ), EMN and rEBUS suggested having reached the location whilst CBCT imaging showed inaccurate positioning ( $n=5$ ), EMN guidance showed inaccurate due to tissue displacement (because of e.g. lower segment breathing motion or due to scope induced tissue manipulation,  $n=4$ ), or need for a trans-parenchymal approach ( $n=6$ ).

**Table 5.2** – Navigation outcome and diagnostic outcome for both study arms. The navigation outcome corresponds to the navigation success of the primary workflow on a per lesion basis. Navigation success was determined by tools proving center lesion access ('Center') or tools being in contact with but not centered within the lesion ('In Contact'). The 'Combined with EMN / CBCT' row showcases outcome when all guidance modalities (CBCT + AF + EMN + rEBUS) were used in combination. The diagnostic accuracy is on a per subject basis (number of subjects between brackets).

Navigation outcome	Primary CBCT and AF approach			Primary EMN approach		
	Center	In Contact	Total	Center	In Contact	Total
Primary navigation	66.1%	10.2%	76.3% <sup>1</sup>	50.1%	2.1%	52.2% <sup>1</sup>
Combined with EMN / CBCT	+10.2%	+3.4%	+13.6% <sup>2</sup>	+25.0%	+10.4%	+35.4% <sup>2</sup>
Total (per lesion)	76.3%	13.6%	89.9% <sup>3</sup>	75.0%	12.5%	87.5% <sup>3</sup>
Total (per subject)	87.2%	8.5%	95.7% <sup>3</sup>	75.0%	15.0%	90.0% <sup>3</sup>
<b>Diagnostic accuracy (subject)</b>	<i>Overall</i>			<i>Overall</i>		
Primary navigation	61.7% (29)			50% (20)		
Combined with EMN / CBCT	+8.5% (4)			+25% (10)		
Overall	70.2% <sup>4</sup> (33)			75% <sup>4</sup> (30)		

<sup>1</sup> Significant navigation success difference between arms (p=0.016).

<sup>2</sup> Significant increases in navigation success by addition of EMN- to primary CBCT-based guidance and by addition of CBCT to primary EMN-based guidance (p=0.043 and p<0.01, respectively).

<sup>3</sup> Nonsignificant differences in final navigation success between study arms.

<sup>4</sup> Diagnostic accuracy significantly lower than navigation success (p<0.01, but non-significant differences between study arms).

### 5.4.5 Trans-parenchymal navigation

In both study arms combined, a trans-parenchymal approach was performed in 18 lesions. CBCT Image guidance was used in all these cases (Figure 5.2). In the EMN arm, trans-parenchymal navigation was successful in 5 out of 8 lesions, with 4 leading to an accurate diagnosis. In the CBCT arm, it was successful in 8 out of 10 cases, resulting in an accurate diagnosis in 7 cases.

### 5.4.6 Complications

Observed complications across both study arms were; pneumothorax (n=3), COPD exacerbation following the procedure (n=1), moderate bleeding intra-procedurally following cryobiopsy (n=1) and minor fever (<4 hrs, n=1). All study subjects – except one pneumothorax requiring chest tube and one case of COPD exacerbation – were able to return home the same day.

**Table 5.3** – Procedural tool use and timing. Average times and counts as derived from procedural report forms. Minimum to maximum range in between brackets. Navigation time definition: from start of navigation modality until decision to start biopsy. Primary EMN navigation also includes the calibration process in timing. Biopsy time definition: From stop of navigation until the last biopsy was taken. Biopsy tools and samples are calculated from lesions where at least one biopsy was taken. CBCTs and fluoroscopy time derived from total amount of procedures. Abbreviations: NS – nonsignificant.

Procedural characteristics	Primary CBCT and AF approach	Primary EMN approach	p
Navigation time	26.9 min (2-69 min)	35 min (4-74 min)	0.039
EMN system calibration time	-	5.7 min (3-11 min)	-
Biopsy time	22.4 min (9-55 min)	25.5 min (2-50 min)	NS
Number of biopsy tools	3.11 (1-7)	3.69 (1-7)	0.042
Number of tissue samples	10.0 (1-23)	9.1 (1-18)	NS
CBCTs made	2.19 (1-5)	1.49 (0-3)	0.0014
CBCT preparation time	4.3 min (2-10 min)	7.9 min (3-11 min)	<0.0001
CBCT segmentation time	5.3 min (2-10 min)	6.4 min (2-14 min)	NS
Fluoroscopy time	9.9 min (1-22 min)	7.3 min (2-23 min)	0.021

## 5.5 Discussion

We show that CBCT and augmented fluoroscopy-based 3D image guidance can be used successfully as a primary tool for navigation bronchoscopy. The addition of CBCT and AF imaging to a workflow where EMN and rEBUS are already being used furthermore significantly improved navigation success. By combining all available guidance modalities, almost 90% of small lesions in these patients were reached. As a single guidance modality, CBCT augmented fluoroscopy guidance had a significantly higher navigation success than EMN-guidance, but, required higher radiation dosage. However, the overall diagnostic accuracy remains considerably lower than the navigation success in both study arms. Improving the tissue acquisition methodology may be crucial to enhance navigation bronchoscopy success.

The discrepancy between navigation success and diagnostic accuracy as found in this study, is significant. We believe that the rigidity of the tools used for sampling, breathing motion and movement due to manipulation of the endoscope and catheter are likely to cause small displacements and thus reduce diagnostic accuracy. In our centimeter sized lesions, the used EMN system was often found inaccurate. Chen *et al.* reported an average of 17.6 mm lesion movement from inspiration to expiration, which is larger than our average lesion long axis diameter [121]. To our opinion, the lack of intuitiveness in combining multiple modalities and tools may be additional important factors in the diagnostic accuracy. In that regard EMN guidance is a useful tool, building on pre-existing endoscopic imaging experience, whilst CBCT based navigation is likely more susceptible to a learning curve. We furthermore cannot assess if other commercially available EMN systems would have resulted in different

findings. Similarly, we do not know if other technology such as robotic bronchoscopes or far smaller bronchoscopes with an outer diameter of <3 mm would have improved both navigation and diagnostic outcome. That being observed, we hypothesize that the combined use of technology needs to become further integrated, adaptive and intuitive.

While the discrepancy in navigation success to diagnostic accuracy might be caused by tool use [41, 122], we did not design the study to compare differences in tool outcome. In this study we however did aim at performing systematic specimen acquisition by using tools in an identical order (brush when central in lesion, followed by needle and forceps biopsy for all others, then if possible and deemed safe; cryobiopsy). In all cases, we had both CBCT-imaging and ROSE available for confirmation of biopsy accuracy. While CBCT had proven lesion access, we found that ROSE often did not provide unambiguous outcome. Despite this observation, in the majority of cases our final analysis would prove diagnostic. A finding also reported by others [122]. Interestingly, Pritchett and colleagues describe fully relying on ROSE while performing repeated attempts and report an impressive diagnostic yield of 83.7% in 93 lesions with 16.0 mm median size [113].

We corroborate previous findings that both lesion size and bronchus sign presence are stringent indicators of navigation success [39,123]. Yet, the presence of a bronchus sign remains subject to debate as it correlates to CT imaging quality and observer interpretation. A bronchus sign that can only be identified by repeatedly following branching of the bronchial tree on high resolution CT with 0.5 mm slice thickness is likely invisible on a coarser 3 mm slice thickness reconstruction.

Utilizing CBCT and AF provides for the option to meticulously reposition and verify access. This is not only essential for gaining accurate trans-parenchymal access but also when performing and monitoring endoscopic treatments [114,124,125]. A trans-parenchymal approach in 18 cases had 72% navigation success leading to an accurate diagnosis in 61% of cases in our study. During the conduct of the study, we were limited to only two differently curved catheters. We feel that the lack of availability of catheters with higher curvature or active steerability prevented lesion access in several cases, as was also postulated by others [109,113].

This study assigned patients to a clinical workflow based on hybrid-OR availability. Due to unanticipated variations in room availability, the group size ended unequal. Since the essential parameters affecting navigation outcome (i.e. lesion volume and bronchus sign presence) were found insignificantly different we feel this did not influence our conclusion. Furthermore, in every primary EMN case, rEBUS was extensively attempted. Only when proven inaccurate with CBCT, additional CBCT image guidance was used. Having CBCT imaging and AF available could have affected our decision making. Additionally, once a confirmation CBCT was made in either study arm, AF was routinely used. It is likely that

the addition of AF enhanced EMN diagnostic accuracy and procedure time, as it provided additional biopsy guidance.

## **5.6 Conclusions**

Cone beam CT and augmented fluoroscopy imaging are highly valuable as a stand-alone means of guiding endobronchial navigation towards peripheral pulmonary lesions. Furthermore, CBCT imaging can significantly enhance navigation success in a workflow where EMN and rEBUS are already being used. While navigation success using all guidance modalities is high, the diagnostic accuracy was significantly lower. Improving the tissue acquisition methodology may be crucial to further enhance navigation bronchoscopy diagnostic accuracy in the future.

## **5.7 Statement of Ethics**

The research was conducted ethically in accordance with the latest World Medical Association Declaration of Helsinki. The study protocol was approved by the independent local medical ethical committee (Arnhem-Nijmegen) and institutional review body before start of subject inclusion. Informed consent was obtained. The study is registered and can be found on ClinicalTrials.gov (identifiers NCT03355586 & NCT03274609).

## **5.8 Acknowledgements**

The authors wish to acknowledge and thank for the support and help given to us by our endoscopy, anesthesia, radiology and pathology team as well as our statistics department and hospital administration. We are appreciative of the technical advice and support from William van der Sterren, Stephanie Schampaert, Lucia Fonseca, and Alessandro Radaelli from the Philips Imaged Guided Therapy team. We further would like to thank the Siemens Healthineers team for their support. The results of this study have been presented as oral presentations at both the 2019 IASLC world conference in Barcelona and the 2019 ERS congress in Madrid. Interim (preliminary) results have furthermore been presented at the 2019 European Congress for Bronchology and Interventional Pulmonology in Dubrovnik.









# CHAPTER 6

Multi-modal tissue sampling in cone beam  
CT guided navigation bronchoscopy; the accuracy  
of different sampling tools and rapid on-site  
evaluation of cytopathology

**Authors**

R.L.J. Verhoeven, S. Vos, E.H.F.M. van der Heijden

*Submitted, 2020*

## 6.1 Abstract

### Introduction

Advanced technological aids are frequently used to improve outcome of transbronchial diagnostics for peripheral pulmonary lesions. Even in cases where lesion access has been confirmed, obtaining an accurate tissue sample however remains difficult.

### Research question

What is the accuracy of different sampling tools and the value of rapid on-site evaluation of cytopathology (ROSE) in navigation bronchoscopy cases where 3D-imaging has confirmed lesion access?

### Methods

Navigation bronchoscopies where lesion access had been verified by cone beam CT and augmented fluoroscopy were included. Individual tool outcomes were compared against one another and follow-up outcome. Clinical decision-making determined tool use and sampling.

### Results

A mean of 11.39 samples using 2.93 tools were obtained in 225 lesions (median diameter 15 mm, 195 patients). An accurate diagnosis was most often obtained by forceps (accuracy 70.6%), followed by 1.1 mm cryoprobe (68.4%), needle aspiration (46.7%), 1.9 mm cryoprobe (41.2%), brush (30.3%) and lavage (23.7%). Procedural outcome corresponded to follow-up outcome in 75.1% of lesions (80.5% of patients). Accurately diagnosed lesions were subjected to significantly more sampling (11.91 vs 9.72 samples,  $p=0.014$ ). In cases where procedural outcome proved malignant, ROSE had also detected this in 47.5%.

### Interpretation

Extensive multi-modal sampling resulted in highest diagnostic accuracy. A hypothetical multi-modal approach of only using forceps and needle aspiration provided eventual diagnostic outcome in 91.7% of successfully diagnosed lesions. Confirmation of malignancy on ROSE did not reduce number of biopsies taken nor biopsy time. Future research on how to improve the accuracy and effectivity of tissue sampling is needed.

## 6.2 Introduction

Despite the development and introduction of several technological platforms to help guide the physician in the past two decades, obtaining an accurate endobronchial diagnosis of small peripheral pulmonary nodules remains a challenge. These platforms allow for both navigation guidance towards a lesion as well as confirming accurate lesion access, which become increasingly important as lesions are small sized and located peripherally in the lung. Techniques include ultrathin bronchoscopy, virtual navigation bronchoscopy, electromagnetic navigation, radial endobronchial ultrasound probes (rEBUS), robotic assisted bronchoscopy and cone beam CT imaging (CBCT) [32,34,39,41,108,109,113,126–128].

Unfortunately, a confirmed successful navigation does not warrant a representative and accurate diagnosis. Several studies report the diagnostic yield being lower than that of navigation success [41,115,122,128]. A study by Coghlin *et al.* shows that the mean % area of samples obtained from visible endobronchial lung cancer on histopathology was only 33.4% and found that 52% of patients had one or multiple fragments collected which contained no tumor at all. As lesions become smaller and are of early stage, the margin of error and the nuance become smaller, and likely even less samples will reveal the true lesion origin.

Obtaining accurate tissue samples for analysis is made difficult due to small lesion size, tumor heterogeneity, and, the ability of making a clear distinction in (early state) disease pathology in samples of limited size. The concurrent decision-making process on which tissue sampling methodology to use and deciding on when sufficient material has been collected add to this complexity. Additional general characteristics influencing the likelihood of a diagnostic outcome are the positioning relative to the bronchus, lobes involved, solidness, malignancy presence, pleural distance and patient characteristics such as emphysema or other comorbidity [34,37,123,129–135]. As two editorials recently concluded, there's however insufficient evidence to – in general - prefer one overall tissue acquisition method over the other, while several studies comparing individual technologies and concurrent methodologies have been published to date [41,129]. Multiple studies suggest trans-bronchial needle aspiration (TBNA) has good outcome [129–131], while the brush, forceps and cryobiopsy probes are other commonly available and successfully used means [41,129,131,134,136–138]. One further promising addition to the routine tissue sampling methodology is Rapid On-site Evaluation of cytopathology (ROSE), providing on-site information on cytology aspirate representativeness and the possibility of malignancy. It may enhance diagnostic yield and reduce complication rates in transbronchial and endobronchial sampling, although there is contradiction in results [139–141].

In this single institution study, we assess the different tissue acquisition methodologies and the value of ROSE in a cohort of patients whom have been navigated to by CBCT guided navigation bronchoscopy for small peripheral pulmonary nodules. This allows for a unique

analysis, as the 3D CBCT image verification provides for analysis of those lesions which have shown to be accurately accessed. By relating biopsy tool outcomes per lesion, a direct paired comparison of tools is enabled whilst simultaneously incorporating clinical decision making on tool use. Combined, we report on overall diagnostic tool accuracy and agreement of ROSE with final pathology outcome in a navigation bronchoscopy setting.

## **6.3 Methods**

### **6.3.1 Study subjects**

All patients receiving a navigation bronchoscopy under guidance of CBCT for diagnosis of a peripheral pulmonary lesion in the period of December 2017 – June 2020 were eligible and prospectively approached for written informed study consent. Study approval was obtained by the local institutional review board. Patients whom did not finally receive a navigation with CBCT imaging (and augmented fluoroscopy), patients in which a navigation setting was deemed unnecessary due to endobronchial findings, or, patients in whom the lesion could not be successfully reached as verified by 3D CBCT, were excluded for analysis. After exclusion, only study subjects and concurrent lesions for which successful lesion access had been verified remained for analysis (Figure 6.1).

### **6.3.2 Materials and Methods**

Conventional bronchoscopes with 2.8 mm working channel (EB19-J10, Pentax Medical, Japan) and consecutive 2.6 mm catheters (Olympus medical guide sheath, Tokyo, Japan & Medtronic extended working channels, Minneapolis, USA) were used to navigate. Navigation was performed by one or a combination of electromagnetic navigation guidance (Medtronic SuperDimension), rEBUS (Olympus UM-S20-17S) and CBCT imaging with augmented fluoroscopy (Philips Allura/Azurion, Best, The Netherlands or Siemens Zeego, Forcheim, Germany). The procedures took place under general anaesthesia. After navigation, lesion access was verified by one or a combination of rEBUS, CBCT and augmented fluoroscopy.

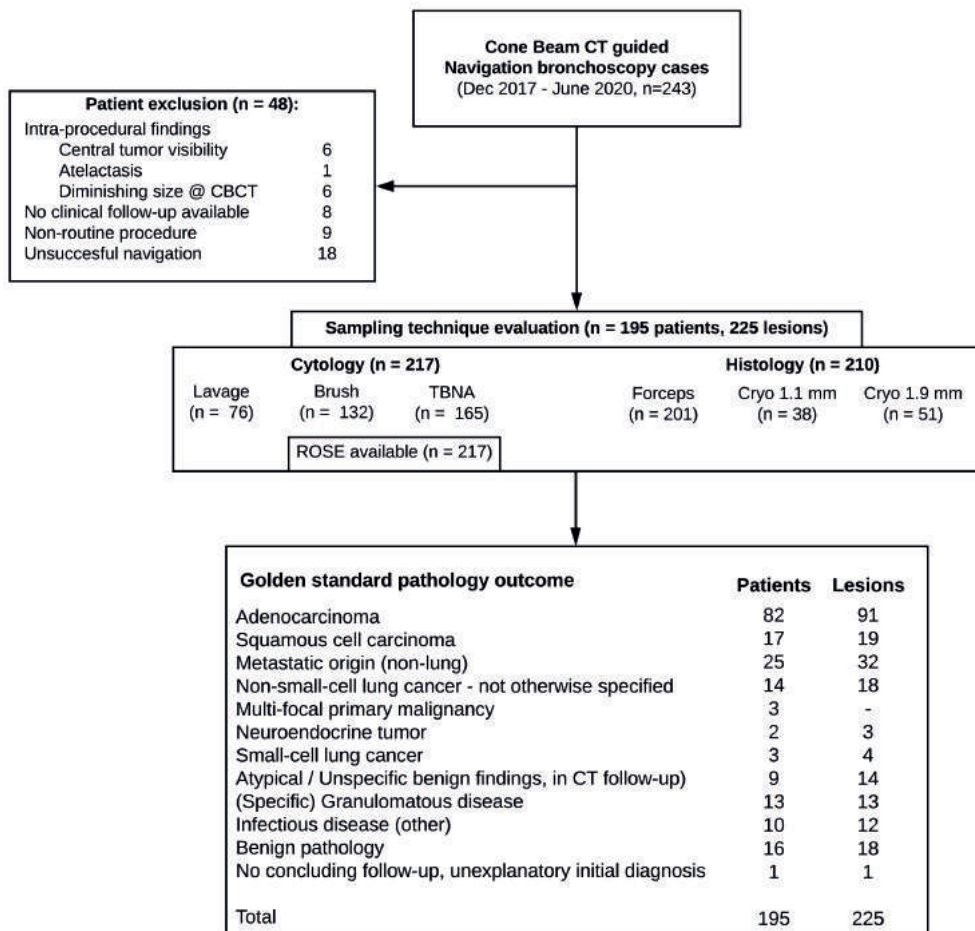
After confirming navigation success, the catheter remained positioned near or within the lesion throughout biopsy specimen acquisition. Biopsy specimen acquisition was performed with intermittent augmented fluoroscopy, CBCT and/or rEBUS imaging. All tool use and the amount of sampling was decided upon by the endoscopy team while taking into account factors such as safety, hypothesized efficacy, intermittent ROSE outcome and lesion characteristics. With the tools that were decided upon, biopsy specimen acquisition was routinely performed in the following order; lavage, brushing, TBNA, followed by forceps and/or cryobiopsy. Lavage included injection of up to 60 ml of 0.9% saline through the catheter or endoscope and subsequent retrieval by aspiration until more than 20 ml had been retrieved for analysis. Brushing for cytopathology was performed by a pushing-pulling technique of the complete tool or retraction-insertion of the 1.8 mm brush in and out of the catheter

(Olympus BC-202D-2010 brush, Medtronic SuperDimension cytology brush or Medi-globe cytology brush, Achenmühle, Germany). Needle aspiration was predominantly performed with 18G needles (Broncus FlexNeedle, San Jose, USA) by means of a similar motion as to that of the brush, with suction being applied by syringe proximally. Twenty-one gauge and 19G needles of other manufacturers were less often used, based upon commercial primary needle availability (Medtronic SuperDimension Aspirating Needle). Serrated or non-serrated oval forceps of 1.8 mm diameter were used to acquire histology specimens (Boston Scientific Pediatric Radial Jaw 4 or Olympus FB-233D biopsy forceps). After advancement through the catheter, the forceps were opened and further pushed into the lumen until traction could be felt, after which they were closed and retracted for histology specimen collection. Cryobiopsy for histopathology was available only through a 1.9 mm cryoprobe until September 2019, after which a 1.1 mm version also became available (Erbe Elektromedizin, Tuebingen, Germany). Due to probe and sample size, the 1.9 mm cryoprobe had to be removed along with catheter and endoscope after an initial freeze of 4-7s. Oppositely, the catheter could be left in place for repeated sampling with the 1.1 mm cryoprobe. Freezing during 5-9s was followed by removal of the 1.1 mm probe for histopathology collection.

Individual cytology samples were divided onto two slides; one Giemsa staining which was also used for ROSE and one slide for Papanicolaou smearing used only for definitive analysis. Remaining material was collected for cell block. Separate collection containers were used for every sampling tool. ROSE was available for all cases, which in our center is performed by trained cytopathology technicians.

### **6.3.3 Analysis**

Descriptive parameters are presented as counts and percentages, along with medians, means and ranges. All individual nodules in which sampling was performed were correlated to a procedural outcome and a golden standard follow-up outcome. Golden standard follow-up was either a surgical resection, additional CT guided TTNA and/or clinical follow up combined with CT for at least 6 months. The comparative accuracy of tools was determined by pairing tool outcome in cases of individual lesions where two or more tools were used. The McNemar chi-squared test was used to test equivalence of tool accuracy. Wilcoxon testing was performed for comparison on not-normally distributed data. Student's t-Tests were used to test accuracy differences between unpaired data. Tests with a p-value of <0.05 were considered significant. For evaluation of ROSE, all procedures where a malignant pathology was found and ROSE was performed were included for analysis. The concordance of overall malignant ROSE outcome by all cytological specimens was compared with both final cytology as well as histology outcome. R and RStudio were used for statistical analysis [68].



**Figure 6.1** – Flow diagram on study inclusion. Unsuccessful navigations were classified as those where imaging showed that the lesion was not successfully reached. A non-routine procedure indicated the primary reason for navigation bronchoscopy was other than diagnostics or different than normal procedural work-up due to study or clinical causes. ROSE was available only per analysis of brush and TBNA smears. Abbreviations: TBNA – Trans-Bronchial Needle Aspiration, ROSE – Rapid On-Site Evaluation of cytopathology.

## 6.4 Results

A total of 195 patients received successful navigation bronchoscopy as verified by CBCT and augmented fluoroscopy imaging, in which a total of 225 lesions were successfully reached (Figure 6.1, Table 6.1). Overall, 76% of patients were diagnosed with malignant disease. Median lesion diameter was 15.0 mm (range 5-65 mm).



**Table 6.1** – Patient, lesion and procedural characteristics. Abbreviations: LUL – Left Upper Lobe; RUL – Right Upper Lobe; RML – Right Middle Lobe; LLL – Left Lower Lobe; RLL – Right Lower Lobe.

Patients, lesions and procedural characteristics		
Patients / Lesions (successfully accessed)	195 / 225	
Age (mean, range)	65.2 (36-85)	
Gender	65.2 (36-85)	
Malignancy prevalence (pt. / lesion)	76% / 75%	
Nodule size (median, range)	15 mm (5-65 mm)	
Bronchus sign (lesion)	64.4%	
Diagnostic accuracy procedure	80.5% (157/195)	
Diagnostic accuracy lesion	75.1% (169/225)	
Lesion locations	LUL / RUL	62 / 77
	/ RML	/ 11
	LLL / RLL	32 / 43

### 6.4.1 Cytology and histology accuracy

The gold standard outcome corresponded to procedural outcome (whilst navigation had showed successful) in 80.5% of cases on a per patient basis, and 75.1% of cases on a per lesion basis. The cytology findings (lavage, brush, TBNA) corresponded to gold standard follow-up outcome in 49.3% of lesions (107/217, Table 6.2). Histology findings (by forceps and cryobiopsy) were more often found accurate (72.4%), but the combination of both cytology and histology remained most accurate (75.1%). Analysis of data wherein both cytology and histology were obtained shows histology was significantly more often accurate, be it either malignant or benign (Table 6.2, p-value <0.01). The histology outcome by itself was significantly more often accurate in benign lesions than in malignant lesions (p<0.01, 88.6% vs 66.9%, respectively). This finding did not similarly hold for cytology outcome (48.5% accuracy in benign lesions and 51.9% accuracy in malignant lesions, Table 6.2).

### 6.4.2 Tissue sampling method accuracy

Repeated sampling and choice of biopsy method were based upon clinical decision making. Analysis of sampling method accuracy shows lesions whom were accurately diagnosed were subjected to a significantly higher amount of sampling (Tables 6.3, p=0.014). An average of 3.83 separate cytology samples (range 0-15) and 7.56 separate histology samples (range 0-18) were acquired per procedure, equivaling an overall average of 11.39 samples (range 1-25). Collection of samples by forceps and 1.1 mm cryobiopsy was performed an average of 7.08 and 6.12 times per lesion, respectively. Brush and TBNA – both enabling ROSE – were used for repeat sampling a respective average of 1.64 and 3.26 times. Forceps biopsy was most often found accurate (70.6%), followed by 1.1 mm cryoprobe findings (68.4%), TBNA (46.7%), 1.9 mm cryoprobe (41.2%) and tiers brush (30.3%) and lavage (23.7%). Further pair-wise tool comparison substantiated these accuracy findings (Table 6.4). The forceps showed superior accuracy when compared against all cytology techniques (lavage,

brush, TBNA,  $p < 0.01$ ), but did not show significantly better than cryobiopsy ( $p = 0.081$ ). Cryobiopsy showed significantly better accuracy than that of lavage and brush ( $p < 0.05$ ), but not TBNA ( $p = 0.40$ ). The 1.1 mm cryoprobe was more often accurate than the 1.9 mm cryoprobe (68.4% vs. 41.2%, respectively).

### 6.4.3 Multi-modal sampling analysis

Overall outcome showed that forceps and TBNA sampling were used most often, respectively having been used in 89.3% and 73.3% of lesions (Tables 6.3 & 6.4). Analysis of a multi-modal sampling approach revealed sampling using forceps combined with TBNA would have provided eventual diagnostic outcome in 155 out of 169 successfully diagnosed lesions (91.7%). In the cases where these were not diagnostic, sampling by 1.1 mm and 1.9 mm cryoprobe correctly diagnosed 2 and 8 lesions whilst brushing and lavage were accurate in 4 and 3 lesions, respectively.

**Table 6.2** – Sampling outcome (per lesion) versus procedural and follow-up gold standard outcome. Results of Rapid On-Site Evaluation (ROSE) of cytopathology are described specifically for malignant disease findings as found per procedural cytopathology outcomes and overall procedural outcomes (being malignant). As clinical decision making decided on tool use, only cases where cytology or histology was available were used for calculation of accuracy. <sup>1</sup> Significant differences ( $p$ -value  $< 0.01$ , McNemar chi-squared test) between accuracies of cytology and histology in benign, malignant and lesions overall were found when assessing paired outcomes. <sup>2</sup> Significant difference ( $p$ -value  $< 0.01$ , unpaired two-sided Student's t-test) between accuracy of histology outcomes in benign and malignant lesions. \* Molecular analysis is only performed upon request (when clinically indicated), denoted here is the number of times it was possible when requested.

Pathology outcome –per lesion basis	%	n
<b>Rapid On-Site Evaluation of Cytopathology</b>		
ROSE correlating to malignant cytopathology findings	72.1%	57/79
ROSE correlating to procedural malignant findings (cytology & histology combined)	47.5%	57/120
<b>Sampling accuracy in malignant lesions</b>		
Cytopathology (procedural) accuracy	48.5% <sup>1</sup>	79/163
Histopathology (procedural) accuracy	66.9% <sup>2</sup>	105/157
Combined pathology (procedural) accuracy	71.0%	120/169
Molecular analysis possible*	83.9%	26/31
<b>Sampling accuracy in benign lesions</b>		
Cytopathology (procedural) accuracy	51.9% <sup>1</sup>	28/54
Histopathology (procedural) accuracy	88.6% <sup>2</sup>	47/53
Combined pathology (procedural) accuracy	87.5%	49/56
<b>Sampling accuracy – lesions overall</b>		
Cytopathology (procedural) accuracy	49.3% <sup>1</sup>	107/217
Histopathology (procedural) accuracy	72.4% <sup>1</sup>	152/210
Overall pathology (procedural) accuracy	75.1%	169/225

### 6.4.4 Rapid on-site evaluation of cytopathology

Rapid on-site evaluation of cytopathology was available in cases where sampling by brush and/or TBNA was performed (n=217). Of 79 lesions where cytology analysis was suggestive of malignancy, ROSE concluded similarly in 57 (69.8%). Due to the discrepancy between cytology results and overall pathology results, ROSE was able to conclude malignancy in 47.5% of cases where procedural outcome showed malignancy (57/120, Table 6.2). In the procedures where ROSE was found suggestive of malignancy, significantly more samples were obtained than where it did not (respective average of 12.65 vs. 10.51 samples, p=0.016, Table 6.3). The biopsy time insignificantly correlated to these findings, taking an average of 25.1 minutes in ROSE findings suggestive of malignancy and 24.2 minutes in non-confirmatory ROSE findings (p=0.36).

**Table 6.3** – Descriptive statistics on procedural sampling techniques. Amount of sampling obtained are computed from cases where the instrument was used to acquire at least one sample. The accuracy are furthermore given by comparing the amount of times the instrument was used and led to an accurate diagnosis as compared against the total times it was used. On the bottom half of the table, the total amount of samples obtained for the different types of procedure characteristics are furthermore given; amount of samples when ROSE concluded malignancy, did not conclude malignancy, amount of samples in undiagnostic lesions and in cases where an accurate diagnosis could be obtained. <sup>1</sup> p-value = 0.016, significantly more samples were obtained when ROSE had concluded malignancy. <sup>2</sup> p-value = 0.014, significantly more samples were obtained in accurate procedures.

Descriptive statistics on sampling techniques	Mean (samples)	Median (samples)	Min-max (samples)	Accuracy (tool)
<b>Cytology</b>	3.83	4	1-15	107/217 (49.3%)
Lavage	1.18	1	1-3	18/76 (23.7%)
Brush	1.64	2	1-4	40/132 (30.3%)
TBNA	3.26	3	1-11	77/165 (46.7%)
<b>Histology</b>	7.56	7	0-18	152/210 (72.4%)
Forceps	7.08	7	1-18	142/201 (70.6%)
Cryobiopsy (1.1 mm)	6.12	7	1-10	26/38 (68.4%)
Cryobiopsy (1.9 mm)	1.15	1	1-2	21/51 (41.2%)
<b>Samples total</b>	11.39	11	1-25	169/225 (75.1%)
ROSE: malignant findings	12.65 <sup>1</sup>	12	4-24	-
ROSE: benign findings	10.51 <sup>1</sup>	10	1-25	-
Unsuccessful diagnosis	9.72 <sup>2</sup>	10	1-23	-
Successful diagnosis	11.91 <sup>2</sup>	12	1-25	-
<b>Tools total</b>	2.93	3	1-6	-

**Table 6.4** – Sampling accuracy of different instruments as used in the navigation bronchoscopy procedure. Diagonal (grey boxes): Accuracy of the individual instrument, as calculated over the amount of times the instrument was used (n/N).  
 Top right half of table: Pair-wise comparison of tool accuracy, calculated by evaluation of cases where both tools were used in the same lesion. The individual tool accuracies as calculated by every time they were pair-wise used are shown in red (rows) and green (columns). I.e. the first row shows how often lavage was accurate (in red) versus how often other tools were accurate (in green), when both were used. In between brackets (in black) the number of times the pair-wise tool comparison was available (as both tools were used in a single lesion), followed by probability of significant accuracy differences between the two tools. Abbreviations: NA – not applicable; TBNA – Trans-Bronchial Needle Aspiration; Cryo – cryoprobe sampling; n – amount of cases; p – probability outcome of McNemar chi-squared test for pair-wise comparison of instruments

	Lavage	Brush	TBNA	Forceps	Cryo 1.1 mm	Cryo 1.9 mm
Lavage	23.7% (18/76)	23.9%/32.8% (n=67, p=0.21)	26.7%/37.8% (n=45, p=0.27)	24.6%/66.2% (n=65, p<0.01)	0%/100% (n=1, p=NA)	0%/46.6% (n=15, p=NA)
Brush		30.3% (40/132)	21.0%/43.2% (n=81, p<0.01)	31.1%/66.9% (n=119, p<0.01)	20%/90% (n=10, p=0.023)	25.8%/38.7% (n=31, p=0.34)
TBNA			46.7% (77/165)	48.1%/72.1% (n=154, p<0.01)	58.8%/67.6% (n=34, p=0.58)	21.9%/37.5% (n=32, p=0.27)
Forceps				70.6% (142/201)	80.6%/72.2% (n=36, p=0.51)	57.1%/42.9% (n=42, p=0.21)
Cryo 1.1 mm					68.4% (26/38)	100%/100% (n=1, p=NA)
Cryo 1.9 mm						41.2% (21/51)

## 6.5 Discussion

In navigation bronchoscopies where access of lesions with a mean 15 mm size had been verified through (repeated) 3D-imaging, we found that procedural pathology outcome corresponded to follow-outcome in 80.5% per patient (75.1% of lesions). In lesions where an accurate diagnosis could be obtained, significantly more sampling was performed (9.72 vs 11.91 samples,  $p=0.014$ ). An accurate diagnosis was most often obtained by forceps (accuracy 70.6%), followed by 1.1 mm cryoprobe (68.4%), TBNA (46.7%), 1.9 mm cryoprobe (41.2%), brush (30.3%) and lavage (23.7%). By these findings, histology results alone were found representative of follow-up outcome in 72.4%, and by cytology in 49.3% of cases (Tables 6.3 & 6.4,  $p$ -value  $<0.01$ ). Due to the discordance of cytology findings with overall procedural findings, and ROSE again being discordant with cytology (in 27.9% of cases), ROSE was able to help predict procedural malignant pathology outcome in only 47.5% of cases.

During the conduct of this study, catheters and (intermittent) 3D-imaging verification were always used. We hypothesize both were essential in maintaining meticulous positioning and acquiring tissue at different sites of hypothesized pathology. It is likely only a minority of tissue samples contains pathologic tissue, as also indicated by Coghlin *et al.* in biopsy samples of visible lung cancers [142]. The NAVIGATE study and a recent systematic review and meta-analysis substantiate these findings, finding a higher procedural success in cases of multi-modal and extensive sampling [122,143]. Our repeated sampling with tools was based on clinical decision making rather than being a randomized and controlled trial. With the differently available tools having different properties, we deemed it relevant to tailor their use to the situation. In general, we chose our tools based upon relative positioning of the catheter to the lesion and secondary adjacent structures (e.g. pleura, vessels, cavities). When a central position in the lesion was obtained, a brush was generally the first choice (followed by secondary sampling tools). When lesion position was eccentric or transparenchymal access was deemed necessary, TBNA was often preferred first. The choice to not perform repeated TBNA, brush or lavage sampling more often was made consciously. EBUS-TBNA and ROSE literature has shown acquisition of more than 4 TBNA samples in EBUS is of minimal additional value and sufficient for enabling molecular analysis in the vast majority of cases [94]. While we cannot perform sampling under direct ultrasonic or video guidance, the motion and straightening of the catheter along with ROSE findings often being consistent in outcome from first to last biopsy made us decide on reducing routine TBNA use to 3-4 times. The choice of forceps and higher amounts of repeat biopsy when compared to other tools was partially based on the observation that precurved catheters as used in this study lost least of their curvature by forceps, consequently allowing for biopsy of different sites. This could also provide for an explanation why we find a significant cytology and histology accuracy difference in both diagnosing benign and malignant lesions (Table 6.2). But where cytology accuracy was similar in malignant and benign lesions (48.5 vs 51.9%,

respectively), histology outcome was of higher variation (66.9% vs 88.6% for malignant and benign outcomes, respectively). We cannot clearly explain this histology accuracy difference in benign and malignant findings, as it is also contrary to generalized findings of other studies [143]. As such, additional research remains needed.

To our knowledge, this is one of first clinical trials to report on 1.1 mm cryoprobes for peripheral lesion biopsy in a through-the-catheter approach. Opposite to that of the 1.9 mm cryoprobe, it allows for repeated sampling while retaining the catheter near the lesion. As descriptively reported, a combination of TBNA with forceps biopsy in a curved guide sheath deprecated the added value of also adding this tool to the inventory in 22 out of 24 cases where it was found diagnostic. It has previously been described that especially lesions non-concentrically positioned around the bronchus would be benefitted by the cryoprobe [134]. Our findings show this might be less valid for the smaller sized probe, which could be caused by its difference in area and tissue penetration.

Folch *et al.* and the NAVIGATE trial report a higher degree of sampling and multi-modal sampling led to higher yield [122,143]. We report routinely sampling more than 10 times per lesion in a multi-modal fashion and similarly see a higher amount of sampling correlating to finding an accurate diagnosis by procedural pathology more often (Table 6.3,  $p=0.014$ ). Our high degree of repeat sampling was in part based on our clinical findings that lesion access by imaging verification was frequent, but a confirmatory diagnosis could then not always be made. The hypothetic TBNA and forceps only scenario as presented in this study however shows we would have found 91.7% of eventual diagnoses by only using these two modalities. It could be suggested that not all lesions require extensive multi-modal sampling. Yet, it can also be concluded that no commercially and readily available tool is currently a do-it-all tool even if lesion access has been confirmed. Therefore, multi-modal and repeated sampling seems to remain the recommended methodology.

As previously found, the ROSE methodology may differ among centers, with no evidence for preferring one above another smearing method [94]. A meta-analysis by Mondoni *et al.* found ROSE increases the procedural yield also in diagnosis of peripheral lesions. Moreover, previous reports have shown that molecular analysis in EBUS-TBNA can be performed more often in a ROSE enhanced procedure [141]. In this study, we uniquely use Cone beam CT imaging to verify in 3D that the lesion has been accurately accessed. Consecutively, extensive sampling was performed. Yet even after having (repeatedly) verified lesion access, a diagnosis indicative of procedural malignant outcome could be obtained by ROSE in only 47.5% of cases (Table 6.2). The discordant findings when related to procedural and cytology outcome may in part be explained by differences in available material. ROSE provides outcome on Giemsa staining, whilst additional material is harbored within Papanicolaou staining and cell block. Another cause of discordance might be related to the cytopathologist's opinion that analysis of peripheral pulmonary lesion smears is different to that of EBUS-TBNA, being

more diverse. With decreasing lesion size and less solidity, differentiating between atypical findings and malignancy becomes more difficult [41]. Combined, we can conclude that ROSE was of additional value in less than 50% of cases, and, that it was not associated with a reduction of total number of samples taken nor with biopsy time. Based on these outcomes we question if ROSE remains justified or that extensive sampling with currently available tools is needed regardless.

## 6.6 Interpretation

This study evaluates the different tissue sampling methodologies and ROSE accuracy in a subset of navigation bronchoscopies where 3D-imaging had verified lesion access. With repeated multimodal sampling based upon clinical decision making, pathology outcome was found corresponding to gold standard follow-up outcome in 75.1% of lesions, resulting in 80.5% of patients obtaining a representative diagnosis. In lesions where an accurate diagnosis could be obtained, significantly more sampling was performed (9.72 vs 11.91 samples,  $p=0.014$ ). An accurate diagnosis was most often obtained by forceps (accuracy 70.6%), followed by 1.1 mm cryoprobe (68.4%), TBNA (46.7%), 1.9 mm cryoprobe (41.2%), brush (30.3%) and lavage (23.7%). Analysis of a multi-modal sampling approach reveals sampling using only forceps and TBNA would have provided eventual diagnostic outcome in 91.7% of successfully diagnosed lesions. In cases where procedural pathology outcome proved malignant, ROSE had precedingly confirmed malignancy in only 47.5%. Confirmation of malignancy on ROSE did not show to reduce number of biopsies taken nor biopsy time. In conclusion, there is currently no single approach or methodology that is a do-it-all. Future research on how to improve the accuracy and effectivity of tissue sampling is needed.

## 6.7 Statement of Ethics

The research was conducted ethically in accordance with the latest World Medical Association Declaration of Helsinki. The study protocol was approved by the independent local medical ethical committee (Arnhem-Nijmegen) and institutional review body before start of subject inclusion. Informed consent was obtained.







# CHAPTER 7

**Cone-beam CT and augmented fluoroscopy  
guided navigation bronchoscopy;  
radiation exposure and learning curve**

**Authors**

R.L.J. Verhoeven, W. van der Sterren, W. Kong, S. Langereis, P. van der Tol,  
E.H.F.M. van der Heijden

*Submitted, 2020*

## 7.1 Abstract

### Background

The endobronchial diagnosis of peripheral lung lesions suspected of lung cancer remains a challenge from a navigation as well as an adequate tissue sampling perspective. Cone beam CT (CBCT) guidance is a relatively new technology and allows for 3D imaging confirmation as well as navigation and biopsy guidance, but, also involves radiation. This study investigates how radiation exposure and diagnostic accuracy in the CBCT guided navigation bronchoscopy evolves with increasing experience, and, with a specific tailoring of CBCT and fluoroscopic imaging protocols towards the procedure.

### Study design

In this observational clinical trial, all 238 consecutive patients undergoing a CBCT guided navigation bronchoscopy from the start of our CBCT guided navigation bronchoscopy program (Dec 2017) until June 2020 were included. Procedural dose characteristics and diagnostic accuracy are reported as a function of time.

### Results

Procedural radiation exposure as measured by the Dose Area Product (DAP) initially was 47.5 Gy·cm<sup>2</sup> (effective dose 14.3 mSv) and gradually reduced to 25.4 Gy·cm<sup>2</sup> (5.8 mSv). The reduction in fluoroscopic DAP was highest, from 19.0 Gy·cm<sup>2</sup> (5.2 mSv) to 2.2 Gy·cm<sup>2</sup> (0.37 mSv, 88% reduction), despite a significant increase of fluoroscopy time. The diagnostic accuracy of navigation bronchoscopy went up from 72% to 90%.

### Conclusion

A significant learning effect can be seen in the radiation safety and diagnostic accuracy of a CBCT and AF guided navigation bronchoscopy. With increasing experience and tailoring of imaging protocols to the procedure, the procedural accuracy improved while effective dose for patients and staff were reduced.

## 7.2 Introduction

Peripheral lung lesions with intermediate to high risk of malignancy should preferably be diagnosed by minimal invasive means before deciding upon treatment strategy [32,37,144,145]. The currently available most sensitive options for obtaining samples from peripheral lung lesions include CT guided trans-thoracic needle biopsy (TTNB) and technology enhanced endobronchial approaches. CT guided TTNB has an overall sensitivity of approximately 90% [32,44] but is also associated with a 19-25% risk of pneumothorax [44]. The endobronchial approach as enhanced by different means of technology has shown a 70-77% pooled sensitivity in meta analysis, with only a 1.5-2.0% risk of pneumothorax [39,143]. Recently, it was shown that utilizing intra-procedural Cone Beam CT (CBCT) image guidance – a relatively new technique in this field - may retain complication risk while further increasing the accuracy of this technology enhanced navigation bronchoscopy procedure [113,128]. Aside of its unique ability to acquire intra-procedural 3D information, deemed valuable for meticulous positioning of tools, the CBCT system can also augment a navigation pathway and lesion position as an overlay on 2D fluoroscopic imaging (also termed augmented fluoroscopy, AF). With this combination of features, CBCT has the potential to meticulously help guide the endoscopist during the different aspects of the procedure.

The use of CBCT imaging systems for guiding the endobronchial diagnosis of suspected peripheral pulmonary lesions solely relies on X-ray imaging through both augmented fluoroscopy imaging as well as repeated CBCT's to navigate and confirm positioning. Since only few reports describe CBCT and AF use in interventional pulmonology, little is known about its radiation safety profile. Steinfurt *et al.* and Casal *et al.* report effective CBCT guided bronchoscopy procedural dose ranges of 9-60.8 mSv [146] and 11-29 mSv (Dose Area Product, DAP: 64.6 Gy·cm<sup>2</sup>, [112]) whereas Pritchett *et al.* report a procedural DAP of only 31 Gy·cm<sup>2</sup> and an effective procedural dose estimation as low as 3 mSv [147].

We hypothesize the radiation exposure to both patients and staff might vary significantly, as it is subject to a learning curve experience. Therein, not only the endoscopist is likely to change its radiation use as experience increases. Tailoring of the CBCT system to the requirements of this relatively new field is also of likely effect. Changing system imaging quality and collimation options could enhance radiation safety to that purpose, without negatively affecting diagnostic accuracy.

In this study, we prospectively evaluate unselected consecutive navigation bronchoscopy cases in order to study two (possibly interrelated) topics: (1) the radiation exposure in the primarily CBCT-guided navigation bronchoscopy procedure over time (with the tailoring of imaging protocols specific to the procedure); (2) the procedural diagnostic accuracy in the CBCT and AF guided navigation bronchoscopy over time.

We hypothesize that more procedural experience and a specific tailoring of CBCT and AF imaging protocols to the navigation bronchoscopy procedure may significantly reduce radiation dose while maintaining or improving procedural accuracy.

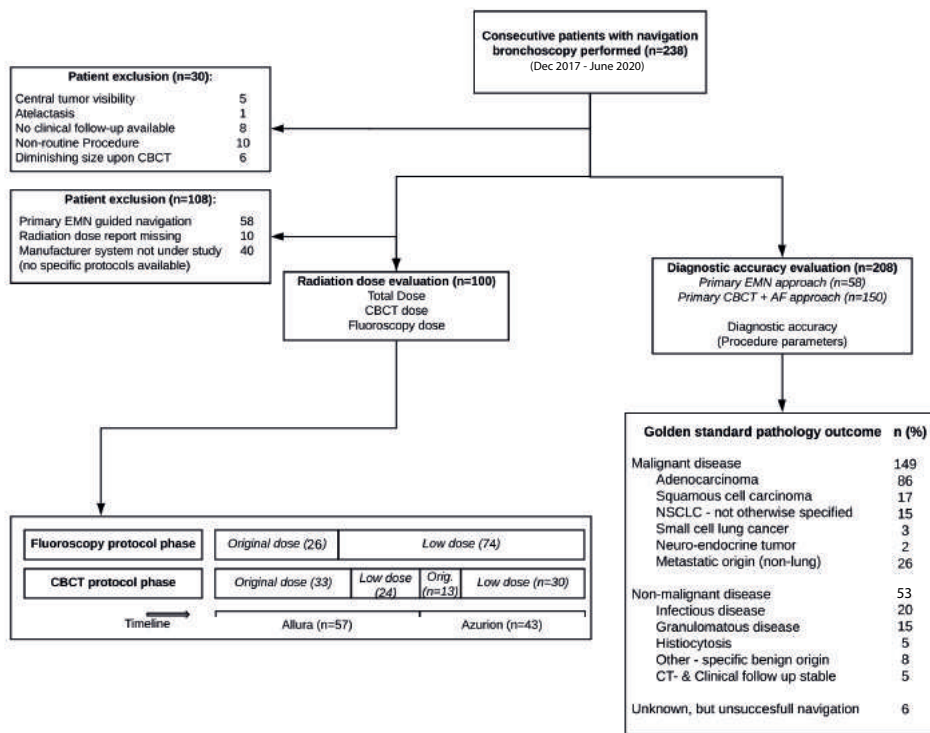
## **7.3 Methods**

### **7.3.1 Study subjects**

This prospective single center study was approved by the local ethical committee. All consecutive patients in the period December 2017 - June 2020 without contra-indications for an endobronchial procedure and a peripheral pulmonary lesion for whom a minimally invasive biopsy was indicated and performed according to routine clinical care were eligible for study inclusion. In our center, CBCT and AF guidance was first choice of procedure (preferred above TTNA), but only indicated for those lesions where advanced navigation guidance and confirmation was deemed necessary (location at least beyond 2<sup>nd</sup> order branches of segmental bronchi). In cases where lesions were thought to be reachable by catheters under r-EBUS mini probe imaging (UM-S20-17S, Olympus, Tokyo, Japan) and C-arm fluoroscopy guidance, procedures were not performed on the CBCT imaging suite. Written informed consent was obtained in all cases. Patients eventually reached and diagnosed without CBCT imaging were excluded for this study. All procedures were performed by the same team of one interventional pulmonologist and one technical physician.

### **7.3.2 Materials and methods**

Procedures were performed under general anesthesia. Standard flexible video bronchoscopes with 2.8 mm working channel (EB19-J10, Pentax Medical, Tokyo, Japan) were used for inspection bronchoscopy and subsequent navigation guidance of commercially available catheters. Catheter navigation was performed only on basis of CBCT and AF guidance in all but the cases where electromagnetic navigation technology (EMN, Medtronic SuperDimension, Minneapolis, USA) was additionally used (Figure 7.1). After navigation, radial EBUS miniprbes and/or CBCT with AF imaging were routinely used to confirm lesion access. Consecutive tissue sampling was performed under guidance of AF. Biopsy tools included brushes, TBNA needles, biopsy forceps and cryoprobes. Rapid on-site evaluation of cytopathology was always available.



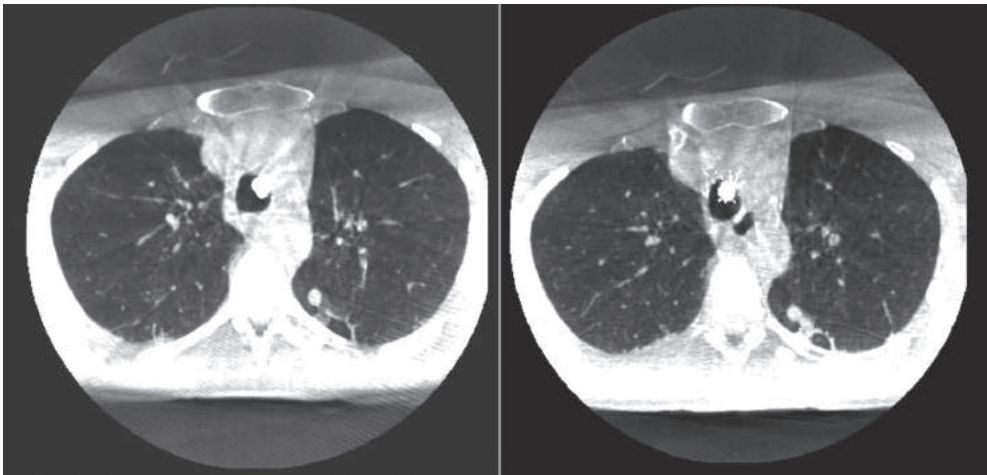
**Figure 7.1** – Flow chart of study inclusion.

The navigation bronchoscopy procedures were performed on three cone beam CT systems; a ceiling mounted Philips Allura Clarity FD20 scanner which was later replaced by a ceiling mounted Philips Azurion scanner (Philips, Best, The Netherlands), and, a floor mounted Siemens Artis Zeego scanner (Siemens Healthineers, Forchheim, Germany). As part of a specific research collaboration, dedicated imaging protocols and software were installed and updated only on the Philips systems. Distinct periods and concurrent imaging methods on these imaging systems can be defined (Figure 7.1). To allow for an accurate learning experience description, the radiation exposure is reported only for the Philips imaging systems. In enabling a description of the diagnostic accuracy learning curve experience, the procedures on all platforms are however taken into account.

### 7.3.3 X-ray imaging

In short, our navigation bronchoscopy program started with imaging protocols only focusing on acquiring the highest imaging quality possible. However, navigation bronchoscopy is not all about maximum image quality and should adhere to the ALARA principle (As Low As Reasonably Achievable). As tools and lesions can often be distinguished from the surrounding lung tissue in navigation bronchoscopy after having obtained initial guidance information, not every detail on subsequent CBCT scans or fluoroscopy imaging is needed.

We therefore changed the availability of thorax CBCT scanning and AF protocols from one to three options. Therewith, quality and concurrent radiation dose could be dynamically decided upon by the endoscopist. For instance, the necessary image quality could be based on requiring only relative positioning information (low dose), identifying if a ground glass lesion had been accurately accessed (medium dose) or to identify different bronchi for navigation towards the lesion (high / original dose, Figure 7.2). The goal of these dedicated imaging protocols was to provide multiple options to the endoscopist, retaining diagnostic accuracy while maintaining or decreasing radiation dose. Protocol changes were made in due time (Figure 7.1). First low dose fluoroscopy protocols became available, afterwards, low dose CBCT protocols. When the Philips Allura system was replaced by the Azurion system, low dose fluoroscopy protocols were immediately transferred. Ten procedures however passed before the low dose CBCT protocols were made available on the Azurion system.



**Figure 7.2** – Example images subsequently obtained from low dose (left) and normal dose (right) imaging protocols for navigating towards a 6x8 mm lesion found in the apical segment of the left lower lobe. As can be seen, artifacts alike the classically known streaking can be seen more strongly in the low dose protocol. Although difficult to appreciate on still images, there is also a further difference in image quality for i.e. allowing recognition of the smallest of bronchi that can be navigated to. Note the minor bleeding lateroposterior to the lesion on the image on the right after having performed initial biopsy.

### 7.3.4 Analysis

Primary study parameters are radiation dose and diagnostic accuracy (over time) in a primary CBCT and AF approach, linked to an initial – generic - imaging protocol and the forthcoming availability of dedicated navigation bronchoscopy imaging protocols (over time).

*Radiation exposure* - To evaluate radiation exposure of navigation bronchoscopies primarily guided by CBCT and AF, cases where other technological modalities were used as primary guidance were excluded for radiation exposure analysis (Figure 7.1). Radiation dose information was obtained using openREM software [148]. Procedural dose was routinely

reported through the DAP. The retrospectively computed effective dose (in mSv) is a less reliable dose estimate because its computation requires several parameters that are difficult to estimate in a continuously changing setting such as with CBCT and AF [149]. For enabling comparison against other imaging modalities, a limited set of average effective doses were however calculated with PCXMC [150]. For quantitative analysis of radiation dose (over time), boxplots and Shewhart individual control charts of accumulated Dose Area Product and counts are presented, further tested for significant differences by Kruskal-Wallis and ANOVA tests.

*Diagnostic accuracy* - To evaluate the continuous diagnostic accuracy of a catheter-based navigation bronchoscopy as primarily or secondarily guided by CBCT and AF in this single institution setting, all navigation bronchoscopies were included (Figure 7.1). Navigation success is defined as cases where imaging gives no doubt about lesion access as confirmed by at least CBCT with AF imaging, but can also include unambiguous r-EBUS imaging or ROSE outcome. Malignant and specific benign findings are considered true positive and negative if not negated by follow-up findings, respectively. Unspecific benign findings are considered true negative only if definitively confirmed by follow up CT guided TTNA, surgical biopsy and/or decisive clinical follow-up of at least 6 months (i.e. no measurable growth). Unrepresentative findings or unsuccessful navigations are considered false negatives regardless of follow-up outcome. The diagnostic accuracy is obtained by relating summed number of true positives and true negatives to total number of procedures. Time-dependent parameters are described by moving averages (10 procedures).

Dichotomous variables were analyzed by a Pearson chi-square test or Fisher exact test. Not normally distributed continuous variables were evaluated by Mann-Whitney-Wilcoxon test. All p-values were two-sided and considered significant if  $<0.05$ . R and R-studio were used for statistical analysis [68].

## 7.4 Results

Patients with informed consent were included from the initiation of our CBCT and AF guided navigation bronchoscopy program (December 2017) until June 2020 (n=238, Figure 7.1). An exclusion of patients was performed for radiation dose evaluation in cases of a missing radiation report (10), a non-primary CBCT and AF based navigation (58), and, cases where navigation bronchoscopy was not performed on the systems under study (40), leaving 100 cases for analysis.

Secondly, 208 patients were eligible and prospectively included for the diagnostic accuracy analysis in this study. These 208 patients had a total of 248 lesions that were navigated to, with a median long axis diameter of 13 mm (range: 5-65 mm, Table 7.1).

### 7.4.1 Radiation exposure

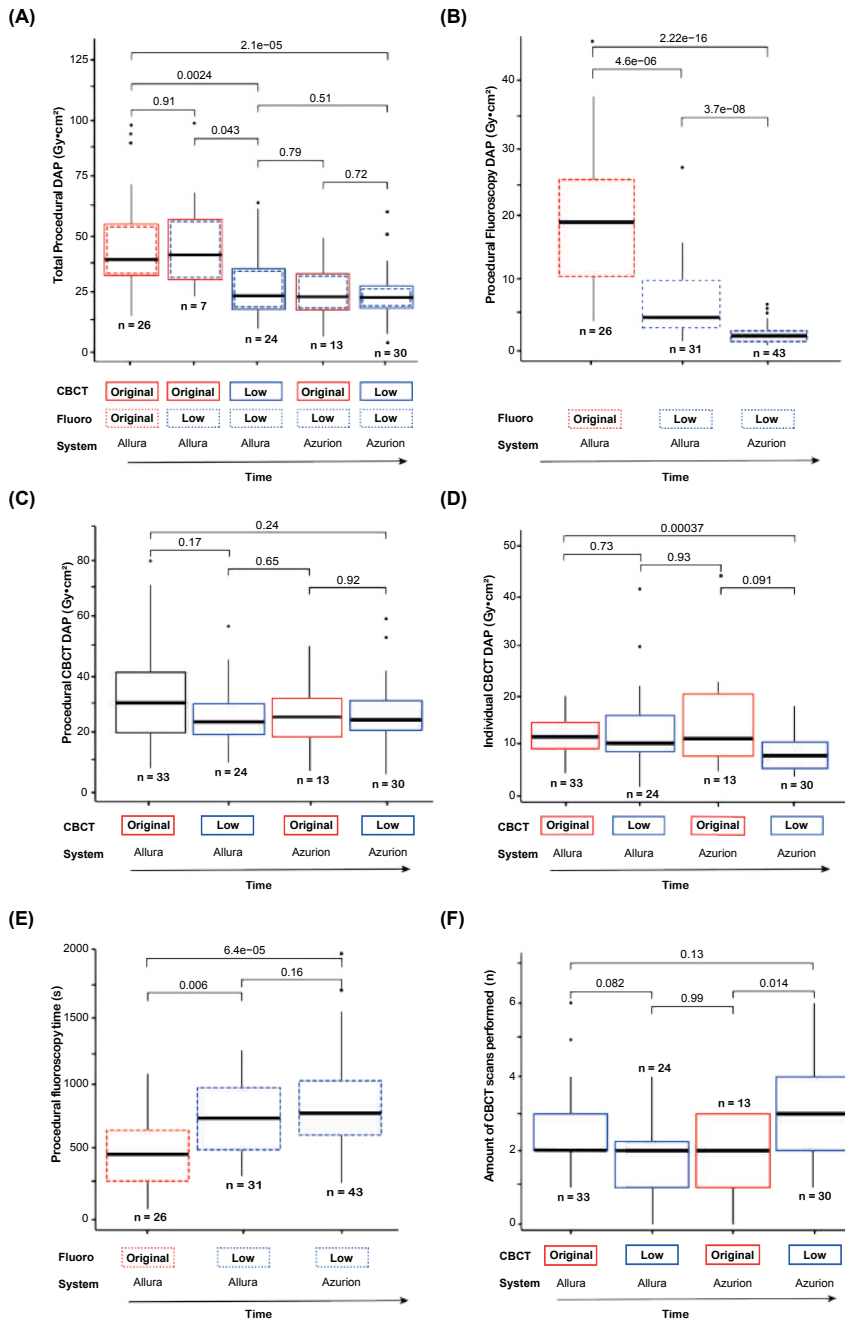
At the start of our CBCT and AF guided navigation bronchoscopy program, average procedural DAP was 47.5 Gy·cm<sup>2</sup> (effective dose 14.3 mSv). Initial average fluoroscopic DAP was 19.0 Gy·cm<sup>2</sup> (5.2 mSv) and the initial total CBCT scan DAP as a consequence of performing 2.47 rotations per procedure was 29.9 Gy·cm<sup>2</sup> (9.1 mSv, 3.7 mSv per scan). As experience increased and the different fluoroscopic and CBCT imaging protocols gradually became available (along with the replacement of the CBCT system, Figure 7.1), procedural DAP gradually declined from 47.5 (estimated effective dose 14.3 mSv, initial period with original protocols) to 25.4 Gy·cm<sup>2</sup> (5.8 mSv, low dose CBCT and fluoroscopy protocols on new Azurion CBCT system). Boxplots and Shewhart individual control charts of DAP per period can be found in Figure 7.3 and 7.4, respectively. Table 7.2 summarizes the average radiation characteristics per period.

**Table 7.1** – Patient, nodule and procedural characteristics. Definitions: Bronchus sign – Image feature showing the lesion to be directly adjacent to a bronchus. Navigation success – CBCT imaging and/or unambiguous r-EBUS imaging verified access of the lesion. Diagn. Acc. (pat) – Procedural outcome of navigation bronchoscopy corresponding to follow-up outcome (see Methods). Abbreviations: LUL – Left Upper Lobe, RUL – Right Upper Lobe, RML – Right Middle Lobe, LLL – Left Lower Lobe, RLL – Right Lower Lobe, Malign. Prev. – Malignancy prevalence.

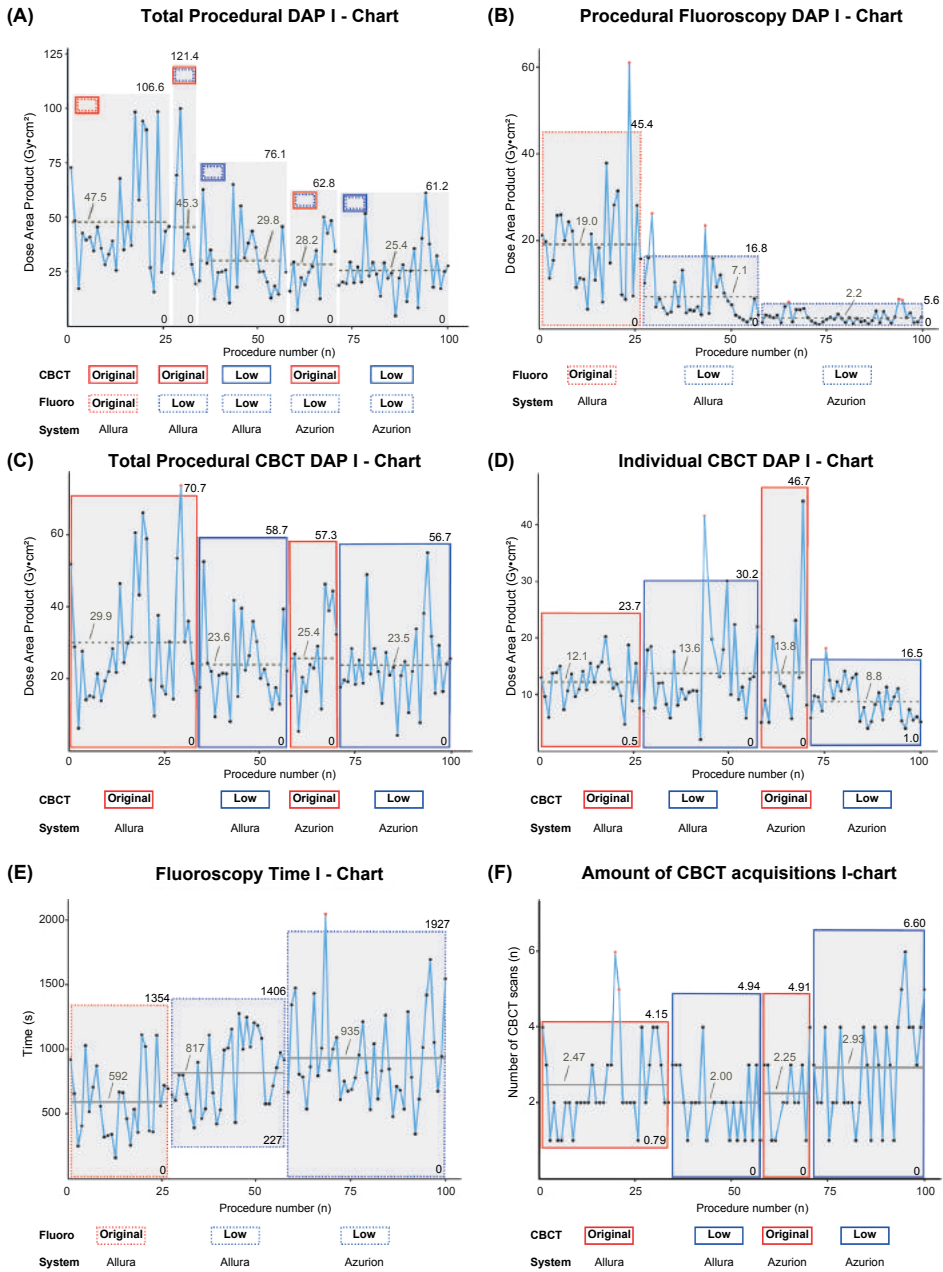
<b>Patient characteristics</b>				
Patients / Lesions (n)	208 / 248			
Sex M/F (n, %)	114 (55%) / 94 (45%)			
Age (min – max)   Length   Weight   BMI	65 y (36-85)   1.72 m   74.9 kg   25.3			
<b>Nodule and procedural characteristics</b>				
Median lesion diameter (min-max)	13 mm (5–65)	Lesion locations	n	
Bronchus sign (@ ≤1 mm CT, lesions)	60.9%	LUL / RUL	67 / 85	
Median navigation time (min-max)	29 min (4 - 100)	/ RML	/ 11	
Mean biopsy time (sd)	25.6 min (10.74)	LLL / RLL	37 / 48	
Mean tissue samples taken (min-max)	11 (0-25)			
<b>Procedural outcome</b>				
<i>Lesion long axis size</i>	<i>n</i>	<i>Nav. Success</i>	<i>Diagn. acc. (Pat)</i>	<i>Malign. Prev.</i>
≤10 mm	36	91.6% (33)	69.4% (25)	75%
>10-20 mm	113	88.5% (100)	73.5% (83)	71.2%
>20-30 mm	32	100% (32)	84.4% (27)	80.6%
>30 mm	27	100% (27)	88.9% (24)	74.1%
<i>Overall</i>	208	92.3%	76.4%	73.7%

The most important cause of the reduction in procedural radiation exposure was an altered use of fluoroscopy (Figure 7.3 & 7.4 - panel B). Becoming more experienced and implementing lower dose fluoroscopy protocols changed average fluoroscopy DAP from 19.0 Gy·cm<sup>2</sup> (effective dose 5.2 mSv) to 2.2 Gy·cm<sup>2</sup> (0.37 mSv, p<0.01). This is counterintuitive to what





**Figure 7.3** – Boxplots of radiation dose over time and per protocol becoming available (left to right). Box indicates 1st to 3rd quartile, line indicating median. Panel A - Total procedure radiation dose area product. Panel B - Procedural Fluoroscopy dose area product. Panel C - Procedural CBCT dose area product. Panel D - Individual CBCT dose area product. Panel E - Procedural fluoroscopy time (s). Panel F - Amount of CBCTs performed per procedure. Also see Figure 7.1 for period partitioning based on CBCT system and protocol availability and Figure 7.4 for corresponding Shewhart Individual Control Charts of radiation exposure data.



**Figure 7.4** – Shewhart individual control charts of procedural radiation characteristics over time. Grey boxes indicate upper and lower confidence limits, horizontal line indicates period mean. Partitioning by the grey boxes based on CBCT system and protocols becoming available (see Figure 7.1 and Figure 7.3)

one would expect based on the monitoring of average total procedural fluoroscopy time. The initial average total fluoroscopy time was 592 seconds (9.9 min), and it gradually increased to an average of 935 seconds (15.6 min,  $p < 0.01$ , Figure 7.3 & 7.4 - panel E).

In the last study period, the bulk of radiation exposure was caused by CBCT acquisitions. While the individual average CBCT scan exposure changed significantly when comparing first to last scanning period (from 12.1 to 8.8 Gy·cm<sup>2</sup>,  $p < 0.01$ , Figure 7.3 & 7.4 - panel D), total CBCT scan exposure did not (from an average of 29.9 to 23.4 Gy·cm<sup>2</sup>,  $p = 0.24$ , Figure 7.3 & 7.4 - panel C). This can be attributed to an increase in average number of CBCTs performed per procedure, from 2.47 to 2.93 (NS, Figure 7.3 & 7.4 - panel F).

**Table 7.2** – Average radiation dose characteristics per period, as defined per imaging protocols available (see Figure 7.1). At first instance, the Allura CBCT imaging system was available with original dose imaging protocols for both fluoroscopy and CBCT (n=26). From there on, consecutive changes were made in system, fluoroscopy or CBCT availability. Dose Area Products (DAP) are given for every subsequent period in Gy·cm<sup>2</sup>. Also see corresponding Figure 7.3 & 7.4. Abbreviations: acq. – CBCT rotational acquisition.

Time period	System	Fluoroscopy			CBCT			Total DAP
		Protocol	DAP	Time	Protocol	DAP / acq.	acq.	
Period 1 (n=26)	Allura	Original dose	19.0	592 s	Original dose	12.1	2.47	47.5
Period 2 (n=7)		Low dose	7.1	817 s	Low dose	13.6	2.0	29.8
Period 3 (n=24)		Low dose	2.2	935 s	Original dose	13.8	2.25	28.2
Period 4 (n=13)	Azurion	Low dose	2.2	935 s	Low dose	8.8	2.93	25.4
Period 5 (n=30)		Low dose	2.2	935 s	Low dose	8.8	2.93	25.4

### 7.4.2 Diagnostic accuracy

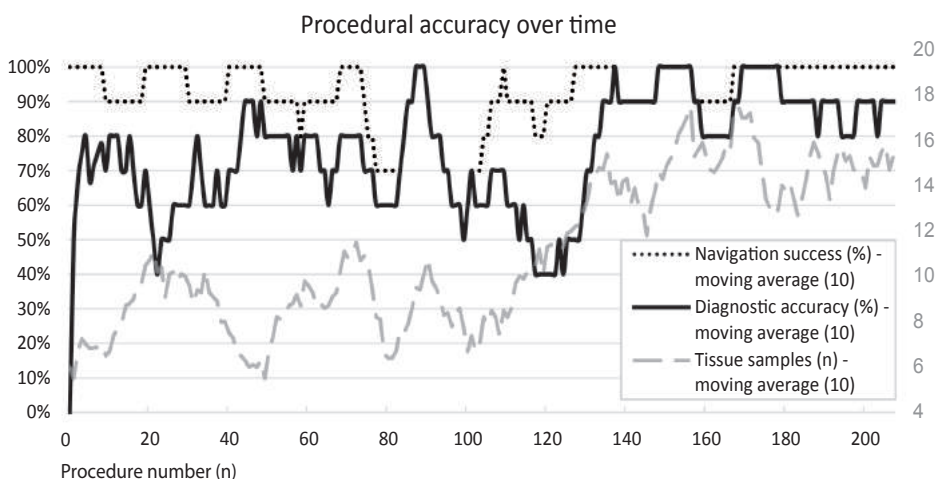
A primary CBCT and AF approach was performed in 150/208 cases. A primary EMN approach was performed in the remaining 58 cases, with 40 of these cases taking place in the first 87 patients during the conduct of our previous study (comparing the EMN and CBCT approach) [128]. The diagnostic accuracy when taking into account all 208 consecutive procedures was 76.4% (Table 7.1). After concluding our previous trial comparing the EMN and CBCT approach at the beginning of 2019 (87 patients, diagnostic accuracy 72.4%, [128]), a temporary drop in accuracy is seen. This drop cannot be explained solely by factors like bronchus sign, lesion size, malignancy prevalence or a decline in navigation success (all  $p > 0.05$ ). In the subsequent period, dynamical decision making by the endoscopy team led to increasing the amount of biopsy samples obtained, as CBCT remained to consistently show accurate lesion access (Figure 7.5). Over the next period diagnostic accuracy gradually rose. From November 2019 to June 2020, the overall diagnostic accuracy was 90.6% whereas navigation success was 98.4% (n=64 procedures).



Statistical analysis of overall procedural characteristics revealed that malignancy prevalence, bronchus sign presence and trans-parenchymal navigation did not have a significant effect on overall diagnostic accuracy. Variables that were statistically related to higher diagnostic accuracy were higher lesion diameter ( $p=0.014$ , 9 versus 15 mm median size), navigation success ( $p<0.001$ ) and a higher number of tissue samples having been obtained ( $p<0.001$ , median 10 versus 12 samples).

### 7.4.3 The Learning curve effect

The learning effect can be derived from combining the information from both radiation exposure as well as diagnostic accuracy analysis. The average procedural DAP went down from  $47.5 \text{ Gy}\cdot\text{cm}^2$  (effective dose: 14.3 mSv) to  $25.4 \text{ Gy}\cdot\text{cm}^2$  (5.8 mSv), while the diagnostic accuracy went up from 72% to 90%. The learning effect in radiation safety is greatest in the use of fluoroscopy, where the total use time went up significantly ( $p<0.01$ ) while a significant reduction in its exposure could simultaneously be seen ( $p<0.01$ , Figure 7.3 & 7.4 – panels B & E).



**Figure 7.5** – Diagnostic accuracy, navigation success and amount of tissue samples over time as found since the introduction of a CBCT and AF based navigation bronchoscopy ( $n=208$  procedures included for analysis, moving average of 10 procedures). Diagnostic accuracy and navigation success on primary axis (left), amount of tissue samples obtained per procedure on secondary axis (right). Moving average plotted using previous values only (aligned right).

## 7.5 Discussion

We show in a prolonged case series that radiation exposure as well as diagnostic accuracy in navigation bronchoscopy guided by CBCT and AF are subject to a significant learning effect. An increase in experience and a tailoring of imaging protocols towards the procedure

significantly reduced the radiation exposure while the diagnostic accuracy was enhanced. Total procedural DAP went down from 47.5 Gy·cm<sup>2</sup> (effective dose: 14.3 mSv) to 25.4 Gy·cm<sup>2</sup> (5.8 mSv), while the diagnostic accuracy went up from 72% to 90%.

The ALARA principle dictates to use radiation as sparsely as possible. The recent forthcoming availability of specific imaging protocols for navigation bronchoscopy that facilitate different steps of the procedure with specific imaging quality shows to help the goal of reducing dose. Interestingly, the significant reduction in radiation dose as seen in our study persisted even though the 2D fluoroscopy time and number of CBCTs performed per procedure increased over time (Figures 7.3 & 7.4). Arguably, the increase in use may be caused by awareness in the reduction of radiation dose by newer protocols. We feel having additional imaging options with lower dose lowered the threshold for additional (confirmatory) imaging. In turn, this additional confirmation might have increased our diagnostic accuracy by more meticulous positioning.

In an increasingly crowded technology field for aiding diagnosis of peripheral pulmonary lesions, the endoscopist likely has to choose between different technological guidance modalities or which combination to use. The endoscopist should aim for high accuracy, keep the amount of radiation involved as low as possible, and, simultaneously take into account the procedural costs. We previously showed that using CBCT and AF only after having performed EMN navigation significantly reduced fluoroscopy time and amount of CBCT scans performed [128]. In the current study we show the radiation dose has decreased significantly since. And while the patient will receive both CBCT as well as fluoroscopy dose, the staff dose is mainly caused by fluoroscopic exposure (as they leave the area during CBCT). Considering the accuracy of the CBCT guided navigation bronchoscopy, the procedural radiation burden for the patient when related to other procedures and associated cost of some of the additional navigation guidance modalities, one needs to individually assess if having multiple navigation guidance modalities remains worthwhile.

As CBCT and AF guidance allows for biopsy with great detail, an elaborate reflection on technique is possible. Shortly after completing our previous study, we observed a decline in diagnostic accuracy (Figure 7.5). As we have real-time CBCT imaging information available and discuss all cases in the multi-disciplinary tumor board shortly following the procedure, we concluded that inadequate tissue acquisition after successful navigation was a likely cause of error. Following these findings, more time was spent on tissue acquisition. Consecutively, the diagnostic accuracy improved to as much as 90.6% in the last 64 procedures (Nov 2019 – June 2020). We experience that having confirmed biopsy positioning on CBCT also provides additional certainty in case of benign pathology findings.

### **7.5.1 Study limitations**

The reduction in radiation dose - as time passed and the team became more experienced - was caused by both dedicated protocols as well as more aggressive collimation and

targeted imaging. Detailed collimation information was not available in our dataset and could therefore not be presented. Furthermore, it is difficult to evaluate how our single center results equate to other centers. For one, average patient BMI should be taken into account (25 in this study, Table 7.1), as this might significantly affect radiation use outcomes. Another limitation herein was our continuous awareness of radiation safety, as it was directly under study. This might have significantly attributed to an increased learning speed.

## **7.6 Conclusion**

In this single institution study, we show radiation dose of a CBCT and AF guided navigation bronchoscopy are of acceptable levels but also subject to a significant learning effect. With the implementation of new specific navigation bronchoscopy imaging protocols along with increasing experience, procedural radiation dose could be reduced from 47.5 Gy·cm<sup>2</sup> (effective dose: 14.3 mSv) to 25.4 Gy·cm<sup>2</sup> (5.8 mSv), while the diagnostic accuracy went up from 72% to 90%. Concluding, navigation bronchoscopy using CBCT and augmented fluoroscopy-imaging as a sole technique for both navigation and sampling is a (relatively) safe and accurate procedure for diagnosis of small peripheral pulmonary lesions.

## **7.7 Statement of Ethics**

The research was conducted ethically in accordance with the latest World Medical Association Declaration of Helsinki. The study protocol was approved by the independent local medical ethical committee (Arnhem-Nijmegen) and institutional review body before start of subject inclusion. Informed consent was obtained.









# CHAPTER 8

Summary



Lung cancer is the most prevalent form of cancer worldwide, exceeding 2.2 million new cases every year. The incidence will continue rising in the upcoming years, with 3.2 million cases expected in 2035 [2]. With approximately 13.800 new lung cancers being diagnosed in 2019, it is also the most prevalent form of cancer in the Netherlands. Unfortunately, the disease often only presents itself with symptoms at a late stage. Consequently, approximately 50% of patients are only diagnosed at end stage disease (stage IV). Once other organs are involved – as indicated by disease stage IV – 5-year overall survival drops to approximately 5%. Comparing this to the 61% 5-year overall survival in patients with stage I disease, a stage where there's no disease present other than a primary tumor, shows earlier diagnosis brings a significantly improved outcome [1]. Yet as even the earliest stage of disease remains to have high mortality, all possibilities of improving outcome should be explored. To do so, one important aspect is to timely and accurately diagnose and stage patients with a suspected or proven lung cancer to prevent unneeded disease progression, under-, and overtreatment. In this thesis it is described how clinical technology in flexible endoscopy might help improve the diagnostic and staging trajectory of lung cancer.

## **Part I – Endoscopic staging of suspected or proven lung cancer using ultrasound techniques**

Flexible endoscopic procedures using the airways and esophagus are a frequently performed and recommended feat in diagnosis and staging of a suspected or proven lung cancer. Once CT and/or FDG-PET imaging have shown a primary tumor finding along with a likely lymph nodal involvement, a combined endobronchial and esophageal ultrasound guided evaluation of mediastinal and hilar lymph nodes should be systematically performed. These so-called EBUS-TBNA and EUS-FNA procedures use a video camera and ultrasound transducer positioned at the distal tip of an endoscope for allowing assessment of the differently defined anatomical lymph node regions. If ultrasound imaging shows lymph node findings, a hollow needle is inserted through the endoscope and into the tissue for ultrasound imaging guided needle aspiration. While PET-CT and/or CT imaging allows for an imaging-based diagnosis, eventual tissue diagnostics will need to provide a definite answer (pathological outcome). During endoscopic evaluation, all lymph nodes of the anatomically defined regions need to be systematically assessed. A systematic assessment implies first evaluating the least suspected contralateral nodes and moving back to the most suspected ipsilateral lymph node regions from there. At least all suspected lymph nodes as identified by increased FDG uptake on PET-scan and enlarged size on CT need to be aspirated by a hollow needle under guidance of ultrasound to obtain cells for cytological examination. In deciding on aspiration of additional nodes or specific nodes within an anatomical lymph node region, ultrasound characteristics are often used.

In **Chapter 2** the feasibility of a relatively new technique in the endobronchial examination of mediastinal and hilar lymph nodes is described; ultrasound strain elastography. Ultrasound strain elastography visualizes relative tissue elasticity by calculating differential tissue motion from subsequently acquired ultrasound images while a deformation of tissue is being induced. The strain is calculated by monitoring the deformation of the different parts of imaged tissue over time. The deformation in endosonographic strain elastography is induced by the cardiovascular system. A lower strain – less deformation over time – is hypothesized to be an indication for malignancy. Chapter 2 describes how and if endobronchial ultrasound strain elastography can help identify malignant lymph nodes in a single center study. By comparing the different available methods of relaying strain information back to the user, the accuracy of endobronchial ultrasound strain elastography for predicting lymph node malignancy was explored in a single center study setting. To evaluate the different scoring methods, endobronchial ultrasound strain elastography measurements of 120 lymph nodes (63 patients) with a suspected or proven lung cancer were analyzed. Measurements were obtained using a standardized measurement protocol as developed preceding to study initiation. It was found a prediction on lymph node malignancy using ultrasound strain elastography was best done by relating the mean relative strain as found in the lymph nodal area against the full remainder of the image, enabling the most objective scoring. The lymph node region of interest was hand-selected by the operator. By using a normalization of the found strain to assure every consecutive image had at least one component with 0 strain and at least one component with a strain of 255, the found strain had range 0-255. Analysis of this scoring method revealed the Receiver Operator Characteristic – Area Under the Curve to be 0.846. A strain cut-off of 78 (range 0-255) then showed to differentiate malignant lymph nodes with a sensitivity of 93%, specificity of 75%, positive predictive value of 69% and negative predictive value of 95% (accuracy; 82%). Lymph nodes with a mean strain <78 (range 0-255) showed to have higher chance of being malignant than lymph nodes which had a mean strain  $\geq 78$ . A further exploratory analysis showed that PET-CT information can potentially be used in adjunct to strain elastography for better stratification of risk of malignancy.

**Chapter 3** describes a prospective multi-center international study (n=5) which evaluated endobronchial ultrasound strain elastography and its predictive value in the clinical lung cancer staging work-up. In this study, a total of 327 patients equivaling a total of 525 lymph node measurements were included according to the insights of the endoscopists. Malignancy prevalence in the included lymph nodes was 0.48. Analysis of the Receiver Operator Characteristic showed the total Area Under the Curve of ultrasound strain elastography for identifying lymph nodal malignancy was 0.77 in this multi-center setting. With this area under the curve it was concluded that strain elastography indeed shows to be of stand-alone predictive value. To identify malignancy with high sensitivity, the strain elastography cut-off value as was presented in chapter 2 however needed revision; from 78 to 115. In this multi-center setting, strain elastography then had 90% sensitivity, 43% specificity and a positive and negative predictive value of 60% and 82%, respectively. As

strain elastography was hypothesized as an adjunct predictor after FDG-PET and CT-scan imaging had already become available, the predictiveness of integrating FDG-PET and size information with ultrasound strain elastography findings was secondarily evaluated. It was found that strain elastography could indeed consistently help identify malignant nodes in multi-modal imaging work-up. Based on these results, two decision trees were presented that could help in routine clinical work-up.

Routine clinical practice and several studies have reported using imaging features as seen on endosonographic B-mode imaging to help the observer decide on the lymph nodes of risk. It was found individual features or a combination thereof might be of predictive value [46–49,88,95–98]. However, the predictive value of the features as described in these predominantly single center studies were concluded to be differing [17]. Possibly, this was (at least in part) caused by a difference in how B-mode features were scored [95,98]. As the outcome of systematic endosonographic assessment and aspiration of lymph nodes can prevent the need of more invasive cervical mediastinoscopy staging and determine follow-up treatment, one can question if subjective scoring of features remains desirable.

**Chapter 4** describes an evaluation on the accuracy and reproducibility of subjectively scored endosonographic B-mode features for identifying malignant lymph nodes. In this chapter, specific focus is placed on the feasibility of B-mode feature scoring in sub-centimeter lymph nodes, as larger lymph nodes should be aspirated regardless [10]. To assess if subjectively scored features are of value, 490 lymph nodes as prospectively scored during the international multi-centric study of chapter 3 were analyzed. In this dataset, the Area Under the Curve of the Receiver Operator Characteristic for ultrasound short axis size to identify lymph node malignancy was 0.78 (95% confidence interval 74-82%). The clinically feasible 8 mm cut-off for routine aspiration showed able to correctly identify 210 out of 237 included malignant lymph nodes (sensitivity 89%, specificity 46%, positive predictive value 61%, negative predictive value 81%). Adding the suggested subjectively scored B-mode criteria was feasible but deemed of limited value. As well known to the frequent ultrasound user, ultrasound is prone to observer interpretation variability. A secondary retrospective scoring of a subset of the collected lymph nodes images (n=200) was performed to assess observer variability. A significant observer variability was found when both experts (>400 procedures, n=5) and experienced endoscopists (50-400 procedures, n=3) were asked to retrospectively classify lymph nodes into malignant or benign based on combined B-mode features. The average inter-observer raw agreement in expert and intermediately experienced observer was 71-74% (Gwet's AC1 0.42-0.48) while the intra-observer raw agreement was 80-86% (Gwet's AC1 0.60-0.76). As the agreement was found to be different for the different subsets of nodes (i.e. <8 mm, ≥8 mm, benign nodes, malignant nodes), risk stratification by means of subjective (B-mode) characteristics was concluded to be of non-uniform and limited predictive value.

## Part II – Clinical technology for the diagnosis of peripheral pulmonary lesions

Imaging modalities like CT are increasingly often performed in routine clinical care for a plurality of diseases or follow-up thereof. Imaging where the lungs have also been depicted reveal the presence of a pulmonary lesion in an average of 13% of CT-scans [32]. When such imaging accidentally reveals a pulmonary nodule without further mediastinal and/or hilar lymphadenopathy, the risk of benign disease is more likely than that of malignant disease. Yet, the diagnosis of a malignancy will eventually be made in approximately 1.5% of these patients [32]. Knowing the potential benefit when diagnosing early stage lung cancer (stage I-II), residing at a far better treatable stage as compared to more advanced disease, follow-up of accidental findings is warranted. The same potential benefit of such early findings is also the reasoning why an increasing number of countries have started or are preparing to start a national lung screening program [25–30]. Studies show that the lung-cancer related mortality risk in a high-risk population can be reduced by at least 20% if a CT-screening is to be introduced [26,31]. These CT-scans in both routine clinical practice as well as a screening setting detect numerous nodules and rapidly increase the demand for minimal invasive accurate and safe diagnostic and therapeutic procedures.

The strategy for obtaining a tissue diagnosis of a peripheral pulmonary lesion is not clear cut, as there's no single 'do it all means' for safely doing so. Potential minimally invasive options are a trans-thoracic CT guided needle biopsy approach and an endobronchial approach. The trans-thoracic needle approach has a high pooled sensitivity of 91% and negative predictive value of 80%, but also results in health complications such as a pneumothorax in more than 20% of cases [32,44]. The historically used alternative endobronchial approach utilizes the airways for navigation and consecutive biopsy of a peripheral pulmonary nodule under guidance of x-ray fluoroscopic imaging. It is a safe method, but also is of poor sensitivity (pooled yield 34%) [34]. The forthcoming availability of new technology in the past decades has however helped the endoscopist to increase the sensitivity of the endobronchial approach to approximately 70-80%, while retaining the complication rate at less than 2.0%. Reported technologies for doing so are based on electromagnetic tracking of tools, miniaturized ultrasound probes for verification of nodule access, virtual endoscopy navigation guidance, robotic assistance and/or ultrathin bronchoscopes [39,41].

**Chapter 5** describes the introduction of a combination of technologies in order to assess if these can help improve the physician in obtaining a safe and accurate endobronchial diagnosis of peripheral pulmonary lesions. In a comparison of workflows, the added value of the differently available technologies was assessed. The first methodology for navigating towards peripheral pulmonary lesions consisted of combining electromagnetic navigation technology with endobronchial mini-probe ultrasound imaging for navigation and confirming nodule access. The second methodology performed navigation by using a cone beam

CT imaging system in combination with the same ultrasound imaging mini-probe for local confirmation of access. After finding either navigation success or failure by the primary methodology of navigation, lesion access was verified by cone beam CT imaging as a golden standard. A total of 87 patients with 107 pulmonary nodules were included in the two workflows. By a primary electromagnetic navigation technology approach, 52.2% of lesions were accurately reached. By a cone beam CT guided navigation, 76.3% of lesions were accurately reached. Being able to combine technology guidance after having initially confirmed an unsuccessful navigation on CBCT imaging showed to increase navigation success to 87.5-89.9% in both arms. Obtaining adequate tissue that was representative of follow-up outcome after a successful navigation was found not self-evident. Patient follow-up revealed that only 72.4% of navigation bronchoscopies eventually resulted in an accurate patient diagnosis. The overall pneumothorax rate was 3.4%. Based on these outcomes it is concluded that the navigation bronchoscopy workflows under study are safe, and, the preferential primary workflow for diagnosis of lesions is the cone beam CT imaging enhanced procedure. Due to the >15% difference in having successfully reached the lesion and obtaining a representative diagnosis, it is secondarily found that there is both a need to improve navigation guidance as well as tissue sampling accuracy.

Chapter 5 describes that there is a difference between successfully reaching the peripheral pulmonary nodule and obtaining an accurate diagnosis. Several factors might be to blame. **Chapter 6** describes an evaluation of the differently available endobronchial tissue sampling tools and rapid on-site evaluation of cytopathology for their yield in procedures where lesion access had been confirmed. This was done by a direct comparison of instruments and procedure reports in a total of 195 successful navigation bronchoscopy procedures. In these 195 procedures, 225 lesions with a median long axis size of 15.0 mm (range 5-65 mm) were sampled with either one or multiple instruments. It was therein found that sampling outcome corresponded to follow-up outcome in 75.1% of lesions, which resulted in a diagnosis in 80.5% of study subjects. Histology findings - as obtained from cryobiopsy and forceps sampling - were found to result in an accurate diagnosis in 72.4% of instances. Cytology findings - considering broncho-alveolar lavage, brush and trans-bronchial needle aspiration - correlated to gold standard follow-up outcome in 49.3% of lesions. Analysis of cases where both cytology and histology were obtained showed histology was significantly more often accurate in all lesions, be it malignant or benign (p-value <0.01). Histology outcomes by themselves furthermore showed accurate significantly more often in benign lesions than in malignant lesions (88.6% vs 66.9%, respectively). These findings did not similarly hold for cytology outcome (48.5% vs 51.9%, respectively). In lesions where an accurate diagnosis was obtained, significantly more sampling was performed (9.72 vs 11.91 samples, p=0.014). An accurate diagnosis was most often obtained by forceps (accuracy 70.6%), followed by 1.1mm cryoprobe (68.4%), trans-bronchial needle aspiration (46.7%), 1.9mm cryoprobe (41.2%), brush (30.3%) and lavage (23.7%). As a consequence of the 49.3% overall cytology sampling accuracy and a discordance of ROSE with final malignant

cytology findings (27.9%), ROSE was found to be correlating to procedural malignant finding outcome in only 47.5% of lesions. Confirmation of malignancy on ROSE also did not reduce amount of biopsies taken nor biopsy time. The results as described in Chapter 6 show there is currently no single approach or methodology that is a do-it-all for obtaining an adequate tissue diagnosis, and, that additional research is therefore warranted.

**Chapter 7** describes the changes in the radiation exposure and diagnostic accuracy of the cone beam CT guided navigation bronchoscopy procedure with increasing experience and the tailoring of imaging protocols to the navigation bronchoscopy setting in a single institution study. The potential learning curve experience of both radiation exposure and diagnostic accuracy were obtained by analyzing all consecutive cone beam CT guided navigation bronchoscopy procedures as performed at the Radboudumc (Dec 2017 – June 2020). It was found that radiation dose during the initial introduction phase of the cone beam CT guided navigation bronchoscopy (Chapter 5) were of acceptable levels (dose area product  $47.5 \text{ Gy}\cdot\text{cm}^2$ , effective dose: 14.3 mSv). After having concluded the comparison of workflows as described in Chapter 5, the choice was made to primarily navigate towards the peripheral nodule using cone beam CT guidance. By the forthcoming availability of new specific navigation bronchoscopy imaging protocols along with becoming increasingly experienced, procedural radiation dose could be reduced from an initial  $47.5 \text{ Gy}\cdot\text{cm}^2$  (effective dose: 14.3 mSv) to  $25.4 \text{ Gy}\cdot\text{cm}^2$  (5.8 mSv). Simultaneously, the diagnostic accuracy went up. The initial diagnostic accuracy as described in chapter 5 was 72.4% in the first 87 patients. After a total of more than 208 procedures, the last 64 patients (November 2019 – June 2020) resulted in a procedural accuracy of 90.6% (navigation success 98.4%). The navigation bronchoscopy procedure was thus found subject to a learning curve, with more experience and a tailoring of imaging protocols resulting in lower radiation exposure and better diagnostic accuracy.









# CHAPTER 9

General discussion and future perspectives



The research described in this thesis was focused on technological innovations in endobronchial lung cancer staging and diagnosis.

Part I of this thesis describes ultrasound strain elastography as a means that can help identify likely malignant lymph nodes in both a single center as well as a multi-center study setting. Whereas it was found of predictive value in the single center setting, the multi-center study further showed that ultrasound strain elastography could be integrated with other clinically available predictors such as FDG-PET and lymph node size for enhancing malignancy risk prediction. These findings were dissimilar to that of subjectively rated ultrasound B-mode characteristics. Subjective B-mode feature scoring was found of limited value for malignancy risk stratification because of suboptimal accuracy and inter- and intra-observer variability in scoring.

Part II of this thesis describes the introduction of the cone beam CT guided navigation bronchoscopy procedure for the diagnosis of suspected peripheral pulmonary lesions. By analysis of two navigation bronchoscopy workflows that comprised a different combination of technological assistance, the comparative diagnostic accuracy was assessed. Navigation to small lesions showed to be most successful if cone beam CT guidance was used as a primary navigation methodology. However, combining the methodologies of both workflows after having found an initial unsuccessful navigation in either resulted in highest success. The peripheral pulmonary lesions were then successfully reached in 88-90% of cases. Follow-up outcome showed this led to an accurate diagnosis in 72% of patients. Additional work was performed to assess how different factors affected the outcome of technology enhanced navigation bronchoscopies. An evaluation of tissue sampling methodologies in imaging verified successful navigations showed that the difference between navigation success and diagnostic accuracy can in part be explained by sampling tool error. Not all acquired tissue will reveal an adequate pathology outcome. As such, it is concluded that future work to increase sampling accuracy is warranted. A secondary evaluation of consecutive cone beam CT guided navigation bronchoscopies showed how procedural accuracy and radiation exposure can evolve over time. Obtaining additional experience in the cone beam CT guided navigation bronchoscopy resulted in an increase in the diagnostic accuracy and navigation success. Becoming more experienced in combination with a tailoring of the cone beam CT imaging protocols to the procedure also showed to significantly reduce procedural radiation dose. Combined, the findings as described in this thesis show that technological guidance can help improve the endobronchial diagnostic and staging accuracy in (suspected) lung cancer. They are small steps towards improving the outcome of lung cancer patients. On basis of these findings, several points for discussion as well as (near) future directives can be given. These points are relevant for the field of pulmonary oncology and interventional pulmonology, but underline the need of a more diverse and multi-disciplinary approach in order to achieve our common goal.

## 9.1 Endosonography and strain elastography

Endoscopic ultrasound evaluation of lymph nodes is routinely performed to stage and therewith prove both absence and presence of disease in individual lymph nodes. If a mediastinal lymphadenopathy remains unproven after endoscopic needle aspiration while earlier PET-CT imaging findings are deemed abnormal, performing a cervical mediastinoscopy is indicated [6]. Current recommendations propose to complete a systematic endosonographic staging by going from the least to the most suspected site. Sampling of at least stations 4R, 7 and 4L along with additional imaging suspected nodes should be performed, by combining an endoscopic assessment from both the airways as well as the esophagus [6,10]. A widely regarded meta-analysis and systematic review by Korevaar *et al.* (2016) found the pooled sensitivity and negative predictive value for detecting metastatic N2/N3 disease in such a combined systematic EBUS-EUS (endobronchial ultrasound & esophageal ultrasound) approach was 86% and 92%, respectively [15]. However, while the included studies focus most on the added value of combining EBUS with EUS for increasing sensitivity, less attention is brought upon the individual study criteria for deciding on aspiration in the first place. A study by Crombag *et al.* (2018) for example stated systematic staging, but further defined that stations 4R, 7 and 4L only needed to be aspirated if the short axis diameter was  $\geq 8$  mm, resulting in a sensitivity of 82% and negative predictive value of 87% for staging of N2/N3 disease [13]. Annema *et al.* (2010) reported a sensitivity of 85%, where sampling involved aspiration of observer interpreted suspicious lymph nodes ( $\geq 10$  mm size, FDG-PET avid and/or those with suspicious ultrasound criteria) [12,46]. Hwangbo *et al.* (2010) found sampling of all  $\geq 5$  mm lymph nodes had 91% sensitivity and 96% negative predictive value, while Ohnishi *et al.* (2011) had similar methodology and found a slightly lower sensitivity of 84% and NPV 94% for identifying malignant N2/N3 disease [151,152]. The similarity of the study outcomes are peculiar when considering the findings presented in part I of this thesis. In the performed multi-center study, strain elastography lymph node measurements were included per judgement of the observer. In total, 31 out of 159 included  $< 8$  mm short axis lymph nodes were found malignant (disease prevalence 0.19). Several of  $< 8$  mm lymph nodes would likely not have been considered for aspiration in some of the aforementioned studies. From these findings it can be hypothesized that systematic EBUS-EUS should routinely include sampling of all  $\geq 5$  mm lymph nodes, if clinically possible. The clinician will however also be well aware that exhaustive staging of lesser suspected lymph nodes is not always possible, and, that there is also the possibility of unrepresentative cytology findings [13,94]. The question then becomes what observer decision making should include. As is described in this thesis, even experienced endoscopists cannot reproducibly score lymph node risk based on B-mode still images. Likely, it is the time-stressed and unrepresentative findings scenario where strain elastography is of most immediate clinical relevance. Strain elastography in combination with other predictive values could help identify likely malignant nodes which should be subject to radiotherapy if exhaustive sampling was not possible, or, could help more objectively decide on which nodes to sample within a certain region intra-procedurally.

## 9.2 Endosonographic staging in early disease

The meta-analysis by Korevaar *et al.* analyzed all available studies that performed systematic endosonographic mediastinal staging for N2/N3 disease and found a pooled sensitivity of 86% and NPV 92% [15]. Detailed information on PET-CT/CT suspicion and pre-procedural imaging based nodal staging in the included studies is lacking. As the intent is to move towards earlier diagnosis of lung cancer, knowing its potential improved outcome, an imaging negative mediastinum and/or hilum is likely to be more frequently found (cN0/cN1). Data on the sensitivity and use of endosonographic staging in these patients is scant. A prospective study by Dooms *et al.* reported using EBUS-TBNA – only sometimes combined with EUS-FNA – in a group of 100 patients suspected of cN1 NSCLC disease. Eventual N2/N3 prevalence was found to be 24%, and endoscopic staging therein identified malignancy with a sensitivity of 38% and specificity of 81%. Only 10 out of 24 metastases were correctly identified. Five out of 14 lymph nodes were missed because of unrepresentative cytology findings or because the lymph nodes were unreachable by endosonography [153]. Ong *et al.* performed a detailed retrospective analysis on 220 patients with cN0 disease. They found cN0 was upstaged because of EBUS in 18 cases (N1=11, N2=6, N3=1), because of surgery in 27 cases (N1=19, N2=8), and because of imaging follow-up in 4 cases (N1=2, N2=2) in a total of 49 out of 220 patients. Overall, this would have resulted in an EBUS sensitivity of 36.7% and NPV of 84.7%. However, an exclusion of the lymph nodal stations that were anatomically unreachable by EBUS-TBNA would lead to a hypothetical sensitivity of 60% and NPV of 93.4% [154]. Yasufuku *et al.* retrospectively assessed potentially resectable cN0/cN1 lung cancer of 163 cases and finds a systematic staging of all  $\geq 5$  mm lymph nodes awarded with a diagnostic accuracy of 96.6% (sensitivity 76.2%). All false negatives were found to be located beyond lymph node region 11 [155]. The limitation that endosonographic staging does not allow easy sampling of regions 3, 5 and 6 is mainly relevant for N2/N3 disease. If we however are able to consistently move towards a need for N0 disease differentiation, a similar problem is found. No endoscope is currently able to evaluate or sample any region beyond station 11 (left or right). And additionally, it is likely clinical N0 staging will not incur (extensive) lymph node evaluation in the first place [32]. Problematic, as our recent in-depth analysis of surgically treated patients for resectable lung cancer showed that clinical N0 staging was found to contain occult nodal involvement (N1/N2) in 23.1% of patients [156]. A finding corroborated by DuComb *et al.* (2020) [157]. Combined, these findings suggest that current (endosonographic) staging solutions are inaccurate in assessing lymph nodal involvement in suspected early stage (N0/N1) lung cancer. Furthermore, whereas surgery would eventually reveal true nodal involvement in case of lobectomy, these adverse findings have important consequences for non-surgical therapies and when considering limited resection. With no currently available means that fill this gap, it seems there is a great need for future technology that would enable more sensitive minimally invasive staging of lung cancer.

### **9.3 Strain elastography standardization**

Strain elastography can help identify malignant hilar and mediastinal lymph by itself, and, in combination with either one or the combination of FDG-PET avidity and short axis size measurements. This was concluded in this thesis by performing an international multicenter study with a standardized measurement protocol, and, by harmonizing the systems and their settings. What should not be disregarded is that ultrasound strain elastography is a semi-quantitative measure, relying on ultrasound processing settings and a customizable methodology for relaying the output back to the user. The future widespread availability of strain elastography will depend on further collaborations with the industry and/or the ability of making a stand-alone (standardized) application that can be run alongside the EBUS-TBNA procedure. Alternatively, development of imaging options that would allow for objective quantification of stiffness would also be of high interest (i.e. shear wave elastography).

### **9.4 Quantitative ultrasound**

Subjectively scored ultrasound B-mode features have repeatedly been studied as potential means of predicting lymph node malignancy [46,47,88,95]. In this thesis it is shown that these features individually indeed have some predictive value, but also showed that their subjective scoring results in considerable intra- and inter-observer disagreement. Future work is needed to assess if subjective means can be replaced by quantitative and therewith objective features. Ultrasound system related features that can be of interest are for example the attenuation coefficient and speckle size [158]. Image segmentation features such as region of interest entropy, volume, and shape can possibly be correlated to earlier studied subjective features and are also relevant. Artificial intelligence-based algorithms for lymph node recognition and risk prediction are another feasible option – at least to obtain a reproducible scoring – but convey the likely need of a large database with standardized image settings for high accuracy. The potential information that is contained within (conventional) ultrasound imaging for identifying malignancy remains to be (objectively) investigated. Moving away from high disease burden will furthermore involve lower lymph node disease burden (and therewith possibly micro-metastatic disease), which can also have a profound consequence on deductible imaging features.

### **9.5 Standardized multi-modal staging**

Lymph nodal staging in lung cancer is highly dependent on the different imaging modalities used and (subjective) expertise of multiple physicians. Each of these modalities have their limitations and detection limits. And while all imaging is performed in (internationally) protocolized fashion, no standard way of interpreting results is available. In clinical practice,



the multi-disciplinary team will have a leading role in determining staging. The CT is interpreted by a radiologist, the PET-CT by the nuclear medicine physician, the EBUS procedure by the pulmonologist and sampling results by the pathologist. The pulmonary physician, surgeon, radiation oncologist and (pulmonary) oncologists will discuss staging results along with patient characteristics in the multi-disciplinary tumor board, from which a strategy is decided upon. An algorithm or standardized model that is able to recombine multi-modality imaging in an accurate and reproducible staging available to the different specialties in the blink of an eye would be of great value.

## 9.6 Navigation bronchoscopy

The Radboudumc is the first center in the Netherlands to implement the cone beam CT guided navigation bronchoscopy procedure in routine clinical care. In Chapter 5 it is described how, in an initial experience, an accurate diagnosis is obtained in 72.4% of patients through this minimally invasive procedure. Subsequently monitoring how the diagnostic accuracy and radiation exposure evolved over time showed that becoming more experienced significantly changed procedural characteristics. While reducing radiation dose, the diagnostic accuracy was increased. As such, it shows the cone beam CT guided navigation bronchoscopy is an adequate methodology for moving towards earlier and improved diagnosis of suspected and/or proven lung cancer. The intent of a minimally invasive safe and accurate means of diagnosis is relevant considering at least 46% of Dutch early stage lung cancer patients in 2017 and 2018 were treated (by surgery or radiotherapy) for a known or suspected lung cancer without having a tissue diagnosis [159]. As the study by IJsseldijk *et al.* (2019) and an accumulation on wedge resection study results also imply, this translates to a significant number of patients receiving radiotherapy or surgery with curative intent for a non-malignant pathology [32,45]. Ideally, one would omit both watchful waiting and therapeutic applications without a diagnosis only if there is a certain benign or malignant finding, respectively. At current, the suboptimal outcome of minimally invasive strategies along with their invasiveness however trouble this. Only limited (American) health technology assessments are furthermore available on the patient outcome and cost-effectiveness of this risk stratification procedure [160–162]. One of aforementioned studies concluded that a diagnostic strategy of PET-CT, navigation bronchoscopy or CT-guided TTNA should be preferred above video-assisted thoracic surgery (VATS) only if chance of malignancy is at least 85%. In their health technology assessment they however did not consider (non-diagnostic) radiotherapy applications nor did they specify that the QALY is reduced in cases where the patient is left with anxiety due to a watchful waiting strategy. Moreover, the estimated accuracy of navigation bronchoscopy might be different from that as described in this thesis. Future research is required to identify the best work-up and further improve the minimally invasive field. One would however expect the cost-effectiveness scenario of needing to diagnose yes or no becomes increasingly ill-posed as the means of minimally invasive diagnosing lesions becomes an increasingly safe, easy and reliable method.

## 9.7 Clinical navigation technology learning and adoption

The implementation of techniques in clinical setting is often directed towards either simplifying or improving routine clinical practice and its outcome. The cone beam CT guided multi-modality navigation bronchoscopy showed the potential to improve clinical outcome, especially when performed by experienced hands. It is however to be questioned if the cone beam CT guided navigation bronchoscopy procedure as introduced in this thesis is simpler (to the less experienced endoscopist) than other previously available means or oncoming techniques like robotic assisted bronchoscopy [41, 163–165]. Initial in-vivo experience reports by robotic bronchoscopy – utilizing pre-procedural CT information and endoscopic imaging along with endoscope position sensing – state their immediate navigation success is >95% [108, 165]. A recently launched integrative guidance system which combines pre-procedural CT with radial ultrasound mini probe imaging and 2D fluoroscopy for augmented fluoroscopic guidance equally reports a 93-95% navigation success rate [163, 164]. As these modalities report a higher navigation accuracy than our initial multi-modal cone beam CT experience (89%), these could prove valuable in improving or simplifying navigation success. Surely, the ease with which the endoscopist is able to navigate towards the lesion and the cost of doing so will have a high impact on the choice of modality. To make the cone beam CT guided navigation bronchoscopy a more widely accepted and implemented methodology, future efforts should be made to improve its intuitiveness. This can for example be done by developing a virtual endoscopic view from the available 3D CBCT and 2D fluoroscopic imaging, or conversely, providing an automatic overlay of the complete endobronchial tree on the 2D fluoroscopic image.

## 9.8 Representative tissue is the issue

Based mostly on the study by Lee *et al.*, it is suggested endosonographic lymph node staging should involve at least 3-4 needle aspirations of individual lymph nodes. Lee *et al.* reports a 95.3% sensitivity of individual lymph nodes and obtaining a sample adequacy of 100% after 3 consecutive aspirations [17, 94, 166]. Needle aspiration is generally performed under direct endosonographic imaging to confirm penetration of the target tissue, supposedly leaving little room for error. One could however reckon that needle revolutions inside an area of interest are not necessarily representative of the complete region of interest, even if several different sites upon consecutive sampling attempts are chosen. This reasoning becomes especially relevant as disease burden in the assessed lymph nodes becomes low. Sampling in navigation bronchoscopy is similarly but even further complicated as there's currently no real-time exact guidance in acquiring histology or cytology specimens. Real-time tissue sampling guidance as used in Chapters 5-7 of this thesis was available only by external imaging such as X-ray fluoroscopy. With modalities such as fluoroscopy imaging from an external reference point in a moving lung, a sampling error is easily made. And with

every sampling instrument having a slightly different rigidity in a very soft and deformable lung, a change in lesion contact and a suboptimal catheter angulation as a consequence of changing catheter shape is easily found. With no means of compensating for this currently available – aside of the robotic endoscope which is not yet available to the European market – it seems there is room for improvement. These findings are corroborated by the majority of studies, which all report a difference between navigation success and diagnostic accuracy (i.e. [41,108,164,167]). The needed meticulous positioning is likely one of reasons we and others find that extensive sampling using multiple sampling instruments enhances diagnostic yield [113,122]. A further reason for this mismatch might be the difficulty in classifying pathology outcome based on only small samples wherein nuances are important. Where lymph node sampling ought to confine itself to only several microscopic imaging scenarios, even the diagnosis of adenocarcinoma in a peripheral pulmonary nodule involves classifying it into a range of pathological states [168]. And as Coghlin *et al.* for example describe in a study on sampling in central endobronchial lesions, lesions are heterogeneous in nature and only a minority of sampling outcome will reveal the true pathology [142]. Concluding, there is a need to develop methodologies for allowing better in-vivo tissue biopsy guidance in both endosonographic needle aspiration and navigation bronchoscopy. Secondly, reducing the repeated sampling need by introducing a sampling device that would enable a complete cross-section biopsy of the entire lymph node and peripheral lesion would also be of great help. To help resolve these issues, a plurality of methodologies and devices has been ideated, which resulted in two patent applications during the conduct of this thesis (P6087546EP, P6091207EP).

## 9.9 Minimally invasive staging and treatment

While diagnosis is currently the most sought-after goal of navigation bronchoscopy, increasing interest is also directed towards enabling local minimally invasive treatment (i.e. [125,169–171]). For this, CBCT imaging might prove essential. Meticulous (transparenchymal) positioning and monitoring of treatment area is possible only by having detailed 3D information available. Current (commercially sponsored) studies seem to suggest a microwave ablation based technique is the optimal means for treating peripheral pulmonary lesions (i.e. [170,171]). Indeed, implementation thereof might be of potential use as neoadjuvant therapy, in metastatic disease, or patients with limited options because of low performance. Its use in early stage disease might however remain limited, as it provides only local control (limited to primary tumor). Microwave ablation is unlikely able to (curatively) treat metastatic spread to nearby (intralobar) lymph nodes in early stage disease. As described in 9.2. 'Endosonographic staging in early disease', occult nodal metastatic disease in these areas are however frequently found [156,157]. To offer a curative endobronchial treatment in early stage disease, both options to endoscopically stage and treat draining lymph nodes should be explored. For example, injection and imaging of specific agents might

allow for improving staging and/or enabling local treatments in early stage disease. If this proves possible, it would allow for a future single minimally invasive diagnosis and curation procedure.

## **9.10 Low and high fidelity approaches**

In routine clinical practice, different patients and concurrent lesions will be seen. Not all cases will require technology utilization to the fullest, especially in an era where containing healthcare cost becomes increasingly important. A work-up tailored to case complexity seems relevant. Navigation to sub-centimeter nodules or any potential treatment will for example benefit from CBCT guidance, while the navigation to a three centimeter peribronchial lesion positioned in the apical segment of the upper lobe could also be reached by less complex technologies such as x-ray fluoroscopy combined with ultrathin bronchoscopy. The first is best performed in an expert center, while the second can also be performed in less experienced centers (if properly guided). While the advent of newer (often expensive) technologies at the forefront of healthcare is exciting, the translation from expert to less experienced centers should not be forgotten. Future technology development should focus on also enabling navigation bronchoscopy in less resourceful and experienced centers, and, allowing for a clear distinction in case needs.

## **9.11 (Multi-disciplinary) Teamwork**

The navigation bronchoscopy implies a multiplicity of technology and instruments, often handled at the same time. Depending on expertise available, a mix of patient and nodule characteristics need to be aligned with ultrasound imaging, electromagnetic tracking, fluoroscopy, endoscopic imaging, instrument properties, pre-operative imaging and so on. When relying on technology, one needs to be considerate of all individual pitfalls. If a future therapeutic or local staging application is also considered, we are yet venturing into another new terrain of expertise. The starting point here is interventional pulmonology. However, what it concerns is unclear. The expertise which it will need is inter-disciplinary, and might be a specialized team of both clinical as well as technical perspective (with a solid base in pulmonary medicine).

## **9.12 Generalized future perspective**

For achieving lung cancer curation it seems unequivocal to target early identification, diagnosis and treatment of peripheral pulmonary lesions. In the upcoming years either one or multiple of non-invasive diagnostics such as breath analysis, liquid biopsy or low-dose

CT screening supported with novel AI-algorithms will surely allow a cost-effective means of at least early identification, and possibly, diagnosis. As current survival numbers show, the next frontier then becomes improving early stage lung cancer outcome. Aside of aiding in diagnostics, the future of (endobronchial) technology in early stage lung cancer is therein possibly two-fold. One is to allow unravelling the mechanisms of early stage lung cancer in-situ, it's micro-environment and impact on local immune-oncological phenomena to improve diagnostic and staging accuracy. Two is to provide a means of minimally invasive curative treatment. Most ideally, future technology and knowledge will allow us to move away from a sequential multi-modal diagnostic and treatment work-up and move towards a single stop diagnose-and-treat. It would however be short sighted to suggest technology is able to do it all. To reach this dot on the horizon, several aspects of lung cancer remain to be studied by the different specialties in pulmonary oncology. An intensive collaboration is needed to fully elucidate what we are aiming for, and only then can we decide where technology should take us.





# CHAPTER 10

Nederlandse samenvatting





Longkanker is de meest voorkomende vorm van kanker wereldwijd, met meer dan 2.2 miljoen gevallen per jaar. De incidentie ervan zal ook in de aankomende jaren blijven groeien, waarbij in 2035 een toename tot 3.2 miljoen nieuwe gevallen per jaar verwacht wordt [2]. In 2019 werden er in Nederland zo'n 13.800 mensen gediagnosticeerd met deze ziekte. Patiënten hebben pas laat klachten, wat er helaas toe leidt dat zo'n 50% van de patiënten al vergevorderde ziekte (stadium IV) hebben op het moment van diagnose. In dit late stadium - waar er ook betrokkenheid is van andere organen - is de overlevingskans na vijf jaar ongeveer 5%. Dit in tegenstelling tot een 5-jaars overleving van zo'n 61% als de patiënt in het vroegste stadium geïdentificeerd kan worden (stadium I) [1]. Om de kans op genezing groter te maken is het derhalve van belang dat longkanker in een zo vroeg mogelijk stadium geïdentificeerd wordt en dat daarnaast het stadium van de ziekte accuraat in kaart wordt gebracht. In dit proefschrift wordt onderzocht of nieuwe technieken het diagnostische traject van longkanker verder kunnen verbeteren, met daarbij de focus op de bijdrage van technieken in de flexibele endoscopie.

## **Deel I - Endoscopische stadiëring van longkanker middels ultrageluid technieken**

Flexibele endoscopische procedures die gebruik maken van de aanwezige luchtwegen of de slokdarm worden frequent uitgevoerd bij een variëteit aan (long)ziekten. Met een stuurbare flexibele slang waarop een videocamera gemonteerd zit kan er door bestaande openingen genavigeerd worden. Specifiek bij longkanker is het gebruik van flexibele endoscopie voor de stadiëring van ziekte aanbevolen zorg. In dat geval is er naast de camera ook nog een echokop geplaatst op het uiteinde van de endoscoop, waarmee echo's gemaakt kunnen worden. Bij een verdenking op longkanker zal er allereerst FDG-PET en/of CT beeldvorming aangevraagd worden, welke informatie kunnen geven over de anatomie en het metabolisme. Laten deze naast een tumor ook zien dat er misschien lymfeklieren betrokken zijn, dan raadt men aan een verdere echo geleide evaluatie van de (hilaire en mediastinale) lymfeklieren door de luchtwegen en slokdarm uit te voeren [10]. Wanneer op echo een lymfeklier gezien wordt, kan deze aangeprikt worden middels een naald die opgevoerd wordt door het werkkanaal. Zo kan er naast de 'beeldende' diagnose door middel van PET-CT en echo beeldvorming ook weefsel verkregen worden voor het stellen van een pathologische diagnose. Tijdens deze endoscopische evaluatie procedure (ook wel EBUS-TBNA/EUS-FNA procedures genoemd) dienen de lymfeklieren van de verschillende regio's systematisch geëvalueerd te worden, waarbij gestart wordt met de minst verdachte klier en teruggewerkt wordt naar de meest nabij gelegen – meer verdachte - klieren. Lymfeklieren worden daarbij aangemerkt als verdacht op basis van een verhoogd metabolisme (FDG-aviditeit) en grootte (CT- en echo beeldvorming). Klieren met deze kenmerken dienen in ieder geval gepuncteerd te worden door middel van een holle naald, om op deze manier cellen voor diagnostiek te verkrijgen.

Naast de FDG-aviditeit en kliergrootte worden veelal ook (subjectieve) echo karakteristieken gebruikt om te beoordelen welke klieren verdacht zijn en gepunteerd moeten worden.

In **hoofdstuk 2** wordt beschreven hoe een relatief nieuwe endoscopische echo techniek, genaamd strain elastografie, mogelijk verdachte lymfeklieren kan identificeren. Echo strain elastografie is een techniek die de relatieve vervorming van weefsel in beeld brengt. Deze vervorming (*strain*) wordt in kaart gebracht door echo signalen opeenvolgend in tijd met elkaar te vergelijken terwijl er een deformatie plaatsvindt. De vervorming geeft een karakteristiek vergelijkbaar met die van de klassieke geneeskundige palpatie. Het wordt verondersteld dat kwaadaardige lymfeklieren een lagere vervorming (ook wel een lagere rek) zullen hebben. In de EBUS-TBNA/EUS-FNA procedures worden deformaties als gevolg van het cardiovasculaire systeem gebruikt om de weefselvervorming in kaart te brengen. De berekende rek is relatief, het geeft weer hoe het ene gebied ten opzichte van het andere vervormt. Omdat de berekende rek een relatieve maat is presenteren we in hoofdstuk 2 een protocol om een zo reproduceerbaar mogelijke meting te verkrijgen met inachtneming van zowel technische als klinische beperkingen. Na het opstellen van het meetprotocol worden er in 63 patiënten met een longkanker verdenking een totaal van 120 lymfeklier strain elastografie metingen verzameld. Met de verzamelde metingen wordt bepaald dat de rek het beste beoordeeld kan worden door het gemiddelde te nemen van de rekwaarden in een geselecteerde regio van interesse ten opzichte van het gehele afgebeelde gebied. Door de rek te normaliseren – in de afbeelding is er altijd een gebied met geen vervorming (0) alsook een gebied met maximale vervorming (255) – krijgt de gebruiker een relatieve vervorming terug. In dit hoofdstuk wordt beschreven dat het oppervlakte onder de ROC-curve voor het voorspellen van kwaadaardige lymfeklieren met deze methodiek 0.846 is. Deze beoordelings-methodiek is daarnaast objectief, er wordt alleen aan de endoscopist gevraagd om de lymfeklier te selecteren, waarna een waarde teruggegeven wordt. Een afkapwaarde van 78 (bereik 0-255) geeft een sensitiviteit van 93%, specificiteit van 75%, positief voorspellende waarde van 69% en negatief voorspellende waarde van 95% (accuraatheid: 82%). Lymfeklieren met een rek van minder dan 78 (een lagere vervorming) blijken een hogere kans te hebben op kwaadaardigheid dan klieren met een rek van >78 (een hogere vervorming). Een eerste verkennende analyse in deze studie laat tevens zien dat de rek-waarde tezamen met FDG-PET en CT informatie gebruikt kan worden om de kans op kwaadaardigheid beter in te schatten.

**Hoofdstuk 3** beschrijft hoe endoscopische echo strain elastografie in een multicenter internationale setting (5 centra) van een voorspellende waarde kan zijn in het klinische traject van longkankerdiagnostiek. In de periode juni 2016 – juli 2018 worden 525 lymfeklier metingen verzameld in een totaal van 327 patiënten. Het verzamelen van metingen gebeurt naar inzicht van de endoscopist en resulteert in een kwaadaardige lymfeklier prevalentie van 0.48. In Receiver Operator Characteristic analyse blijkt strain elastografie een oppervlakte onder de curve te hebben van 0.77, welke aangeeft dat strain elastografie een voorspellende

waarde heeft. Om de vertaalslag te maken naar de mogelijke toepassing in de reguliere kliniek wordt er gekeken naar de voorspellende waarde van verschillende afkappunten van vervorming. Omdat de correcte identificatie van maligniteiten het belangrijkste wordt geacht, wordt een afkapwaarde geprefereerd voor een hoge sensitiviteit en negatief voorspellende waarde. Op basis van deze voorkeur wordt geconcludeerd dat de eerder gevonden afkapwaarde van 78 in hoofdstuk 2 naar 115 bijgesteld moet worden. Met deze afkapwaarde blijkt strain elastografie voor het identificeren van kwaadaardige lymfeklieren 90% sensitief, 43% specifiek en heeft het een positief en negatief voorspellende waarde van respectievelijk 60 en 82% in een internationale multicenter studie. Daarnaast blijkt uit hoofdstuk 3 dat deze echo strain elastografie metingen verder gecombineerd kunnen worden met FDG-PET informatie en echo-gebaseerde kliergrootte om de kans op maligniteit nog beter in te schatten. Om dit te vertalen naar klinisch toepasbare scenario's worden twee beslisbomen gepresenteerd; een beslisboom die kliergrootte en gemiddelde vervorming combineert en een beslisboom die FDG-PET-aviditeit, kliergrootte en gemiddelde vervorming combineert.

In de huidige klinische praktijk wordt er naast FDG-PET en CT-grootte frequent gebruik gemaakt van subjectieve conventionele echo karakteristieken voor het bepalen of lymfeklieren wel of niet kwaadaardig zijn, en of de lymfeklier derhalve aangeprikt moet worden. Karakteristieken die in verband gebracht worden met kwaadaardige lymfeklieren zijn: heterogene klier echogeniciteit, afwezigheid van een centrale klier-hilus, aanwezigheid van centrale klier necrose, bolronde kliervorm (t.o.v. langwerpig) en scherp afgrensbare klier marges. In **hoofdstuk 4** wordt beschreven wat de invloed is van kliergrootte op de voorspellende waarde van deze karakteristieken, en, of de endoscopist deze karakteristieken reproduceerbaar samen kan vatten om een oordeel te vellen over lymfeklier kwaadaardigheid. Ter beoordeling van de individuele voorspellende waarde van deze karakteristieken worden de verzamelde lymfeklieren beoordelingen uit de multicenter internationale studie van hoofdstuk 3 gebruikt. Wanneer een  $\geq 8$  mm korte as van de klier gebruikt wordt als voorspeller van kwaadaardigheid blijken 210 van de 237 kwaadaardige lymfeklieren correct geïdentificeerd, terwijl 110 van de 253 goedaardige klieren correct als niet kwaadaardig worden geclassificeerd (sensitiviteit 89%, specificiteit 46%, positief voorspellende waarde 61%, negatief voorspellende waarde 81%). Het verder toevoegen van de voorgestelde echo karakteristieken blijkt van gelimiteerde waarde, ook wanneer er gekeken wordt naar de reproduceerbaarheid van deze beoordelingen. Wanneer experts ( $>400$  procedures,  $n=5$ ) en ervaren endoscopisten (50-400 procedures,  $n=3$ ) gevraagd worden om een willekeurige subset van in totaal 200 lymfeklieren te scoren op meest waarschijnlijke diagnose (kwaadaardig of goedaardig), is de overeenkomst tussen beoordelaars slechts 71-74% (Gwet's agreement coëfficiënt 1 0.42-0.48). Wanneer een beoordelaar de lymfeklier herhaaldelijk scoort, resulteert dit slechts in 80-86% van de gevallen in dezelfde uitkomst (Gwet's agreement coëfficiënt 1 0.60-0.76). Omdat deze variabiliteit bij verdere analyse verschillend blijkt te zijn voor klieren  $< 8$  mm,  $\geq 8$  mm en goedaardige of kwaadaardige klieren, wordt er geconcludeerd dat een risico stratificatie

aan de hand van subjectieve echo karakteristieken geen eenduidige voorspellende waarde heeft en van beperkte waarde is.

## **Deel II - Klinische technologie ter diagnose van perifere afwijkingen in de long**

Beeldvormende modaliteiten zoals CT waarop de longen afgebeeld staan worden uitgevoerd in routinematige klinische zorg voor een veelvoud aan ziekten. In gemiddeld zo'n 13% van de CT scans die worden gemaakt voor een reden anders dan longkanker blijkt één of meerdere kleine afwijkingen in de longen gezien te worden. Wanneer deze afwijkingen bij toeval gevonden worden, dan is de kans op goedaardige ziekte veel groter dan die van een kwaadaardigheid. Echter, uiteindelijk blijkt toch zo'n 1.5% van deze scans tot een diagnose van longkanker te leiden [32]. Het opvolgen van deze afwijkingen in patiënten zonder klachten is gerechtvaardigd omdat het vroeg identificeren van ziekte belangrijke gezondheidswinst oplevert. Meerdere studies beschrijven daarnaast ook wat de potentiële overlevingswinst zou zijn wanneer een populatie met verhoogde kans op longkanker door middel van CT-scans specifiek gescreend zou worden voor deze ziekte. Het blijkt dat een dergelijke CT screening de longkanker mortaliteit met tenminste 20% kan verlagen [26,31]. De behaalde gezondheidswinst wordt hierin voornamelijk toegeschreven aan het vinden van longkanker in een vroeg stadium. Aan de hand van onder andere deze resultaten wordt de nationale implementatie van screeningsprogramma's aanbevolen door talrijke gremia in vele landen [25–30]. De CT-scans die in de reguliere klinische diagnostiek alsook die in een screeningsprogramma worden gemaakt zullen veel afwijkingen vinden en aanvullende weefseldiagnostiek vereisen. De vraag naar een accurate, makkelijke en veilige manier om deze afwijkingen te diagnosticeren is dan ook groot.

De gebruikte strategie voor het diagnosticeren van kleine afwijkingen in de long is momenteel onderhevig aan nationale en internationale variatie. Deze variatie is tot stand gekomen doordat er momenteel geen simpele en veilige universele methode beschikbaar is om tot een diagnose te komen. De keuze voor een diagnostische methode wordt gemaakt aan de hand van centrum afhankelijke variabelen zoals de beschikbaarheid over klinische technologie, aanwezige expertise en procedurele risico's. De meest gebruikte minimaal invasieve opties zijn de trans-thoracale CT geleide punctie of de trans-bronchiale (flexibel endoscopische) benadering. De trans-thoracale CT geleide punctie maakt gebruik van een CT-scanner om beeldgestuurd een instrument door de borstkas en in de afwijking te prikken. Deze methode heeft een hoge sensitiviteit van 91% en een negatief voorspellende waarde van 80%, maar leidt ook tot complicaties zoals een pneumothorax in meer dan 20% van de gevallen [32,44]. Het historisch beschikbare alternatief is de flexibele endoscopische benadering waarbij enkel gebruikt wordt van conventionele röntgen doorlichting en de natuurlijke luchtwegen. Omdat de conventionele endoscopen te groot zijn voor de kleine luchtwegen moet er onder beperkt

zicht gezocht worden naar de spreekwoordelijke speld in een hooiberg. Via de natuurlijke luchtwegen worden instrumenten opgevoerd tot de plek waar de afwijking verwacht wordt, waarna herhaaldelijk weefselbipten afgenomen worden. Deze benadering is aanzienlijk minder traumatisch (kans op pneumothorax <2%), maar heeft in combinatie met röntgen doorlichting geleiding ook slechts een sensitiviteit van 34% [34]. In het afgelopen decennium zijn er echter technologische ontwikkelingen geweest die de endoscopist kunnen helpen bij het endoscopisch bereiken dan wel aanprikken van afwijkingen. Dit heeft de sensitiviteit van de procedure omhoog gebracht tot zo'n 70%-80%, waarin nog steeds minder dan 3.0% complicaties gerapporteerd worden [39,41]. Deze technieken berusten op het gebruik van elektromagnetisme voor het traceren en navigeren van instrumenten, geminiaturiseerde echo beeldvorming voor endobronchiale visualisatie van de afwijking in het longparenchym, de ontwikkeling van kleinere endoscopen om zodanig verder in de long te kunnen komen maar recentelijk ook bijvoorbeeld de introductie van robotica [41,49].

**Hoofdstuk 5** beschrijft de evaluatie van twee combinaties van technieken voor het diagnosticeren van kleine afwijkingen in de longen middels flexibele endoscopie. De hypothese is dat deze twee methodieken beide veilig en accuraat een weefsel diagnose kunnen verkrijgen. De beide methodologieën verschillen enkel in het eerste gedeelte van de procedure, wanneer er getracht wordt naar de afwijking te navigeren. De eerste methodologie maakt voor de navigatie naar de afwijking gebruik van een combinatie van elektromagnetische navigatie techniek en geminiaturiseerde echo beeldvorming. De tweede methodologie maakt gebruik van een zogenaamd cone beam CT systeem ter navigatie, in combinatie met eenzelfde echo systeem als in de eerste methodologie. Het cone beam CT systeem, welke gesitueerd is op de interventie radiologie alsook de hybride operatiekamer, maakt het mogelijk om zowel 2D röntgen als 3D CT-scan gelijkende beeldvorming te produceren. Beschikbare software en de kalibratie van dit systeem met de operatietafel maakt het verder mogelijk om de opgenomen 3D beelden te segmenteren en intra-procedureel op 2D beelden te projecteren. Zo kan een aanvankelijk op 2D röntgen onzichtbare afwijking met behulp van de segmentatie op eerdere 3D beeldvorming toch gevisualiseerd worden. De bewegingsmogelijkheden van het systeem maakt het daarnaast mogelijk om in meerdere vlakken deze projecties te verzorgen, zodat de endoscopist in meerdere vlakken onder röntgendoorlichting bevestiging kan krijgen. In dit hoofdstuk wordt geëvalueerd of de primaire methodiek succesvol of onsuccesvol is door na de navigatie fase een cone beam CT-scan te maken ter confirmatie van het bereiken van de afwijking. Met behulp van de cone beam CT beeldvorming wordt er vervolgens besloten of het zinvol is om een oversteek naar de andere navigatie methodiek te maken. Indien de navigatie succesvol blijkt op cone beam CT beeldvorming, wordt er in beide methodieken weefsel afgenomen onder verdere geleide van cone beam CT beeldvorming en röntgendoorlichting. In totaal worden 87 patiënten met 107 afwijkingen geïncludeerd. De gemiddelde lange as diameter van de afwijkingen is 14.2 mm in de elektromagnetische navigatie arm en 16.6 mm in de cone beam CT arm. Het blijkt dat de elektromagnetische navigatie techniek minder vaak succesvol is dan de

navigatie onder geleide van cone beam CT en bijbehorende röntgendoorlichting, leidend tot een succesvolle navigatie in respectievelijk 52.2% en 76.3%. Het verder combineren van de technieken als de navigatie eerder onsuccesvol blijkt resulteert dat uiteindelijk in beide armen 87.5-89.9% van de afwijkingen succesvol bereikt worden. Het weefsel dat door middel van een navigatie afgenomen wordt resulteert echter slechts in 72.4% van de gevallen in een accurate diagnose. In 3.4% van de patiënten leidt deze procedure tot een pneumothorax. Er wordt geconcludeerd dat een navigatie bronchoscopie een veilige diagnose kan stellen in meer dan 70% van de gevallen, en dat een primaire cone beam CT geleide navigatie hierin de voorkeur heeft. Om daarnaast nog betere resultaten te bereiken in de toekomst zal er - naast het verbeteren van de navigatietechniek - een verbeteringslag gemaakt moeten worden in het verkrijgen van voldoende adequaat weefsel voor het stellen van een correcte diagnose.

In hoofdstuk 5 blijkt dat het verkrijgen van een accurate diagnose na een succesvolle navigatie niet vanzelfsprekend is. Er wordt een discrepantie tussen het bereiken van de afwijking en een adequate diagnose gezien. Dit kan veroorzaakt worden door meerdere factoren. Kleine afwijkingen vereisen een minutieuze positionering van instrumenten ter accurate afname van weefsel. Daarnaast is een afwijking vaak heterogeen van aard, niet elk biopt zal een diagnose geven die correspondeert met de oorspronkelijke aard van de afwijking. In **hoofdstuk 6** wordt geanalyseerd hoe de verschillende beschikbare instrumenten voor het verkrijgen van weefsel (cytologie alsook histologie) bijdragen aan een accurate diagnose na een succesvolle navigatie. Tevens wordt er gekeken naar de accuraatheid van ROSE, een methodiek die intra-procedureel direct uitsluitel kan geven over het representatief zijn van cytologie en de aanwezigheid van kwaadaardige aandoeningen daarin. Het blijkt dat de forceps biopteur (een grijper-achtig instrument) bij gebruik het vaakst weefsel oplevert wat tot de diagnose leidt (70.6%), daarna volgen de 1.1 mm cryoprobe (68.4%), de holle naald (46.7%), de 1.9 mm cryoprobe (41.2%), de borstel (30.3%) en de lavage (23.7%). Met deze resultaten blijkt dat histologische weefsel afname technieken verhoudingsgewijs vaker tot een correcte diagnose leiden dan cytologische weefsel diagnostiek (respectievelijk 72.4% versus 49.3%). Ook blijkt dat het afnemen van meer biopten dan aanvankelijk nodig geacht een verbeterde kans geeft op een adequate uitkomst. Omdat cytologie in slechts 49.3% van de gevallen tot een accurate diagnose leidt, kan ROSE (een analyse van cytologie) ook in minder dan de helft van de kwaadaardige afwijkingen correct uitsluitel geven. Met deze uitkomsten wordt er geconcludeerd dat er geen enkele weefselafname methodiek is die garant staat voor een accurate diagnose. Vooral nog blijft een multi-modale manier van weefsel diagnostiek in de navigatie bronchoscopie aan te raden. Hiermee wordt tevens gesuggereerd dat onderzoek naar een verbetering van de weefsel diagnostiek een belangrijke factor is in de verdere ontwikkeling van de navigatie bronchoscopie procedure.

**Hoofdstuk 7** beschrijft de veranderingen van de diagnostische accuraatheid en de procedurele stralingsdosis van de navigatie bronchoscopie naarmate de ervaring toeneemt. Door alle patiënten zoals geïnccludeerd voor een navigatie bronchoscopie procedure op chronologische volgorde te bekijken, kan een potentiële leercurve afgeleid worden. Na de initiële introductie van de navigatie bronchoscopie zoals beschreven in hoofdstuk 5 wordt er nadien bewust gekozen voor een cone beam CT geleide methodiek als primaire navigatie methode. Dit hoofdstuk laat zien dat specifiekere instellingen van de röntgenapparatuur voor deze procedure leidt tot een significante reductie in procedurele stralingsdosis van zowel 3D cone beam CT-scans als 2D röntgen doorlichting, van in totaal  $47.5 \text{ Gy}\cdot\text{cm}^2$  (effectieve dosis:  $14.3 \text{ mSv}$ ) tot  $25.4 \text{ Gy}\cdot\text{cm}^2$  ( $5.8 \text{ mSv}$ ) per procedure. De reductie is het grootst in stralingsdosis als gevolg van röntgendoorlichting. De accuraatheid van de procedure laat eveneens een leercurve zien. In hoofdstuk 5 (de eerste 87 patiënten) wordt een accurate diagnose gesteld in 72.4% van de patiënten. Na 208 procedures (248 afwijkingen) loopt deze inmiddels op tot 76.4%. Als we daarbij verder opsplitsen naar periodes zien we dat in de laatste 64 patiënten (november 2019 – juni 2020) een accuraatheid van 90.6% gehaald wordt (en een succesvolle navigatie in 98.4% van de gevallen). Een toenemende ervaring met het uitvoeren van de navigatie bronchoscopie procedure leidt dus vaker tot zowel een accurate navigatie alsook een accurate diagnose, terwijl de stralingsdosis af kan nemen.

## Discussie en toekomstperspectief

De bevindingen in het eerste deel van dit proefschrift laten zien dat echo strain elastografie van een toegevoegde waarde kan zijn voor de systematische stadiëring van longkanker met een verdenking op lymfeklier metastasen. Er wordt gezien dat deze techniek als individuele voorspellende waarde alsook in combinatie met andere technieken gebruikt kan worden om kwaadaardige lymfeklieren beter te identificeren. Er worden echter ook verschillende uitdagingen blootgelegd. De endoscoop is op dit moment niet geschikt voor evaluatie van de meest perifeer gelegen lymfeklieren. Echo-geleide endoscopische evaluaties worden daarnaast mogelijk nog niet voldoende uitputtend uitgevoerd, met name minder verdachte klieren zouden mogelijk vaker aangeprikt moeten worden. Additioneel onderzoek is daarnaast nodig om echo strain elastografie als een gestandaardiseerde (meet-)methode beschikbaar te maken voor het brede publiek. En alhoewel subjectieve echo karakteristieken in dit proefschrift van gelimiteerde waarde blijken te zijn, zou een methode om deze objectief te kwantificeren mogelijk toch een voorspellende waarde van deze karakteristieken kunnen laten zien.

In het tweede deel van dit proefschrift wordt beschreven dat de flexibele endoscopisch diagnose van kleine afwijkingen in de long belangrijk significant kan worden door gebruik te maken van technologische hulpmiddelen. Door het gebruik van cone beam CT beeldvorming en een uitvoerige analyse van de diagnostiek worden er echter ook belangrijke verbetermogelijkheden vastgesteld. Om de prestatie van deze *navigatie*

*bronchoscope* procedures te verbeteren is niet alleen ervaring benodigd. Er blijkt een belangrijke discrepantie te zitten tussen het bereiken van de afwijking en het verkrijgen van een accurate diagnose. Derhalve zullen de methoden om weefsel te verkrijgen verbeterd moeten worden. De cone beam CT systemen blijken daarnaast geschikt voor minutieuze positionering van instrumenten, maar ook onderhevig aan een leercurve. Om de leercurve te verkleinen en adoptie van deze techniek te vergroten is verdere ontwikkeling van de navigatie bronchoscope techniek en haar gebruikers wenselijk. Tegelijkertijd is de cone beam CT geleide navigatie bronchoscope nu al een platform wat zich zou kunnen lenen voor de toekomstige beantwoording van een pluraliteit aan vraagstukken. Één daarvan is bijvoorbeeld de mogelijkheid van flexibele endoscopische behandelingen van vroege stadia longkanker. Omdat de werkingsmechanismen van (long)kanker echter nog steeds niet volledig ontrafeld zijn, zullen de verschillende specialismen de handen op korte termijn ineen moeten slaan om meerdere vraagstukken samen te beantwoorden. Met het ontrafelen van deze mechanismen kan er pas bepaald worden wat er van toekomstige klinische technologie verwacht wordt.









# Appendices

**Bibliography**

**Research data management**

**PhD portfolio**

**List of publications & presentations**

**Dankwoord**

**Curriculum Vitae**



## Bibliography

- 1 Integraal kankercentrum Nederland. Nederlandse Kankerregistratie Cijfers Available from: [iknl.nl/nkr-cijfers](http://iknl.nl/nkr-cijfers)
- 2 Bray F, Ferlay J, Soerjomataram I, Siegel RL, Torre LA, Jemal A. Global cancer statistics 2018: GLOBOCAN estimates of incidence and mortality worldwide for 36 cancers in 185 countries. *CA Cancer J Clin.* 2018;68(6):394–424.
- 3 Dutch National Institute for Public Health and Environment. Ranglijst aandoeningen op basis van ziektelast (DALY's) Available from: <https://www.volksgezondheidenzorg.info/ranglijst/ranglijst-aandoeningen-op-basis-van-ziektelast-dalys>
- 4 Travis WD, Brambilla E, Nicholson AG, Yatabe Y, Austin JHM, Beasley MB, et al. The 2015 World Health Organization Classification of Lung Tumors: Impact of Genetic, Clinical and Radiologic Advances since the 2004 Classification. *J Thorac Oncol.* 2015;10(9):1243–60.
- 5 Brambilla E, Travis WD, Colby T V., Corrin B, Shimosato Y. The new World Health Organization classification of lung tumours. *Eur Respir J.* 2001;18(6):1059–68.
- 6 De Leyn P, Dooms C, Kuzdzal J, Lardinois D, Passlick B, Rami-Porta R, et al. Revised ESTS guidelines for preoperative mediastinal lymph node staging for non-small-cell lung cancer. *Eur J Cardiothorac Surg.* 2014 May;1–12.
- 7 International Association for the Study of Lung Cancer. Staging Manual in Thoracic Oncology, second edition. 2016.
- 8 PENTAX Medical. EB1970UK Ultrasound video bronchoscope. Available from: <https://www.pentaxmedical.com/pentax/en/95/1/EB-1970UK-Ultrasound-Video-Bronchoscope/>
- 9 Silvestri GA, Gonzalez A V, Jantz MA, Margolis ML, Gould MK, Tanoue LT, et al. Methods for staging non-small cell lung cancer: Diagnosis and management of lung cancer, 3rd ed: American college of chest physicians evidence-based clinical practice guidelines. *Chest.* 2013;143:211–50.
- 10 Vilman P, Clementsen PF, Colella S, Siemsen M, De Leyn P, Dumonceau J-M, et al. Combined endobronchial and oesophageal endosonography for the diagnosis and staging of lung cancer: European Society of Gastrointestinal Endoscopy (ESGE) Guideline, in cooperation with the European Respiratory Society (ERS) and the European Society of Tho. *Eur J Cardio-thoracic Surg.* 2015 Jul;46(1):40–60.
- 11 Rusch VW, Asamura H, Watanabe H, Giroux D, Rami-porta R, Goldstraw P, et al. A Proposal for a New International Lymph Node Map in the Forthcoming Seventh Edition of the TNM Classification for Lung Cancer. *J Thorac Oncol.* 2009;4(5):568–77.
- 12 Annema JT, van Meerbeeck J, Rintoul RC, Dooms C, Deschepper E, Dekkers M, et al. Mediastinoscopy vs Endosonography for Mediastinal Nodal Staging of Lung Cancer: A Randomized Trial. *JAMA - J Am Med Assoc.* 2012;304(20):2245–52.
- 13 Crombag LMM, Dooms C, Stigt JA, Tournoy KG, Schuurbiens OCJ, Ninaber MK, et al. Systematic and combined endosonographic staging of lung cancer (SCORE study). *Eur Respir J.* 2019;53(2):1–10.

- 14 Usluer O, Kaya SO. Endobronchial ultrasound-guided transbronchial needle aspiration of mediastinal lymphadenopathy: effect of the learning curve. *Interact Cardiovasc Thorac Surg.* 2014;(19)4:693-695.
- 15 Korevaar DA, Crombag LM, Cohen JF, Spijker R, Bossuyt PM, Annema JT. Added value of combined endobronchial and oesophageal endosonography for mediastinal nodal staging in lung cancer: a systematic review and meta-analysis. *Lancet Respir Med.* 2016;4(12):960–8.
- 16 Catalano MF, Sivak M V., Rice T, Gragg LA, Van Dam J. Endosonographic features predictive of lymph node metastasis. *Gastrointest Endosc.* 1994;40(4):442–6.
- 17 Wahidi MM, Herth F, Yasufuku K, Shepherd RW, Yarmus L, Chawla M, et al. Technical aspects of endobronchial ultrasound-guided transbronchial needle aspiration - CHEST guideline and expert panel report. *Chest.* 2016;149 (3):816–35.
- 18 Ying L, Hou Y, Zheng H-M, Lin X, Xie Z-L, Hu Y-P. Real-time elastography for the differentiation of benign and malignant superficial lymph nodes: a meta-analysis. *Eur J Radiol.* 2012;81(10):2576–84.
- 19 Itoh A, Ueno E, Tohno E, Kamma H. Breast Disease: Clinical Application of US Elastography for Diagnosis. *Radiology.* 2006;239(2):341–50.
- 20 Szabo TL. *Diagnostic Ultrasound Imaging: Inside out.* 1th ed. Boston: Elsevier; 2004.
- 21 Shung KK. *Diagnostic ultrasound - imaging and blood flow measurements.* 1th ed. Boca Raton: Taylor & Francis Group; 2006.
- 22 Shiina T, Nitta N, Ueno E, Bamber J. Real time tissue elasticity imaging using the combined autocorrelation method. *J Med Ultrason.* 2002;29:119–28.
- 23 Ophir J, Céspedes I, Ponnekanti H, Yazdi Y, Li X. Elastography: a quantitative method for imaging the elasticity of biological tissues. *Ultrason Imaging.* 1991;13(2):111-34.
- 24 Shiina T, Nightingale KR, Palmeri ML, Hall TJ, Bamber JC, Barr RG, et al. WFUMB Guidelines and Recommendations for Clinical Use of Ultrasound Elastography: Part 1: Basic principles and terminology. *Ultrasound Med Biol.* 2015;41(5):1161–79.
- 25 Yousaf-Khan U, van der Aalst C, de Jong PA, Heuvelmans M, Scholten E, Lammers J-W, et al. Final screening round of the NELSON lung cancer screening trial: the effect of a 2.5-year screening interval. *Thorax.* 2017;72(1):48-56.
- 26 The National Lung Screening Trial Research Team. Reduced Lung-Cancer Mortality with Low-Dose Computed Tomographic Screening. *N Engl J Med.* 2011;365(5):395–409.
- 27 Rzyman W, Szurowska E, Adamek M. Implementation of lung cancer screening at the national level: Polish example. *Transl Lung Cancer Res.* 2019;8(Suppl 1):S95–105.
- 28 Pedersen JH, Sørensen JB, Saghir Z, Fløtten Ø, Brustugun OT, Ashraf H, et al. Implementation of lung cancer CT screening in the Nordic countries. *Acta Oncol (Madr).* 2017;56(10):1249–57.
- 29 Pastorino U, Sverzellati N, Sestini S, Silva M, Sabia F, Boeri M, et al. Ten-year results of the Multicentric Italian Lung Detection trial demonstrate the safety and efficacy of biennial lung cancer screening. *Eur J Cancer.* 2019;118:142–8.
- 30 Oudkerk M, Devaraj A, Vliementhart R, Henzler T, Prosch H, Heussel CP, et al. European position statement on lung cancer screening. *Lancet Oncol.* 2017;18(12):e754–66.

- 31 De Koning HJ, Van Der Aalst CM, De Jong PA, Scholten ET, Nackaerts K, Heuvelmans MA, et al. Reduced lung-cancer mortality with volume CT screening in a randomized trial. *N Engl J Med*. 2020;382(6):503–13.
- 32 Callister MEJ, Baldwin DR, Akram AR, Barnard S, Cane P, Draffan J, et al. BTS Guidelines for the Investigation and Management of Pulmonary Nodules. *Thorax*. 2015;70:ii1–54.
- 33 MacMahon H, Naidich DP, Goo JM, Lee KS, Leung ANC, Mayo JR, et al. Guidelines for Management of Incidental Pulmonary Nodules Detected on CT Images: From the Fleischner Society 2017. *Radiology*. 2017;284(1):228–43.
- 34 Rivera MP, Mehta AC, Wahidi MM. Establishing the diagnosis of lung cancer: Diagnosis and management of lung cancer, 3rd ed: American college of chest physicians evidence-based clinical practice guidelines. *Chest*. 2013;143(5 Suppl):e142S–e165S.
- 35 McWilliams A, Tammemagi MC, Mayo JR, Roberts H, Liu G, Soghrati K, et al. Probability of Cancer in Pulmonary Nodules Detected on First Screening CT. *N Engl J Med*. 2013;369(10):910–9.
- 36 Herder GJ, van Tinteren H, Golding RP, Kostense PJ, Comans EF, Smit EF, et al. Clinical Prediction Model To Characterize Pulmonary Nodules. *Chest*. 2005;128(4):2490–6.
- 37 Gould MK, Donington J, Lynch WR, Mazzone PJ, Midthun DE, Naidich DP, et al. Evaluation of individuals with pulmonary nodules: When is it lung cancer? Diagnosis and management of lung cancer, 3rd ed: American college of chest physicians evidence-based clinical practice guidelines. *Chest*. 2013;143(5):e93s–e120s.
- 38 Asano F, Eberhardt R, Herth FJF. Virtual bronchoscopic navigation for peripheral pulmonary lesions. *Respiration*. 2014;88(5):430–40.
- 39 Wang Memoli JS, Nietert PJ, Silvestri GA. Meta-analysis of guided bronchoscopy for the evaluation of the pulmonary nodule. *Chest*. 2012;142(2):385–93.
- 40 Gilbert C, Akulian J, Ortiz R, Lee H, Yarmus L. Novel bronchoscopic strategies for the diagnosis of peripheral lung lesions: Present techniques and future directions. *Respirology*. 2014;19(5):636–44.
- 41 Fielding D, Oki M. Technologies for targeting the peripheral pulmonary nodule including robotics. *Respirology*. 2020;25(9):914–23.
- 42 Mehta AC, Hood KL, Schwarz Y, Solomon SB. The Evolutional History of Electromagnetic Navigation Bronchoscopy: State of the Art. *Chest*. 2018;154(4):935–47.
- 43 Steinfort DP, Bonney A, See K, Irving LB. Sequential multimodality bronchoscopic investigation of peripheral pulmonary lesions. *Eur Respir J*. 2016;47(2):607–14.
- 44 Heerink WJ, de Bock GH, de Jonge GJ, Groen HJM, Vliegenthart R, Oudkerk M. Complication rates of CT-guided transthoracic lung biopsy: meta-analysis. *Eur Radiol*. 2017;27(1):138–48.
- 45 Jsseldijk MA, Shoni M, Siegert C, Wiering B, van Engelenburg KCA, Lebenthal A, et al. Survival After Stereotactic Body Radiation Therapy for Clinically Diagnosed or Biopsy-Proven Early-Stage NSCLC: A Systematic Review and Meta-Analysis. *J Thorac Oncol*. 2019;14(4):583–95.
- 46 Fujiwara T, Yasufuku K, Nakajima T, Chiyo M, Yoshida S, Suzuki M, et al. The utility of sonographic features during endobronchial ultrasound-guided transbronchial needle aspiration for lymph node staging in patients with lung cancer: A standard endobronchial ultrasound image classification system. *Chest*. 2010;138(3):641–7.

- 47 Evison M, Morris J, Martin J, Shah R, Barber P V, Booton R, et al. Nodal staging in lung cancer: a risk stratification model for lymph nodes classified as negative by EBUS-TBNA. *J Thorac Oncol*. 2015;10(1):126–33.
- 48 Satterwhite LG, Berkowitz DM, Parks CS, Bechara RI. Central intra-nodal vessels to predict malignancy during EBUS-TBNA. *J Bronchol Interv Pulmonol*. 2011;18(4):322–8.
- 49 Wang Memoli JS, El-Bayoumi E, Pastis NJ, Tanner NT, Gomez M, Huggins JT, et al. Using endobronchial ultrasound features to predict lymph node metastasis in patients with lung cancer. *Chest*. 2011;140 (6):1550–6.
- 50 Garcia-Olivé I, Monsó E, Andreo F, Sanz J, Castellà E, Llatjós M, et al. Sensitivity of Linear Endobronchial Ultrasonography and Guided Transbronchial Needle Aspiration for The Identification of Nodal Metastasis in Lung Cancer Staging. *Ultrasound Med Biol*. 2009;35(8):1271–7.
- 51 Gong X, Xu Q, Xu Z, Xiong P, Yan W, Chen Y. Real-time elastography for the differentiation of benign and malignant breast lesions: A meta-analysis. *Breast Cancer Res Treat*. 2011;130(1):11–8.
- 52 Sadigh G, Carlos RC, Neal CH, Dwamena BA. Accuracy of quantitative ultrasound elastography for differentiation of malignant and benign breast abnormalities: A meta-analysis. *Breast Cancer Res Treat*. 2012;134(3):923–31.
- 53 Sun J, Cai J, Wang X. Real-time Ultrasound Elastography for Differentiation of Benign and Malignant Thyroid Nodules. *J Ultrasound Med*. 2014;33(3):495–502.
- 54 Dietrich CF, Jenssen C, Arcidiacono PG, Cui XW, Giovannini M, Hocke M, et al. Endoscopic ultrasound: Elastographic lymph node evaluation. *Endosc Ultrasound*. 2015;4(3):176–90.
- 55 He H-Y, Chen J-L, Ma H, Zhu J, Wu D-D, Lv X-D. Value of Endobronchial Ultrasound Elastography in Diagnosis of Central Lung Lesions. *Med Sci Monit*. 2017;23:3269–75.
- 56 Xu W, Shi J, Zeng X, Li X, Xie W-F, Guo J, et al. EUS elastography for the differentiation of benign and malignant lymph nodes: a meta-analysis. *Gastrointest Endosc*. 2011;74(5):1001-1009.
- 57 Nakajima T, Inage T, Sata Y, Morimoto J, Tagawa T, Suzuki H, et al. Elastography for predicting and localizing nodal metastases during endobronchial ultrasound. *Respiration*. 2015;90(6):499–506.
- 58 Korrungruang P, Boonsarngsuk V. Diagnostic value of endobronchial ultrasound elastography for the differentiation of benign and malignant intrathoracic lymph nodes. *Respirology*. 2017;22(5):972–7.
- 59 Izumo T, Sasada S, Chavez C, Matsumoto Y, Tsuchida T. Endobronchial Ultrasound Elastography in the Diagnosis of Mediastinal and Hilar Lymph Nodes. *Jpn J Clin Oncol*. 2014;6:1–7.
- 60 Rozman A, Malovrh MM, Adamic K, Subic T, Kovac V, Flezar M. Endobronchial ultrasound elastography strain ratio for mediastinal lymph node diagnosis. *Radiol Oncol*. 2015;49(4):334–40.
- 61 Dietrich CF, Săftoiu A, Jenssen C. Real time elastography endoscopic ultrasound (RTE-EUS), a comprehensive review. *Eur J Radiol*. 2014;83(3):405–14.
- 62 Steinfort DP. Elastography in endobronchial ultrasound: Stretching the boundary of minimally invasive staging further. *Respirology*. 2017;22(5):843–4.
- 63 Huang H, Huang Z, Wang Q, Wang X, Dong Y, Zhang W, et al. Effectiveness of the benign and malignant diagnosis of mediastinal and hilar lymph nodes by endobronchial ultrasound elastography. *J Cancer*. 2017;8(10):1843–8.



- 64 Bediwy, A.S., Hantira, M.S., Sharawy, D.E., Sawa AE. The role of endobronchial ultrasound elastography in the diagnosis of mediastinal lymph nodes. *Egypt J Bronchol.* 2018;12(1):33–40.
- 65 Havre RF, Waage JR, Gilja OH, Ødegaard S, Nesje LB. Real-Time Elastography: Strain Ratio Measurements Are Influenced by the Position of the Reference Area. *Ultraschall der Medizin - Eur J Ultrasound.* 2012;33(06):559–68.
- 66 Săftoiu A, Vilmann P, Gorunescu F, Janssen J, Hocke M, Larsen M, et al. Accuracy of endoscopic ultrasound elastography used for differential diagnosis of focal pancreatic masses: A multicenter study. *Endoscopy.* 2011;43(7):596–603.
- 67 Boellaard R, Delgado-Bolton R, Oyen WJG, Giammarile F, Tatsch K, Eschner W, et al. FDG PET/CT: EANM procedure guidelines for tumour imaging: version 2.0. *Eur J Nucl Med Mol Imaging.* 2014;42(2):328–54.
- 68 R Core Team. R: A language and environment for statistical computing. 2019. Available from: <https://www.r-project.org>
- 69 Mittal S, Madan K. Correspondence: Endobronchial ultrasound elastography for the differentiation of benign and malignant lymph nodes. *Respirology.* 2017;22(5):972–7.
- 70 Evans A, Whelehan P, Thomson K, McLean D, Brauer K, Purdie C, et al. Quantitative shear wave ultrasound elastography: initial experience in solid breast masses. *Breast cancer Res.* 2010;12(6):R104.
- 71 Miyaji K, Furuse A, Nakajima J, Kohno T, Ohtsuka T, Yagyu K, et al. The stiffness of lymph nodes containing lung carcinoma metastases: a new diagnostic parameter measured by a tactile sensor. *Cancer.* 1997;80(10):1920–5.
- 72 García FA, Ángela C, Clemente C, Santos S, Barroso ÁB, Gallego H, et al. Initial Experience With Real-Time Elastography Using an Ultrasound Bronchoscope for the Evaluation of Mediastinal Lymph Nodes. *Arch Bronconeumol.* 2015;51(2):9–12.
- 73 Inage T, Nakajima T, Yoshida S, Yoshino I. Endobronchial elastography in the evaluation of esophageal invasion. *J Thorac Cardiovasc Surg.* 2015;149(2):576–7.
- 74 Okasha H, Elkholy S, Sayed M, El-Sherbiny M, El-Hussieny R, El-Gemeie E, et al. Ultrasound, endoscopic ultrasound elastography, and the strain ratio in differentiating benign from malignant lymph nodes. *Arab J Gastroenterol.* 2018;19(1):1–9.
- 75 Siemens healthineers. eSie Touch Elasticity imaging. Available from: <http://usa.healthcare.siemens.com/ultrasound/tissue-strain-analytics>
- 76 General Electric Company. GE Healthcare Introduces New Ultrasound Elastography Capability. Available from: <https://www.ge.com/news/press-releases/ge-healthcare-introduces-new-ultrasound-elastography-capability>
- 77 Hitachi Medical Systems. Hitachi Medical Systems products: Hi Vision Preirus. Available from: <http://www.hitachi-medical-systems.be/products-and-services/ultrasound/platforms/hi-vision-platforms/hi-vision-preirus.html>
- 78 Havre RF, Elde E, Gilja OH, Odegaard S, Eide GE, Matre K, et al. Freehand real-time elastography: impact of scanning parameters on image quality and in vitro intra- and interobserver validations. *Ultrasound Med Biol.* 2008;34(10):1638–50.

- 79 Kallel F, Varghese T, Ophir J, Bilgen M. The nonstationary strain filter in elastography: Part II. lateral and elevational decorrelation. *Ultrasound Med Biol.* 1997;23(9):1357–69.
- 80 Popescu A, Saftoiu A. Can elastography replace fine needle aspiration? *Endosc Ultrasound.* 2014;3(2):109.
- 81 Parker KJ, Huang SR. Tissue response to mechanical vibrations for “sonoelasticity imaging.” *Ultrasound Med Biol.* 1990;16(3):241–6.
- 82 Cespedes I, Ophir J, Ponnekanti H, Maklad N. Elastography: Elasticity Imaging Using Ultrasound with Application to Muscle and Breast In Vivo. *Ultrason Imaging.* 1993;73–88.
- 83 Ciurea AI, Dumitriu D, Ciortea C, Botar-Jid C, Dudea SM. Artifacts and pitfalls in breast elastoultrasonography: a pictorial essay. *Med Ultrason.* 2008;10(2):93–8.
- 84 Darwiche K, Freitag L, Nair A, Neumann C, Karpf-Wissel R, Welter S, et al. Evaluation of a novel endobronchial ultrasound-guided lymph node forceps in enlarged mediastinal lymph nodes. *Respiration.* 2013;86(3):229–36.
- 85 Herth FJF, Krasnik M, Kahn N, Eberhardt R, Ernst A. Combined endoscopic-endobronchial ultrasound-guided fine-needle aspiration of mediastinal lymph nodes through a single bronchoscope in 150 patients with suspected lung cancer. *Chest.* 2010;138(4):790–4.
- 86 Herth FJF, Eberhardt R, Krasnik M, Ernst A. Endobronchial ultrasound-guided transbronchial needle aspiration of lymph nodes in the radiologically and positron emission tomography-normal mediastinum in patients with lung cancer. *Chest.* 2008;133(4):887–91.
- 87 Oki M, Saka H, Ando M, Kitagawa C, Kogure Y, Seki Y. Endoscopic ultrasound-guided fine needle aspiration and endobronchial ultrasound-guided transbronchial needle aspiration: Are two better than one in mediastinal staging of non-small cell lung cancer? *J Thorac Cardiovasc Surg.* 2014;148(4):1169-1177.
- 88 Hylton DA, Turner J, Shargall Y, Finley C, Agzarian J, Yasufuku K, et al. Ultrasonographic characteristics of lymph nodes as predictors of malignancy during endobronchial ultrasound (EBUS): A systematic review. *Lung Cancer.* 2018;126:97–105.
- 89 Chen YF, Mao XW, Zhang YJ, Zhang CY, Yu YF, Qin E, et al. Endobronchial Ultrasound Elastography Differentiates Intrathoracic Lymph Nodes: A Meta-Analysis. *Ann Thorac Surg.* 2018;106(4):1251–7.
- 90 Verhoeven RLJ, de Korte CL, van der Heijden EHF. Optimal Endobronchial Ultrasound Strain Elastography Assessment Strategy: An Explorative Study. *Respiration.* 2019;97(4):337–47.
- 91 Verhoeven RLJ, de Korte CL, van der Heijden EHF. Optimal Endobronchial Ultrasound Strain Elastography Assessment Strategy: An Explorative Study - Online Data Supplement. Available at: <https://dx.doi.org/10.6084/m9.figshare.7466873>
- 92 Robin X, Turck N, Hainard A, Tiberti N, Lisacek F, Sanchez JC, et al. pROC: An open-source package for R and S+ to analyze and compare ROC curves. *BMC Bioinformatics.* 2011;12(1):77.
- 93 Bousema JE, Dijkgraaf MGW, Papen-Botterhuis NE, Schreurs HW, Maessen JG, van der Heijden EHF, et al. MEDIASTinal staging of non-small cell lung cancer by endobronchial and endoscopic ultrasonography with or without additional surgical mediastinoscopy (MEDIASTrial): study protocol of a multicenter randomised controlled trial. *BMC Surg.* 2018;18(1):27.
- 94 van der Heijden EHF, Casal RF, Trisolini R, Steinfort DP, Hwangbo B, Nakajima T, et al. Guideline for the Acquisition and Preparation of Conventional and Endobronchial Ultrasound-Guided

- Transbronchial Needle Aspiration Specimens for the Diagnosis and Molecular Testing of Patients with Known or Suspected Lung Cancer. *Respiration*. 2014;88(6):500–17.
- 95 Hylton DA, Turner S, Kidane B, Spicer J, Xie F, Farrokhyar F, et al. The Canada Lymph Node Score for prediction of malignancy in mediastinal lymph nodes during endobronchial ultrasound. *J Thorac Cardiovasc Surg*. 2020;159(6):2499-2507.
- 96 Alici IO, Yılmaz Demirci N, Yılmaz A, Karakaya J, Özyaydin E. The sonographic features of malignant mediastinal lymph nodes and a proposal for an algorithmic approach for sampling during endobronchial ultrasound. *Clin Respir J*. 2016;10(5):606–13.
- 97 Shafiek H, Fiorentino F, Peralta AD, Serra E, Esteban B, Martinez R, et al. Real-Time Prediction of Mediastinal Lymph Node Malignancy by Endobronchial Ultrasound. *Arch Bronconeumol*. 2014;50(6):228–34.
- 98 Schmid-Bindert G, Jiang H, Kahler G, Saur J, Henzler T, Wang H, et al. Predicting malignancy in mediastinal lymph nodes by endobronchial ultrasound: A new ultrasound scoring system. *Respirology*. 2012;17(8):1190–8.
- 99 Verhoeven RLJ, Trisolini R, Leoncini F, Candoli P, Bezzi M, Messi A, et al. Predictive Value of Endobronchial Ultrasound Strain Elastography in Mediastinal Lymph Node Staging: The E-Predict Multicenter Study Results. *Respiration*. 2020;99(6):484–92.
- 100 Kemp S V., El Batrawy SH, Harrison RN, Skwarski K, Munavvar M, Roselli A, et al. Learning curves for endobronchial ultrasound using cusum analysis. *Thorax*. 2010;65(6):534–8.
- 101 Wahidi MM, Hulett Dr. C, Pastis N, Shepherd RW, Shofer SL, Mahmood K, et al. Learning experience of linear endobronchial ultrasound among pulmonary trainees. *Chest*. 2014;145(3):574–8.
- 102 Sehgal IS, Dhooria S, Aggarwal AN, Agarwal R. Training and proficiency in endobronchial ultrasound-guided transbronchial needle aspiration: A systematic review. *Respirology*. 2017;22(8):1547–57.
- 103 Gwet KL. Computing inter-rater reliability and its variance in the presence of high agreement. *Br J Math Stat Psychol*. 2008;61(1):29–48.
- 104 Feinstein AR, Cicchetti D V. High agreement but low Kappa: I. the problems of two paradoxes. *J Clin Epidemiol*. 1990;43(6):543–9.
- 105 Nguyen P, Bashirzadeh F, Hundloe J, Salvado O, Dowson N, Ware R, et al. Optical differentiation between malignant and benign lymphadenopathy by grey scale texture analysis of endobronchial ultrasound convex probe images. *Chest*. 2012;141(3):709–15.
- 106 Folch EE, Pritchett MA, Nead MA, Bowling MR, Murgu SD, Krinsky WS, et al. Electromagnetic Navigation Bronchoscopy for Peripheral Pulmonary Lesions: One-Year Results of the Prospective, Multicenter NAVIGATE Study. *J Thorac Oncol*. 2019;14(3):445–58.
- 107 Casal RF. Cone Beam CT-Guided Bronchoscopy. Here to stay? *J Bronchol Interv Pulmonol*. 2018;25(4):255–6.
- 108 Fielding DIK, Bashirzadeh F, Son JH, Todman M, Chin A, Tan L, et al. First Human Use of a New Robotic-Assisted Fiber Optic Sensing Navigation System for Small Peripheral Pulmonary Nodules. *Respiration*. 2019;98(2):142–50.
- 109 Yarmus L, Akulian J, Wahidi M, Chen A, Steltz JP, Solomon SL, et al. A Prospective Randomized Comparative Study of Three Guided Bronchoscopic Approaches for Investigating Pulmonary Nodules. *Chest*. 2020;157(3):694–701.

- 110 Steinfort DP, Vrijlic I, Irving LB. Augmented Fluoroscopy for Guidance of Bronchoscopic Biopsy of Pulmonary Nodules. *J Bronchology Interv Pulmonol*. 2019;26(2):e27–9.
- 111 Park SC, Kim CJ, Han CH, Lee SM. Factors associated with the diagnostic yield of computed tomography-guided transbronchial lung biopsy. *Thorac Cancer*. 2017;8(3):153–8.
- 112 Casal RF, Sarkiss M, Jones AK, Stewart J, Tam A, Grosu HB, et al. Cone beam computed tomography-guided thin/ultrathin bronchoscopy for diagnosis of peripheral lung nodules: A prospective pilot study. *J Thorac Dis*. 2018;10(12):6950–9.
- 113 Pritchett MA, Schampaert S, De Groot JAH, Schirmer CC, Van Der Bom I. Cone-Beam CT with Augmented Fluoroscopy Combined with Electromagnetic Navigation Bronchoscopy for Biopsy of Pulmonary Nodules. *J Bronchol Interv Pulmonol*. 2018;25(4):274–82.
- 114 Sobieszczyk MJ, Yuan Z, Li W, Krinsky W. Biopsy of peripheral lung nodules utilizing cone beam computer tomography with and without trans bronchial access tool: a retrospective analysis. *J Thorac Dis*. 2018;10(10):5953–9.
- 115 Hohenforst-Schmidt W, Zarogoulidis P, Vogl T, Turner JF, Browning R, Linsmeier B, et al. Cone beam Computertomography (CBCT) in interventional chest medicine - high feasibility for endobronchial realtime navigation. *J Cancer*. 2014;5(3):231–41.
- 116 Ost D, Shah R, Anasco E, Lusardi L, Doyle J, Austin C, et al. A randomized trial of CT fluoroscopic-guided bronchoscopy vs conventional bronchoscopy in patients with suspected lung cancer. *Chest*. 2008;134(3):507–13.
- 117 Heyer CM, Kagel T, Lemburg SP, Walter JW, De Zeeuw J, Junker K, et al. Transbronchial biopsy guided by low-dose MDCT: A new approach for assessment of solitary pulmonary nodules. *Am J Roentgenol*. 2006;187(4):933–9.
- 118 Hautmann H, Henke MO, Bitterling H. High diagnostic yield from transbronchial biopsy of solitary pulmonary nodules using low-dose CT-guidance. *Respirology*. 2010;15(4):677–82.
- 119 Shinagawa N, Yamazaki K, Onodera Y, Miyasaka K, Kikuchi E, Dosaka-Akita H, et al. CT-guided transbronchial biopsy using an ultrathin bronchoscope with virtual bronchoscopic navigation. *Chest*. 2004;125(3):1138–43.
- 120 Tsushima K, Sone S, Hanaoka T, Takayama F, Honda T, Kubo K. Comparison of bronchoscopic diagnosis for peripheral pulmonary nodule under fluoroscopic guidance with CT guidance. *Respir Med*. 2006;100(4):737–45.
- 121 Chen A, Pastis N, Furukawa B, Silvestri GA. The effect of respiratory motion on pulmonary nodule location during electromagnetic navigation bronchoscopy. *Chest*. 2015;147(5):1275–81.
- 122 Gildea T, Folch E, Khandhar S, Pritchett M, Linden P, Arenberg D, et al. the Impact of Biopsy Tool Choice and Rapid on-Site Evaluation on the Diagnostic Accuracy for Malignant Lesions in the Prospective, Multicenter Navigate Study. *Chest*. American College of Chest Physicians; 2019; pp A827–9.
- 123 Ali MS, Sethi J, Taneja A, Musani A, Maldonado F. Computed Tomography Bronchus Sign and the Diagnostic Yield of Guided Bronchoscopy for Peripheral Pulmonary Lesions. A Systematic Review and Meta-Analysis. *Ann Am Thorac Soc*. 2018;15(8):978–87.
- 124 Bowling MR, Brown C, Anciano CJ. Feasibility and Safety of the Transbronchial Access Tool for Peripheral Pulmonary Nodule and Mass. *Ann Thorac Surg*. 2017;104(2):443–9.

- 125 Lau K, Spiers A, Pritchett M, Krinsky W. P1.05-06 Bronchoscopic Image-Guided Microwave Ablation of Peripheral Lung Tumours – Early Results. *J Thorac Oncol*. 2018;13(10):S542.
- 126 Oki M, Saka H, Asano F, Kitagawa C, Kogure Y, Tsuzuku A, et al. Use of an Ultrathin vs Thin Bronchoscope for Peripheral Pulmonary Lesions: A Randomized Trial. *Chest*. 2019;156(5):954–64.
- 127 Ali EAA, Takizawa H, Kawakita N, Sawada T, Tsuboi M, Toba H, et al. Transbronchial Biopsy Using an Ultrathin Bronchoscope Guided by Cone-Beam Computed Tomography and Virtual Bronchoscopic Navigation in the Diagnosis of Pulmonary Nodules. *Respiration*. 2019;98(4):321–8.
- 128 Verhoeven RLJ, Fütterer JJ, Hoefsloot W, van der Heijden EHF. Cone-Beam CT Image Guidance With and Without Electromagnetic Navigation Bronchoscopy for Biopsy of Peripheral Pulmonary Lesions. *J Bronchology Interv Pulmonol*. 2021;28(1):60–9.
- 129 Mondoni M, Sotgiu G, Bonifazi M, Dore S, Parazzini EM, Carlucci P, et al. Transbronchial needle aspiration in peripheral pulmonary lesions: A systematic review and meta-analysis. *Eur Respir J*. 2016;48(1):196–204.
- 130 Ost DE, Ernst A, Lei X, Kovitz KL, Benzaquen S, Diaz-Mendoza J, et al. Diagnostic yield and complications of bronchoscopy for peripheral lung lesions: Results of the AQUIRE registry. *Am J Respir Crit Care Med*. 2016;193(1):68–77.
- 131 Trisolini R, Cancellieri A, Tinelli C, Paioli D, Scudeller L, Forti Parri SN, et al. Performance characteristics and predictors of yield from transbronchial needle aspiration in the diagnosis of peripheral pulmonary lesions. *Respirology*. 2011;16(7):1144–9.
- 132 Choi SH, Chae EJ, Kim JE, Kim EY, Oh SY, Hwang HJ, et al. Percutaneous CT-guided aspiration and core biopsy of pulmonary nodules smaller than 1 cm: Analysis of outcomes of 305 procedures from a tertiary referral center. *Am J Roentgenol*. 2013;201(5):964–70.
- 133 De Filippo M, Saba L, Concarì G, Nizzoli R, Ferrari L, Tiseo M, et al. Predictive factors of diagnostic accuracy of CT-guided transthoracic fine-needle aspiration for solid noncalcified, subsolid and mixed pulmonary nodules. *CHEST Radiol*. 2013;118(7):1071–81.
- 134 Kho SS, Chan SK, Yong MC, Tie ST. Performance of transbronchial cryobiopsy in eccentrically and adjacently orientated radial endobronchial ultrasound lesions. *ERJ Open Res*. 2019;5(4):00135–2019.
- 135 Nasu S, Okamoto N, Suzuki H, Shiroyama T, Tanaka A, Samejima Y, et al. Comparison of the utilities of cryobiopsy and forceps biopsy for peripheral lung cancer. *Anticancer Res*. 2019;39(10):5683–8.
- 136 Chao TY, Chien M Te, Lie CH, Chung YH, Wang JL, Lin MC. Endobronchial ultrasonography-guided transbronchial needle aspiration increases the diagnostic yield of peripheral pulmonary lesions: A randomized trial. *Chest*. 2009;136(1):229–36.
- 137 Herath S, Yap E. Novel hybrid cryo-radial method: An emerging alternative to CT-guided biopsy in suspected lung cancer. A prospective case series and description of technique. *Respirol Case Reports*. 2018;6(2):1–6.
- 138 Schuhmann M, Bostanci K, Bugalho A, Warth A, Schnabel PA, Herth FJF, et al. Endobronchial ultrasound-guided cryobiopsies in peripheral pulmonary lesions: A feasibility study. *Eur Respir J*. 2014;43(1):233–9.

- 139 Chen X, Wan B, Xu Y, Song Y, Zhan P, Huang L, et al. Efficacy of rapid on-site evaluation for diagnosing pulmonary lesions and mediastinal lymph nodes: A systematic review and meta-analysis. *Transl Lung Cancer Res.* 2019;8(6):1029–44.
- 140 Mondoni M, Carlucci P, Di Marco F, Rossi S, Santus P, D'Adda A, et al. Rapid on-site evaluation improves needle aspiration sensitivity in the diagnosis of central lung cancers: A randomized trial. *Respiration.* 2013;86(1):52–8.
- 141 Trisolini R, Cancellieri A, Tinelli C, De Biase D, Valentini I, Casadei G, et al. Randomized trial of endobronchial ultrasound-guided transbronchial needle aspiration with and without rapid on-site evaluation for lung cancer genotyping. *Chest.* 2015;148(6):1430–7.
- 142 Coghlin CL, Smith LJ, Bakar S, Stewart KN, Devereux GS, Nicolson MC, et al. Quantitative analysis of tumor in bronchial biopsy specimens. *J Thorac Oncol.* 2010;5(4):448–52.
- 143 Folch EE, Labarca G, Ospina-Delgado D, Kheir F, Majid A, Khandhar SJ, et al. Sensitivity and Safety of Electromagnetic Navigation Bronchoscopy for Lung Cancer Diagnosis. *Chest.* 2020 Oct;158(4):1753–69.
- 144 Ettinger DS, Wood DE, Aggarwal C, Aisner DL, Akerley W, Bauman JR, et al. Guidelines on Non-small Cell lung cancer v1.2020. *J Natl Compr Cancer Netw*
- 145 Louie A V., Senan S, Patel P, Ferket BS, Lagerwaard FJ, Rodrigues GB, et al. When is a biopsy-proven diagnosis necessary before stereotactic ablative radiotherapy for lung cancer? A decision analysis. *Chest.* 2014;146(4):1021–8.
- 146 Steinfurt DP, D'Agostino RD, Vrijlic I, Einsiedel P, Prasad JD, Jennings BR, et al. CT-Fluoroscopic guidance for performance of targeted transbronchial cryobiopsy: A preliminary report. *Respiration.* 2018;96(5):472–9.
- 147 Pritchett M, Radaelli A, Schampaert S, van der Bom I. Cone Beam CT-Guided Endobronchial Biopsy Assisted by Augmented Fluoroscopy. *Chest.* 2017;152(4):A887.
- 148 McDonagh E. OpenREM - Free and Open Source Radiation Exposure Monitoring for the physicist Available from: [openrem.org](http://openrem.org)
- 149 Clement CH, Hamada N, Rehani MM, Gupta R, Bartling S, Sharp GC, et al. Annals of the International Commission on Radiological Protection - Radiological Protection in Cone Beam Computed Tomography (CBCT). 2015. Available from: [www.icrp.org](http://www.icrp.org)
- 150 Tapiovaara M, Lakkisto M, Servomaa A, Siiskonen T. A PC based Monte Carlo program for calculating patient doses in medical x-ray examinations. 2008.
- 151 Hwangbo B, Lee GK, Lee HS, Lim KY, Lee SH, Kim HY, et al. Transbronchial and transesophageal fine-needle aspiration using an ultrasound bronchoscope in mediastinal staging of potentially operable lung cancer. *Chest.* 2010;138(4):795–802.
- 152 Ohnishi R, Yasuda I, Kato T, Tanaka T, Kaneko Y, Suzuki T, et al. Combined endobronchial and endoscopic ultrasound-guided fine needle aspiration for mediastinal nodal staging of lung cancer. *Endoscopy.* 2011;43(12):1082–9.
- 153 Dooms C, Tournoy KG, Schuurbiens O, Decaluwe H, De Ryck F, Verhagen A, et al. Endosonography for mediastinal nodal staging of clinical N1 non-small cell lung cancer: A prospective multicenter study. *Chest.* 2015;147(1):209–15.

- 154 Ong P, Grosu H, Eapen GA, Rodriguez M, Lazarus D, Ost D, et al. Endobronchial ultrasound-guided transbronchial needle aspiration for systematic nodal staging of lung cancer in patients with N0 disease by computed tomography and integrated positron emission tomography-computed tomography. *Ann Am Thorac Soc.* 2015;12(3):415–9.
- 155 Yasufuku K, Nakajima T, Waddell T, Keshavjee S, Yoshino I. Endobronchial ultrasound-guided transbronchial needle aspiration for differentiating N0 versus N1 lung cancer. *Ann Thorac Surg.* 2013;96(5):1756–60.
- 156 Beyaz F, Verhoeven RLJ, Schuurbiens OCJ, Verhagen AFTM, van der Heijden EHF. Occult lymph node metastases in clinical N0/N1 NSCLC; A single center in-depth analysis. *Lung Cancer.* 2020;150:186–94.
- 157 DuComb EA, Tonelli BA, Tuo Y, Cole BF, Mori V, Bates JHT, et al. Evidence for Expanding Invasive Mediastinal Staging for Peripheral T1 Lung Tumors. *Chest.* 2020;158(5):2192–9.
- 158 Weijers G, Wanten G, Thijssen JM, van der Graaf M, de Korte CL. Quantitative Ultrasound for Staging of Hepatic Steatosis in Patients on Home Parenteral Nutrition Validated with Magnetic Resonance Spectroscopy: A Feasibility Study. *Ultrasound Med Biol.* 2016;42(3):637–44.
- 159 Dutch Institute for Clinical Auditing. Surgical and Radiotherapeutic treatment of suspected or proven Lung Cancer in the Netherlands 2017-2018. Available from: <https://dica.nl/>
- 160 Arias S, Yarmus L, Argento AC. Navigational transbronchial needle aspiration, percutaneous needle aspiration and its future. *J Thorac Dis.* 2015;7:S317–28.
- 161 Dale CR, Madtes DK, Fan VS, Gorden J a, Veenstra DL. Navigational Bronchoscopy with biopsy versus Computed Tomography-guided biopsy for the diagnosis of a solitary pulmonary nodule - A Cost-Consequence analysis. *J Bronchology Interv Pulmonol.* 2012;19(4):294–303.
- 162 Deppen SA, Davis WT, Green EA, Rickman O, Aldrich MC, Fletcher S, et al. Cost-Effectiveness of Initial Diagnostic Strategies for Pulmonary Nodules Presenting to Thoracic Surgeons. *Ann Thorac Surg.* 2015;98(4):1214–22.
- 163 Pritchett MA. Prospective Analysis of a Novel Endobronchial Augmented Fluoroscopic Navigation System for Diagnosis of Peripheral Pulmonary Lesions. *J Bronchology Interv Pulmonol.* 2021;28(2):107-115
- 164 Cicienia J, Bhadra K, Sethi S, Nader DA, Whitten P, Hogarth DK. Augmented Fluoroscopy - A new and novel navigation platform for peripheral bronchoscopy. *J Bronchology Interv Pulmonol.* 2021;28(2):116-123
- 165 Chen A, Pastis N, Mahajan A, Khandhar S, Simoff M, Machuzak M, et al. Multicenter, Prospective Pilot and Feasibility Study of Robotic-Assisted Bronchoscopy for Peripheral Pulmonary Lesions. *Chest.* 2019;156(4):A2260–1.
- 166 Lee HS, Lee GK, Lee HS, Kim MS, Lee JM, Kim HY, et al. Real-time endobronchial ultrasound-guided transbronchial needle aspiration in mediastinal staging of non-small cell lung cancer: How many aspirations per target lymph node station? *Chest.* 2008;134(2):368–74.
- 167 Chaddha U, Kovacs SP, Manley C, Hogarth DK, Cumbo-Nacheli G, Bhavani S V., et al. Robot-assisted bronchoscopy for pulmonary lesion diagnosis: Results from the initial multicenter experience. *BMC Pulm Med.* 2019;19(1):1–7.
- 168 Iwata H. Adenocarcinoma containing lepidic growth. *J Thorac Dis.* 2016;8(9):E1050–2.

- 169 Pritchett MA, Schirmer CC, Laeseke P. Melting the tip of the iceberg: bronchoscopic-guided transbronchial microwave ablation. *Transl Lung Cancer Res.* 2020;9(4):960–3.
- 170 Ethicon. NEUWAVE Flex Microwave Ablation System in the Ablation of Primary Soft Tissue Lesions of the Lung. 2018. Available from: <https://clinicaltrials.gov/ct2/show/NCT03603652>
- 171 Medtronic. NAVIGATE: Clinical Evaluation of superDimension™ Navigation System for Electromagnetic Navigation Bronchoscopy™. 2015. Available from: <https://clinicaltrials.gov/ct2/show/NCT02410837>



## Research data management

This thesis is based on the results of human studies, which were conducted in accordance with the principles of the Declaration of Helsinki. The medical and ethical review board Committee on Research Involving Human Subjects Region Arnhem Nijmegen, (Nijmegen, the Netherlands) gave approval to conduct all of these studies. In case of the multi-center studies as described in Chapters 3-4, participating other centers also had local ethical committee approval.

All standardized paper case report forms collected during the studies as described in this thesis were entered into the computer by use of Castor EDC. Imaging and clinical data which need not or could not be captured by Castor EDC were collected through direct exports of (image and clinical) data from their respective sources. The Castor EDC database and additional source data were correlated and analyzed with R and Rstudio.

Analog files and digital files as collected in the studies described in this thesis have been stored at the department of Pulmonary diseases (route 614). Binders containing analog documentation are stored in the Pulmonary diseases research archive closets, and will be relocated with the movement of the department of Pulmonary Diseases (expected to happen in less than 3 years). Both RLJ Verhoeven and EHFM van der Heijden will assure that all of the research data are then properly and coherently moved. Digital source files of manageable size (<50 Gb) and files related to the analysis of the study are stored at the research server of the department of Pulmonary Diseases (\\umcms033\Researchafdeling Longziekten) under their acronym, of which a back-up is continuously made. Chapter 2-4 acronym; E-predict, Chapter 5 acronym; CONTROL A & CONTROL E, Chapter 6-7 acronym; Navigation bronchoscopy database. Source files of more than 50 Gb size and not deemed directly necessary to answer the primary or secondary questions nor relevant for analysis of the studies described in this thesis are stored on external hard disks in two-fold, which are kept together with their respective analog study files.

The privacy of the participants in this study is warranted by use of encrypted and unique individual subject codes. This code corresponds with the code on the case report form, image data and other source files. The code is stored separately from the study data.

The data will be saved for 15 years after termination of the studies. Using the patient data in future research is possible if it is research directly related to the original subject and does not require additional patient contact or imply additional patient burden, as is recorded in the informed consent. The datasets analyzed during the studies as described in this thesis are available from both RLJ Verhoeven and EHFM van der Heijden upon reasonable request.

## PhD Portfolio

**Name PhD candidate:** R.L.J. Verhoeven

**PhD period:** 16-06-2017 –15 -12-2020

**Department:** Pulmonary diseases &  
Medical Ultrasound Imaging Center (Radiology)

**Promotor(s):** Prof. C.L. de Korte

**Graduate School:** Radboud Institute for Health Sciences

**Co-promotor(s):** Dr. E.H.F.M. van der Heijden

<b>TRAINING ACTIVITIES</b>	Year(s)	ECTS
<b>Courses &amp; Workshops</b>		
- RIHS Introduction course	2017	1
- BROK course	2017	1.2
- Cone Beam CT imaging workshop (Radboudumc)	2017	0.2
- Electromagnetic navigation bronchoscopy training (IRCAD)	2017	0.7
- Science & Skills: Figure making (RIHS)	2018	0.1
- Techmed workshop series, Twente University	2018	0.3
- Briskr workshop series, Novio Tech Campus	2018	0.4
- Digital Operating Room Summer School (Universitat Leipzig)	2018	1.5
- Entrepreneurship and innovation course (RU)	2019	3
- Grant writing and presenting for funding committees course (RU)	2019	1
<b>Seminars &amp; lectures</b>		
- Excellence statements for grant and career development	2018	0.1
- How to search for grants via the online database	2018	0.1
- Radboud research rounds: rare cancers†	2019	0.1
<b>(Inter)national Symposia &amp; congresses</b>		
- World Congress on Bronchology and Interventional Pulmonology†	2016, 2020	2
- European Lung cancer management summit	2017, 2018	1.5
- European Respiratory Society congress††	2017-2019	4
- European congress for Bronchology and Interventional Pulmonology†	2017	1
- Raakvlakken in de zorgketen – Nationaal Longkanker symposium Radboudumc	2017	0.2
- Technical Innovations in Medicine symposium†	2018, 2020	0.4
- European Congress for Radiology†	2018	1
- Dutch conference on Biomedical Engineering†	2018	0.3
- Conference of the European Society for Molecular Imaging††	2019	1.5
- 31 <sup>st</sup> congress of the EFSUMB†	2019	0.8
- World Conference on Lung Cancer†	2019	1
- Masterclass long-oncologie voor de verpleegkundig specialist†	2019	0.3
- International Interventional Pulmonology virtual meet - Linear EBUS†	2020	0.2
- Acoustics Virtually Everywhere - Acoustic Society America†	2020	0.3
- Mastery in Interventional Pulmonology: innovation in EBUS and navigation†	2020	0.2

**Other**

- Radboudumc Intraoperative imaging group (study group)	2017-2019	0.8
- Simulation for bronchoscopy (NVALT study group)	2017-2019	0.3
- NVMU bi-annual meeting(s)	2017-2018	0.6
- IKNL werkgroepvergadering long†	2019	0.1
- Radiology research meetings	2017-2018	0.8

**TEACHING ACTIVITIES**

**Lecturing**

- Practical assignment: bronchoscopy (students Medicine)	2016-2019	3
- Regional education AIOS Pulmonary Diseases	2018	0.2
- Navigation bronchoscopy in clinical practice (nurses)	2018	0.1
- Clinical endoscopy (nurses)	2018	0.1
- Regional education AIOS radiotherapy: navigation bronchoscopy	2020	0.1

**Supervision of internships / other**

- Supervision of MDO/TGO Technical Medicine students (3x)	2017-2020	2
- Supervision of M2 internships Technical Medicine (3x)	2017, 2019	4
- Supervision of M3 internships Technical Medicine (3x)	2019, 2020	8
- Supervision of MBRT graduation internship (1x)	2018	1
- Supervision of BMW bachelor internship (1x)	2019	1
- Supervision of BMW/Medicine student project: grant proposal / science project (2x)	2018, 2019	1
- Supervision of Medicine student internship (2x)	2020	3.2

**TOTAL** **50.7**

† Indicates oral presentation, ‡ Indicates poster presentation

A

## List of publications & presentations

### Papers in international journals

**R.L.J. Verhoeven**, C.L. de Korte, E.H.F.M. van der Heijden. Optimal Endobronchial Ultrasound Strain Elastography Assessment Strategy: An Explorative Study. *Respiration*. 2018; 97(4): 337–347.

**R.L.J. Verhoeven**, R. Trisolini, F. Leoncini, P. Candoli, M. Bezzi, A. Messi, M. Krasnik, C.L. de Korte, J.T. Annema, E.H.F.M. van der Heijden. Predictive Value of Endobronchial Ultrasound Strain Elastography in Mediastinal Lymph Node Staging: The E-Predict Multicenter Study Results. *Respiration*, 2020;99(6):484-492.

**R.L.J. Verhoeven**, F. Leoncini, D.J. Slotman, R. Trisolini, E.H.F.M. van der Heijden. Accuracy and reproducibility of endoscopic ultrasound B-mode features for observer-based lymph nodal malignancy prediction. Accepted for publication in *Respiration*, 2021.

R. Trisolini\*, **R.L.J. Verhoeven\***, A. Cancellieri, A. de Silvestri, F. Natali, E.H.F.M. van der Heijden. Role of endobronchial ultrasound strain elastography in the identification of fibrotic lymph nodes in sarcoidosis: A pilot study. *Respirology*, 2020; 25: 1203-1206. \* *Both authors contributed equally.*

**R.L.J. Verhoeven**, J.J. Fütterer, W. Hoefsloot, E.H.F.M. van der Heijden. Cone-Beam CT Image Guidance With and Without Electromagnetic Navigation Bronchoscopy for Biopsy of Peripheral Pulmonary Lesions. *Journal of Bronchology & Interventional Pulmonology*, 2020; 28(1):60-69.

**R.L.J. Verhoeven**, S. Vos, E.H.F.M. van der Heijden. Multi-modal tissue sampling in cone beam CT guided navigation bronchoscopy; the accuracy of different sampling tools and rapid on-site evaluation of cytopathology. Submitted, 2020.

**R.L.J. Verhoeven**, W. van der Sterren, W. Kong, S. Langereis, P. van der Tol, E.H.F.M. van der Heijden. Cone-beam CT and augmented fluoroscopy guided navigation bronchoscopy; radiation exposure and learning curve. Submitted, 2020.

F. Beyaz, **R.L.J. Verhoeven**, O.C.J. Schuurbijs, A.F.T.M. Verhagen, E.H.F.M. van der Heijden. Occult lymph node metastases in clinical N0/N1 NSCLC; A single center in-depth analysis. *Lung Cancer*, 2020; 150: 186-194

## Conference presentations

European Congress for Bronchology and Interventional Pulmonology, Belgrado, Serbia, 2017.

**R.L.J. Verhoeven**, C.L. de Korte, E.H.F.M. van der Heijden. Oral presentation.

*EBUS elastography – Technical aspects and considerations.*

European Respiratory Society International Congress, Milan, Italy, 2017.

**R.L.J. Verhoeven**, C.L. de Korte, E.H.F.M. van der Heijden. Poster presentation.

*Single center study: predicting lymph nodal malignancy through EBUS strain elastography.*

European Congress of Radiology, Vienna, Austria, 2018.

**R.L.J. Verhoeven**, C.L. de Korte, E.H.F.M. van der Heijden. Poster presentation.

*Single center study: predicting lymph nodal malignancy through EBUS strain elastography.*

Winter Conference of the European Society for Molecular Imaging, Chamonix, France, 2018.

**R.L.J. Verhoeven**, C.L. de Korte, E.H.F.M. van der Heijden. Poster presentation and consecutive oral presentation for best poster award.

*Endobronchial ultrasound strain elastography imaging and scoring of mediastinal lymph nodes; can it predict malignancy?*

Dutch Biomedical Engineering Conference, Egmond, The Netherlands, 2018.

**R.L.J. Verhoeven**, C.L. de Korte, E.H.F.M. van der Heijden. Poster presentation.

*Endobronchial ultrasound strain elastography imaging and scoring of mediastinal lymph nodes; can it predict malignancy?*

EUROSON, 31st congress of the EFSUMB, Granada, Spain, 2019.

**R.L.J. Verhoeven**, C.L. de Korte, E.H.F.M. van der Heijden. Invited oral presentation.

*Predicting mediastinal lymph node malignancy through endobronchial ultrasound strain elastography.*

5th European congress for Bronchology and interventional pulmonology, Dubrovnik, Croatia, 2019.

**R.L.J. Verhoeven**, J.J. Fütterer, W. Hoefsloot, E.H.F.M. van der Heijden\*. Oral Presentation\*.

*Augmented cbCT based 3D navigation for small pulmonary nodules.*

European Respiratory Society International Congress, Madrid, Spain, 2019.

**R.L.J. Verhoeven**, J.J. Fütterer, W. Hoefsloot, E.H.F.M. van der Heijden\*. Poster presentation\*. *Real-time 3D cone beam CT imaging guidance for advanced navigation bronchoscopy to centimeter sized lesions.*

European Respiratory Society International Congress, Madrid, Spain, 2019.

**R.L.J. Verhoeven**, J.J. Fütterer, W. Hoefsloot, E.H.F.M. van der Heijden\*. Poster presentation\*. *Added value of cone beam CT imaging to electromagnetic navigation bronchoscopy in diagnosing small pulmonary lesions.*

European Respiratory Society International Congress, Madrid, Spain, 2019.

**R.L.J. Verhoeven**, C.L. de Korte, E.H.F.M. van der Heijden. Poster presentation. *EBUS Strain Elastography for predicting lymph node malignancy: standardization of assessment technique.*

European Respiratory Society International Congress, Madrid, Spain, 2019.

**R.L.J. Verhoeven**, R. Trisolini, F. Leoncini, P. Candoli, M. Bezzi, A. Messi, M. Krasnik, C.L. de Korte, J.T. Annema, E.H.F.M. van der Heijden. Oral presentation. *Predictive value of EBUS strain elastography in mediastinal lymph node staging; the E-Predict multicenter study results.*

World Conference on Lung Cancer, Barcelona, Spain, 2019.

**R.L.J. Verhoeven**, R. Trisolini, F. Leoncini, P. Candoli, M. Bezzi, A. Messi, M. Krasnik, C.L. de Korte, J.T. Annema, E.H.F.M. van der Heijden. Oral presentation. *Predictive value of EBUS strain elastography in mediastinal lymph node staging; the E-Predict multicenter study results.*

World Conference on Lung Cancer, Barcelona, Spain, 2019.

**R.L.J. Verhoeven**, J.J. Fütterer, W. Hoefsloot, E.H.F.M. van der Heijden\*. Oral presentation\*. *Cone beam CT imaging for transbronchial navigation in small peripheral pulmonary lesions.*

World Conference on Bronchology and Interventional Pulmonology, Shanghai hybrid event, 2020.

**R.L.J. Verhoeven**, R. Trisolini, F. Leoncini, P. Candoli, M. Bezzi, A. Messi, M. Krasnik, C.L. de Korte, J.T. Annema, E.H.F.M. van der Heijden. Invited oral presentation. *Ultrasound based Strain Elastography in the EBUS-TBNA procedure for predicting lymph node malignancy.*

World Conference on Bronchology and Interventional Pulmonology, Shanghai hybrid event, 2020.

**R.L.J. Verhoeven**, J.J. Fütterer, W. Hoefsloot, E.H.F.M. van der Heijden\*. *Oral presentation\**  
*Cone Beam CT: A New Perspective for Diagnosis of Peripheral Pulmonary Nodules?*

World Conference on Bronchology and Interventional Pulmonology, Shanghai hybrid event, 2020.

**R.L.J. Verhoeven**, J.J. Fütterer, W. Hoefsloot, E.H.F.M. van der Heijden\*. *Oral presentation\**  
*cbCT Augmented Fluoroscopy Based Navigation in Clinical Practice.*

Acoustics Virtually Everywhere, Virtual conference by the Acoustical Society America, Virtual, 2020.

**R.L.J. Verhoeven**, R. Trisolini, F. Leoncini, P. Candoli, M. Bezzi, A. Messi, M. Krasnik, C.L. de Korte, J.T. Annema, E.H.F.M. van der Heijden. *Invited oral presentation.*  
*Identifying likely malignant lymph nodes in lung cancer through endobronchial ultrasound strain elastography and multi-modality imaging in a multi-center international prospective study.*

Technical Innovations in Medicine webinar, 2020.

**R.L.J. Verhoeven**, E.H.F.M. van der Heijden. *Invited oral presentation*  
*Een vroeg stadium longkanker verdenking; een klinisch probleem waarop de techniek geen antwoord weet?*

International Interventional Pulmonology virtual meet - Linear EBUS, 2020.

**R.L.J. Verhoeven**, R. Trisolini, F. Leoncini, P. Candoli, M. Bezzi, A. Messi, M. Krasnik, C.L. de Korte, J.T. Annema, E.H.F.M. van der Heijden. *Invited oral presentation.*  
*EBUS Elastography: Known and Unknown.*

## Dankwoord

Een promotietraject heeft in mijn optiek enige gelijkenis met de koers; een uitgezet traject met een start en als het goed is ook een finish. Maar waar ik aanvankelijk dacht dat het traject veel weg had van een wegkoers, bleek het toch al vrij vlot meer weg te hebben van een mountainbike marathon. De ene keer moest er vanwege obstakels op de baan een klein stukje afgeweken worden van het oorspronkelijke traject, terwijl er de andere keer überhaupt geen andere keus was dan een complete nieuwe weg. Achteraf gezien ook de langste en meest uitdagende koers waar ik tot nu toe aan begonnen ben. Misschien is het geen toeval dat ik in deze een sterke persoonlijke voorkeur heb voor de mountainbike boven die van de racefiets. Gebaande paden zijn té makkelijk en weinig avontuurlijk. De afleiding, de vrijheid om te ontdekken, de benodigde keuze in focus en de coaching van langs de kant maken ook dat ik het promotietraject als plezierig heb ervaren. En dat laatste is mogelijk wel een van de belangrijkste factoren. Jezelf jarenlang vastbijten op een traject (of; probleem) is alleen leuk in een stimulerende omgeving die resulteert in (incrementele) vordering en uitdaging. In het promotietraject van de afgelopen jaren heb ik ontzettend veel geluk gehad. Naast het vanzelfsprekend interessante onderwerp voelde het alsof er veel mensen betrokken en geïnteresseerd waren in het Radboudumc en daarbuiten. Ik zou daarvoor graag iedereen die betrokken was willen bedanken.

Allereerst **Chris**. Mijn eerste 10 weekse stage was onder jouw en MUSIC's hoede. Het was het begin van de rest van dit proefschrift. Wat was ik verbaasd over hoe gezellig en hecht de MUSIC groep was en wat vond ik jouw manier van begeleiden fijn. Kwam het eenmaal op de inhoud aan dan kon je kritisch zijn en liet je je kennis voor je spreken, maar dat kon pas nadat er eerst een goed informeel gesprek geweest was. En alhoewel ik nooit veel heb gekund met je koffiemok gezien mijn gebrek aan het volgen van de voetbalsport, hebben we 2 van onze 3 buitenlandse congressen samen toch goed weten te combineren met ook een aantal niet werk-gerelateerde activiteiten. Op de weg kon ik je bijhouden, maar op de latten was je mij te snel af ;-). Daarnaast was er natuurlijk ook altijd gezelligheid tijdens het aanvullen van de energietekorten. Ontzettend bedankt voor je sturing, je begeleiding alsook jou als persoon.

Ook tijdens mijn allereerste stage leerde ik **Erik** kennen. Aan de ene kant neig ik nu naar het maken van een geintje, aan de andere kant slechts naar het tonen van respect. Maar misschien moet ik het een tikkeltje serieus houden, zodat we het in het normale leven des te luchtiger kunnen houden en ik misschien nog een keer met jou en Barbara op vakantie mag ;-). Erik, ik blijf jou vooralsnog dag in dag uit lastig vallen met mijn eeuwige vragen. Ik ben je bijzonder dankbaar voor je geduld, de vrijheden en kansen die je mij tot nu toe hebt gegeven. Voor mij en elke patiënt zijn je praktische aanpak en eeuwige inzet voor zowel onderzoek en kliniek goud waard. Ik verbaas me elke keer weer over je reacties op mijn vragen om 1u 's nachts, om vervolgens om 07.50 weer de OK binnen te komen ('Is de patiënt er al?'). Joop Zoetemelk zou zijn wijsheden tweemaal moeten checken en de lokale Belg zou



je aanmanen om jezelf koest te houden. Erik, ik heb bewondering voor wat jij voor elkaar krijgt en ik hoop dat we in de toekomst samen nog vele uitdagingen mogen ondernemen.

**Prof. Verhagen**, beste Ad, als voorzitter van de manuscript commissie wil ik je bedanken voor de tijd en moeite die je genomen hebt om dit manuscript te lezen en beoordelen. Daarnaast wil ik je ontzettend graag bedanken voor je kennis en kunde waarmee je niet alleen op dagelijkse basis patiënten levens redt, maar ook de onwetende onderzoeker zoals ik verder op weg helpt. Hopelijk zullen we na afloop van een volgend congres of symposium samen niet wéér in een vreemde stad eindigen, ook al was het (late) etentje onverwachts meer dan het benoemen waard.

**Prof. Roovers**, beste Maroeska, bedankt dat je de moeite en tijd genomen hebt om dit manuscript te lezen en beoordelen. Daarnaast ook een welgemeend dankjewel voor je inzet en expertise omtrent de Health Evidence en Health Technology Assessment. Ik blijf mij keer op keer verbazen over de ondoorzichtigheid van het zorgsysteem en het uitblijven van objectief bewijs voor de effectiviteit of ineffectiviteit van het een of het ander. Jij bent een boegbeeld in dit gebied en kietelt de zorg om alleen voor betaalbaar en effectief beter te gaan. Ik hoop dat dit onderwerp steeds meer zal gaan leven, zodat we als zorgverleners maar ook als maatschappij kritisch blijven acteren. Een goede aanzet tot dit doel vind ik het onder de loep nemen van de navigatie bronchoscopie, zoals we dit nu met Tim Govers doen. Dank voor deze samenwerking, ook richting Tim, en hopelijk op naar meer.

**Prof. Slebos**, beste Dirk Jan, als buitenlid van de manuscriptcommissie en vooraanstaand lid van de interventie longziekten wil ik ook jou graag bedanken voor de tijd en moeite die je hebt genomen om dit manuscript te beoordelen en je inzet in de dagelijkse zorg. Een eerste kennismaking vond plaats toen jij onze posters over de navigatie bronchoscopie in Madrid tijdens het ERS congres beoordeelde. Daarop volgde een levendig gesprek welke interessante mogelijkheden aanstippelde voor verder onderzoek. Het is bewonderenswaardig hoe jij een volledig nieuw procedure in Nederland op de kaart hebt gezet en eigen hebt gemaakt, en, daar niet bij stopt. Ondanks dat het inmiddels even geleden is, hoop ik dat de uitnodiging tot een bezoek nog steeds staat. Het is een stukje reizen, maar ik denk dat het een leerzame en interessante reis zou zijn!

As the defense of the work described in this thesis wouldn't be worth much without critical questions, I'd like to thank the corona for their time and efforts in studying the manuscript and participating in this defense.

**Prof. Fütterer**, beste Jurgen, naast het plaatsnemen in de corona zou ik je graag willen bedanken voor je aandeel in het opzetten van de navigatie bronchoscopie procedure en de wetenschappelijke beargumentatie daarachter. Ik ben positief verbaasd over hoe jij zoveel dingen weet te begeleiden en hoop vanzelfsprekend dat er in de toekomst een verdere

samenwerking inzit wanneer we de mogelijkheden van de navigatie bronchoscopie kunnen uitbreiden.

**Prof. Trisolini**, dear Rocco, thank you for all the kindness and hospitality during my visit of Italy, the occasional memorable meet (and lovely dinners) at conferences, but also the fruitful collaborations we had. Your positiveness and everlasting enthusiasm is admirable. Also, a thank you for taking the time to participate in my defense. I'm sure all your interesting ideas will certainly point us towards more collaborations in the future.

**Prof. Mischi**, dear Massimo, we've only briefly met in Granada, but I'm honored that you are willing to invest your time and efforts to take place in the corona. Although the work presented in this manuscript is mostly based on clinical measurements, I hope you see room for discussing possible improvements on the technology and signal processing side of things.

Dear **E-predict study team**; Rocco, Fausto, Piero, Michela, Alessandro, Mark, Chris, Jouke and Erik. Thank you all for your hospitality during the visits of your centers, your teamwork and the significant time and effort you put in to successfully complete this trial.

Dear **Fausto**, thank you for the nice conversations, good company and the teamwork. Your input has been of high value for this manuscript and your unrelentless motivation is admirable. Let's hope that we can team up again in the future.

Klinische diagnoses zijn aardig maar er is er eigenlijk maar één die echt het laatste woord heeft; de patholoog. **Shoko**, naast je waardevolle klinische werk zou ik je ook graag willen bedanken voor je vriendelijkheid, wetenschappelijke input en je interesse. Elke keer als wij elkaar spreken leer ik weer ontzettend veel. Hopelijk heb ik je niet al te veel belast met alle vragen.

Tijdens zo'n beetje elk endoscopieprogramma bellen we ze plat en moeten ze heel wat meters maken om ons van een advies te voorzien; de analisten van de pathologie. **Lia, Anne, Danny en Tini**, heel erg bedankt voor jullie inzet maar ook jullie interesse en behulpzaamheid. Ontzettend leuk dat ik af en toe mee mag kijken en weer van jullie observaties mag leren. Overigens, mijn excuses dat ik jullie af en toe een beetje vervloek als jullie zeggen dat er geen representatief materiaal uitkomt. ;)

Je ziet ze niet vaak rondlopen, maar ze zijn een stille kracht die de ziekenhuis faciliteiten op de been houden; de klinische fysici. Bedankt **Pieterneel, Wens, Joost en Erik** voor jullie dagelijkse inzet maar ook het meedenken, of dat nou enkel wetenschappelijk of klinisch was. Wens en Pieterneel, zonder de prettige samenwerking met jullie was ik er zeker niet uit

gekomen. Joost en Erik, een ander domein, maar net zo belangrijk. Bedankt voor jullie advies en behulpzaamheid.

Toen het navigatie bronchoscopie programma van de grond kwam was het wennen. Het pad dat we bewandelde was eigenlijk voor niemand bekend. Een dankwoord zou ik daarbij uit willen spreken richting de laboranten van de interventie radiologie. **Tom, Gretha, Ichelle, Mark, Peggy en Thessa** maar ook de rest van de collega's, jullie hulp en inzet was en is van grote waarde. Het specialisme longziekten is misschien niet jullie meest logische gast, maar fijn dat jullie ons de weg laten zien.

Graag wil ik ook de endoscopie verpleegkundigen bedanken. **Ineke, Beppie, Annelou en Hennie** maar natuurlijk ook de rest van de afdeling. Het is altijd gezellig met jullie als collega's, ook al is het vaak flink doorwerken. Jullie bijdrage is onmisbaar groot en is tenminste elke week bij het navigatie programma een kleine volksverhuizing. Ik beloof plechtig dat ik niemand van jullie meer op de kast zal zetten.

Veel tijd bracht ik gedurende het schrijven van dit manuscript door op route 614, Longziekten. Allereerst wil ik het stafsecretariaat bedanken; Rob, Hilda en Joyce. Jullie regelen meer dan dat ik waarschijnlijk ooit door zal hebben en krijgen het ook maar elke keer weer voor elkaar. Ook zou ik de **verpleegkundige specialisten, back-office, stafleden, research verpleegkundigen** maar ook de **AIOS** en **ANIOS** en **alle andere collega's van de longziekten** willen bedanken. Er wordt altijd tijd gemaakt voor een gezellige kop koffie, samen lunchen, of het kleine praatje op de gang. Pauzes zijn over het algemeen niet mijn sterkste punt, maar ik doe mijn best. Specifiek wil ik graag nog **Wouter en Olga** bedanken, voor de dingen die jullie mij geleerd hebben alsook de vriendelijke en collegiale sfeer die er altijd hing tijdens de endoscopie programma's. Ik ben blij dat jullie ruimte zagen voor mij als vreemde klinische technoloog en dat jullie haast vanzelfsprekend willen bijdragen aan de wetenschappelijke vragen die ter discussie staan. En Wouter, misschien dat ik in de toekomst ooit nog zo'n gekke hersenkronkel krijg zoals jij en dat we nog een keer samen ergens gaan trailrunnen. Tot die tijd hou ik het even bij dat moment in Belgrado, waarna ik na 3 dagen nog steeds krom liep van de spierpijn. Olga, ontzettend fijn dat je er weer bent. Ook verdienen **Petra en Michel** een specifieke benoeming. Ontzettend veel dank voor jullie vertrouwen alsook steun. De positiviteit van jullie beiden zorgt voor inzet en slagkracht. Met jullie aan het roer krijgt de afdeling Longziekten veel voor elkaar. **Milou**, je bent een fijne kamergenoot en sparringpartner. Soms hard werken, maar soms ook even gewoon niet. Die blessures met al dat hardlopen, ik snap dat gewoon nog steeds niet. Een fiets is toch gewoon sneller, kost minder moeite, en, minder blessuregevoelig? **Ineke**, jij verdient het om nogmaals genoemd te worden. Jouw tomeloze inzet voor de longziekten is gigantisch, je kwebbel oneindig, en de vrolijkheid en drukte waarmee je altijd rondstormt is een gezicht op zich. Bedankt!

Toen ik voor het eerst stage ging lopen in het Radboudumc deed ik dat voornamelijk bij de **MUSIC** groep. Ik voelde mij destijds vrijwel direct op mijn plek in een gezellige en hechte groep. Een gevoel van thuiskomen. In mijn latere afstudeerstage alsook het vervolg heb ik ontzettend veel mogen leren van de verschillende MUSICi. De technische kennis staat er buiten kijf en het groepsgevoel is sterk. Ik kijk met veel plezier terug op zo'n beetje elk moment dat ik weer tussen de MUSICi verbleef, ondanks dat ik zeker vaker de tijd had moeten nemen om te socializen. Mooi om te zien hoe deze onderzoeksgroep zichzelf zo vormt en stuurt. Graag wil ik ieder van hen bedanken voor hun oprechte interesse, gezelligheid, kennis en ook de samenwerkingen. Specifiek wil ik daarbij **Gert** noemen voor zijn hulp en expertise op het gebied van kwantitatieve echo. Bedankt voor jouw behulpzaamheid en inzet voor het exploreren van de waarde hiervan binnen de longkanker diagnostiek Gert. Hopelijk blijf ik ondanks mijn aanstelling binnen de Longziekten ook in de toekomst nog welkom binnen de groep.

Tijdens dit promotietraject heb ik de eer gehad om meerdere stages te mogen begeleiden. De verschillende studie en bachelor opdracht groepjes wil ik graag bedanken voor hun telkens unieke kijk op de stof, jullie enthousiasme maar ook de uitdagende vragen die jullie soms stelden. **Nienke, Eline** en **Irene**, bedankt voor jullie individuele bijdragen aan de verschillende onderwerpen binnen dit proefschrift. **Jorik**, de resultaten in dit manuscript zijn ook zeker voor een deel jouw werk, waarvoor dank. Jij ging als een gemotiveerde sneltrein, en je was bereidwillig om zelfs na je stage periode nog even door te denderen. Ik waardeerde onze gesprekken, discussies en gezamenlijke leermomenten enorm. **Renée**, meermaals heb ik mij verbaasd over jouw oprechte interesses in iedereen, dat ontzettend grote en snel lerende geheugen en je actiepunten afwerk tempo. Op de Longziekten wachten we allemaal op je wederkeren als AIOS ;-). **Desi**, je begon ontzettend enthousiast aan het ontrafelen van taal met rare tekens en circuitjes. Volgens mij hebben we samen nogal wat uitprobeerde (en wat frustraties geuit). Inmiddels succesvol bezig met een andere opdracht met en na je afstuderen; je opgewektheid en eerlijkheid brengen leven in de brouwerij en kunnen nog wel eens veel impact gaan hebben! **Nienke**, jij laat je niet gauw uit het veld slaan. Binnen een mum van tijd heb je technisch ingewikkelde dingen aan elkaar weten te knopen (letterlijk en figuurlijk) om die dan ook nog eens naast de patiënt te kunnen valideren. Een mooi voorbeeld van de TG'er. Succes met je vervolg onderzoek in een nieuw veld! **Ferhat** en **Souraya**, ik beschrijf jullie samen omdat ik jullie ook een beetje als een (ambitieuze) duo zie. Was de een er, dan de ander ook. Jullie werk is echt een ontzettend mooie basis die de wetenschap ook in de toekomst nog vooruit gaat helpen, dank daarvoor. Ferhat, ook na je stage ben je aan je onderwerp blijven doorwerken om het richting een succesvolle publicatie te krijgen. Een mooi resultaat, wat een van de problemen van de huidige longkankerdiagnostiek goed blootlegt.

My research has been supported in different ways by **Pentax Medical Europe**, the **Ankie Hak fund**, **AstraZeneca**, **Medtronic**, **Siemens Healthineers**, **Philips medical** as well as the

Radboudumc (**MITeC**) itself. I am very grateful to all for their support. I'd furthermore like to thank several people individually. **Amilcar**, ever since we met in Strasbourg you've never stopped to challenge and question me. Thank you for your kindness and hospitality, even though we are now both in a different place and into different body parts. **Sander**, thank you for the never-ending information exchange, the help, the good conversations, straight forwardness and hands-on mentality. **Stephanie, William, Marco, Lucia, Alessandro but also the rest of the team**; thank you for the intensive collaboration, the nice conversations and the continuous progress you are making, it really helps both the patients and clinicians a whole lot.

Zo af en toe moet je je uitleven, en een significante noemer daarvoor is mijn fiets. Bedankt ook richting het **KMC mountainbike team** voor hun support. **Martin**, blij met je nuchtere blik op de wereld en het aangrijpen van elke uitdaging, hoe extreem dan ook. Een eer dat ik onderdeel van je equipe uit mag maken en mezelf daarin tot het uiterste mag drijven. Ook een specifiek dankwoord aan (oud-)ploeggenoten **Gerben** en **Tim**. Tim omdat ik nog krediet op moet bouwen voor de aankomende duo meerdaagsen (hij gaat me toch uitwringen..) en Gerben omdat ik nog steeds hoop dat ie terug komt.. **Ramses** moet ik misschien ook bedanken, maar het zit vaker toch meer tussen een mening over krankzinnigheid en inspiratie in. Maar natuurlijk ook aan de andere concullega's; ik hoop nog veel mooie momenten samen met jullie mee te mogen maken.

Al sinds jaar en dag vanaf het moment dat ik naar Enschede verhuisde kan ik van hun op aan; studievrienden. Inmiddels enigszins verspreid over Nederland, maar de afstand voelt nooit groot. Fijn om altijd op jullie terug te kunnen vallen **Sander, Simon, Ruben, Ruud** (en jullie wederhelften natuurlijk!). Samen hebben we veel geleerd maar ook veel beleefd. Bedankt voor de goede discussies onder een glas whisky, het samen tot 'rust' te komen op vakanties of dagen weg, het meedenken, maar ook bijvoorbeeld bedankt voor de onverwachte support op het WK in Singen of de meer dan avontuurlijke support in Combloux. Daarnaast ook richting alle andere vrienden om mij heen; bedankt, jullie verrijken mijn leven!

Last but not least wil ik graag **ons thuis** bedanken. Dat kan ik in heel veel woorden doen, maar over het algemeen weet ik dat het bij ons juist vaak onuitgesproken blijft. **Renée** en **Martijn**, ondanks onze verschillende richtingen heb ik toch altijd wat aan jullie advies en is het altijd gezellig als we elkaar weer zien. Een gesprek met jullie richt je hart en hersenen weer de goede kant op en houdt je met beide benen op de grond. **Pap, mam**, zonder jullie was ik nooit tot hier gekomen. Ik ben jullie dankbaar voor de normen en waarden, opvoeding, de ontelbare keren hulp, jullie enthousiasme, support, en, het feit dat jullie meer dan 24 uur in één dag weten te krijgen om ons als kinderen te helpen. **Kelly**, samen zijn wij een nieuw ons thuis ;-). Bedankt voor jou en de momenten samen, in zijn algeheel.



## Curriculum Vitae



Roel (Lambertus Johannes) Verhoeven was born in 's-Hertogenbosch, the Netherlands, on May 20<sup>th</sup> 1992. After finishing his secondary education at the Mondriaan college in Oss, he started the Technical Medicine program at Twente University in 2010 (Enschede, The Netherlands). He completed his bachelors degree in technical medicine by finishing a project wherein a mitral valve surgery simulator giving real-time feedback was developed. Interested by the possibilities of the technical physician, he further enrolled and completed the Technical

Medicine master-track 'Medical Imaging and Interventions' with cum laude honors in 2017. During his master he obtained internship experiences at various institutes. Key words of these internships were; (suspected) cancer, surgery, (flexible) endoscopy, ultrasound, robotic soft- and hardware, artificial intelligence, image analysis, MedTech development and intra- and entrepreneurial skills. An additional 6-month Erasmus exchange program with the Norwegian University of Science and Technology (Trondheim, Norway) allowed him to study ultrasound and neuroscience in-depth in between internships. The topic of his master thesis was "Innovation in bronchoscopy" and the research performed therein was continued into this PhD dissertation. The results of the research Roel performed have at least in part been described in this thesis. With his appointment as a technical physician at the Dept. of Pulmonary Diseases in the Radboudumc, he wants to continue working towards development of technology and methodologies for improving lung cancer diagnosis, staging and improving chances of curation.

Roel carried and continues to carry out the research in combination with being an elite endurance athlete. While finishing the Embrunman full-distance triathlon in 2015 at an 18<sup>th</sup> place (Embrun, France) was an escapade, his main focus is ultra-distance and multi-day mountainbike events. In doing so, he's participated in the UCI world mountainbike marathon championships of 2017 (66<sup>th</sup>) and 2018 (56<sup>th</sup>), and consistently finished in the top 10 of the national championships for the past years. Since 2019 he is contracted by the KMC mountainbike-team.

